Weathering the Storm: Supply Chains and Climate Risk*

Juanma Castro-Vincenzi
Harvard University

Gaurav Khanna
University of California, San Diego

Nicolas Morales
Federal Reserve Bank of Richmond

Nitya Pandalai-Nayar
University of Texas at Austin and NBER

May 2024

Abstract

We characterize how firms structure supply chains under climate risk. Using new data on the universe of firm-to-firm transactions from an Indian state, we show that firms diversify sourcing locations, and that suppliers exposed to climate risk charge lower prices. Our event-study analysis shows firms with suppliers in flood-affected districts experience a temporary decline in inputs, followed by a return to original levels. We develop a general equilibrium spatial model of firm input sourcing under climate risk. Firms diversify identical inputs from suppliers across space, trading off the probability of a climate disruption against higher input costs. We quantify the model using data on 271 Indian regions, showing real wages vary across space and are correlated with geography and productivity. Wages are inversely correlated with sourcing risk, giving rise to a cost minimization-resilience tradeoff. Supply chain diversification unambiguously reduces real wage volatility, but ambiguously affects their levels, as diversification may come with higher input costs. While diversification helps mitigate climate risk, it exacerbates the distributional effects of climate change by reducing wages in regions prone to more frequent shocks.

JEL: F14, L14
Keywords: Production networks, supply chains, firm dynamics, climate change

*We thank Claire Conzelmann and Simon Farbman for outstanding research assistance and Swapnika Rachapalli for sharing inventory data. We also thank Pol Antràs, Adrien Bilal, Chris Boehm, Olivier Coibion, Elhanan Helpman, Andrei Levchenko, Andres Rodriguez-Clare, Alireza Tahbaz-Salehi, and Jose Vasquez as well as seminar and conference participants at University of Michigan, St Louis Fed, Warwick, UT Austin, Midwest Macro, TIGN, Empirical Macro Workshop and Kiel-CEPR Geopolitics Conference for helpful comments. The views expressed are those of the authors and do not necessarily reflect those of the Federal Reserve Bank of Richmond or the Board of Governors. Email: jcastrovincenzi@fas.harvard.edu, gakhanna@ucsd.edu, nicolas.morales@rich.frb.org and npnayar@utexas.edu.

1 Introduction

The intersection of complex supply chains and climate risk presents a critical challenge to the global economy. Complex supply chains have yielded significant efficiency gains worldwide, enabling firms to procure inputs from the most efficient suppliers regardless of their location. Yet, escalating climate risk raises concerns about the vulnerability of interlinked production networks and the ensuing broader economic fragility (Barrot and Sauvagnat, 2016; Boehm et al., 2019). Increasing global risk of climate change also heightens the likelihood of natural disasters such as flooding and storm surges. In response, forward-looking firms may choose their production locations (Castro-Vincenzi, 2024), or diversify the locations of their suppliers based on geographic variability in climate threats to mitigate the impact of disruptions to their productive activities. Therefore, our understanding of how climate change may reshape economic production and its implications for welfare across regions hinges on firms' adaptive sourcing decisions in response to escalating hazards. In this paper, we provide a theoretical, empirical, and quantitative analysis of the spatial consequences of supply chain restructuring in light of increased climate risk.

Studying the general equilibrium consequences of how firms structure supply chains when faced with climate hazards raises two important challenges. First, for empirical evidence on how firms respond to climate risk, we need high-frequency data on transactions along the supply chain, the precise locations of establishments, and meaningful variation in weather-related events. Second, to quantify the broader economy-wide consequences, we require a general equilibrium model of firm input sourcing under climate risk, where firms face trade-offs such as the lower probability of climate shocks against higher-cost, less productive inputs or higher shipping costs.

To address the first challenge, we obtain the universe of establishment-to-establishment level transactions from a large state in India, as long as one node of the transaction (either buyer or seller) is in the state (the other node can be anywhere in the country). This dataset contains the precise zip code of the establishments, the value of the transaction, the product code, the date, the quantity (and so the unit values), and the unique tax ID of the establishment. Using these data, we document important new motivating facts suggesting firms are optimizing supply chains to mitigate climate risk. First, firms diversify the locations they source from, even within narrow product codes. Second, firms that multisource the same product buy from farther distances, dryer regions and pay higher prices. And third, suppliers in regions that are more exposed to climate risk tend to charge lower prices.

A key advantage of our setting is that India experiences monsoonal rainfall that follows a somewhat predictable spatial pattern every year, although the intensity and timing can

vary. Regions across India are regularly and increasingly experiencing large flooding events that disrupt firm supply chains. Firms operating in this environment might reasonably consider the probability of climate-related disruptions in their operations, as suggested by our descriptive analysis.

To provide causal evidence of firm responses to climate shocks, we leverage the exogenous geographic and temporal variation in flooding events using a staggered event study design. We show that the sales of flood-hit suppliers fall drastically over three months but recover by five months after a flood. Further, the total purchases of downstream buyers decrease substantially, and they are unlikely to substitute to other suppliers. Yet, we detect no change in the sales of these downstream buyers. Prices increase in the short run, but once again recover. Importantly, we show no difference in affected and unaffected firms in the pre-period. In sum, all of our empirical evidence together suggests firms plan for climate-related risk and recover from the realized shocks relatively quickly. These empirical patterns serve to motivate and discipline our general equilibrium framework.

Our second contribution is theoretical. To address the challenge of quantifying economy-wide impacts, we build a spatial general equilibrium model of firm sourcing under climate risk. Motivated by our empirical results and the patterns in the data, firms diversify their sourcing of otherwise identical inputs across locations to mitigate climate risk. Such diversification comes with a trade-off: places with lower climate risk might be less productive, or geographically distant, necessitating payment of higher trade costs.

A key feature of the model is that firms' expected profit functions in the presence of sourcing risk are concave in input orders. That is, firms behave as if they are risk-averse, even in the absence of explicit risk aversion in preferences.[1] This implies that firms from each region will choose to diversify their input sourcing across regions if they face heterogeneous shock probabilities, even in the extreme case where regional fundamentals are constant across space, and trade is costly (a "symmetric" economy). In a comparative statics exercise, we show that in this setting, there might be no conventional gains from trade, but trade still occurs purely due to the diversification motives of firms. As a result, despite identical fundamentals, "safer" regions see higher real wages in general equilibrium, while more distant or riskier regions see lower real wages.

Interestingly, this comparative statics exercise implies that the prices of inputs and, therefore, of regional consumption, are higher under costly trade than regional autarky. A stark insight from this exercise is that the average expected regional real wage can be lower under costly trade than under autarky, but its volatility is also lower. In other words, under commonly used consumer preferences that do not have an explicit role for the volatility

[1] Blaum et al. (2024) study firm input sourcing under shipping time risk where firms face a similar problem. In contrast, our focus is the multi-region general equilibrium.

of real wages in welfare, costly trade might be welfare decreasing. We show, however, that free trade in the symmetric economy brings both the diversification benefits of lower wage volatility and higher expected real wages compared to costly trade.

This stark result depends on the calibrated trade costs and disruption probabilities. We show that while consumers are risk neutral, their welfare is also concave in input orders, albeit less so than firms' for common parameter calibrations. As a result, for high enough trade costs, firms will choose to diversify more than is optimal for the consumer, and costly trade can be welfare decreasing. This implies that in general, autarky and trade cannot be Pareto ranked, and in some instances, depending on the trade costs and disruption probabilities, autarky will be Pareto-improving over trade.

We quantify this model using a census of manufacturing firms across the country, allowing us to estimate location-specific productivities and labor shares. We implement the model on 271 regions in India. Our model implies that bilateral sourcing shares are a function of all regional labor endowments, productivities, and bilateral trade costs, as well as the risk of sourcing in each region. Given estimates of regional labor, productivity, and bilateral trade costs, we back out the model-implied regional risk that is necessary to fit observed sourcing shares. To validate our framework, we project the model-implied risk on climate observables such as rainfall and floods as well as other risk-related variables such as court capacity to capture institutional features that affect firm decisions. We find that climate-related risk is positively correlated with the estimated risk probabilities. The positive correlation suggests that firms take into account several sources of risk when they form their supply chains, a feature that has been largely ignored by the literature (an exception is Kopytov et al. (2021) who study how supply chains adapt to supplier volatility).[2]

While the comparative statics exercises provide stark analytical insights about the possible impacts of diversification, the effects of firm diversification in a realistic economy will, in general, depend on the variation in fundamentals and "standard" motives for trade, such as geography and productivity in addition to risk-mitigation incentives. Our third contribution is, therefore, quantitative: we compute expected real wages across districts in our calibrated model, given model-implied sourcing risk. Our framework implies that as a result of firm sourcing decisions, real wages in each district will depend on the geography, productivity, and climate risk of all districts.

We perform several quantitative exercises in our calibrated model. First, we validate the insight from our comparative statics exercises regarding wage volatility. We find that under the estimated trade costs and climate risk, the variance of real wages is 113% higher in autarky. On the other hand, expected real wages do not always have to be lower than

[2]In an alternative exercise, we parameterize the regional risk as a function of climate-related variables and estimate the relevant parameters. Our quantitative results remain similar.

in autarky. In our calibrated model, they are, on average, 3.2% lower, although 1.1% of districts see expected real wages that are higher than in autarky.

We then study how regional wages change in general equilibrium under alternative shock probabilities to capture scenarios of changing climate risk and to highlight our new channel. We use the correlation of flood, heat, and precipitation risk with our estimated district-level risk probabilities to infer how these probabilities would change given IPCC projections of flood, heat, and precipitation risk. We then compute expected real wages, input prices, and wage volatility under the scenario of flood, heat, and precipitation risk increasing as projected. We find that the average risk of districts increases by 1.49p.p., but there is wide heterogeneity. Expected real wages decline on average by 2%, their volatility decreases slightly by an average of 1.2%. Nearly 44% of districts see real wage increases, however. In particular, safer districts largely see expected real wage increases. In sum, our model and quantification show that firm sourcing decisions help mitigate the effects of climate shocks and have quantitatively important implications in general equilibrium for real wages in safer regions relative to riskier ones.

Our results highlight two economic implications of climate change. On the positive side, the risks of climate change are mitigated since firms anticipate climate risk and diversify their sourcing decisions to minimize the volatility due to climate shocks. This implies that more volatile weather does not necessarily translate into higher aggregate output volatility. On the negative side, climate change will have even larger redistributive effects across regions than commonly believed. Regions with more climate risk will face the direct effects of the shocks themselves, but additionally will also become less appealing to other regions as a source of inputs. As a result, demand for products from these regions will decline, and real wages will fall. The converse will occur in "safer" regions. In other words, diversification will amplify the distributional effects of climate change.

Related literature. A growing literature studies how climate change shapes economic activity. Several papers focus on the long run, assessing how the distribution of economic activity changes within and across regions, and countries (Bilal and Rossi-Hansberg, 2023; Cruz and Rossi-Hansberg, 2023; Desmet et al., 2021; Farrokhi and Lashkaripour, 2024; Hsiao, 2023; Jia et al., 2022; Nath, 2022). A smaller subset considers optimal medium-term policy responses (Balboni, 2021). Another branch of the literature studies the effects of extreme weather events on firms' employment and location decisions as well as on FDI (Castro-Vincenzi, 2024; Gu and Hale, 2022; Indaco et al., 2020; Pankratz and Schiller, 2021). In this paper, we study the general equilibrium impacts of endogenous firm supply network decisions under climate risk. While we emphasize how firms can use their supply networks to mitigate the risk of extreme weather events, our model is well suited to

analyze the general equilibrium effects of supply network formation under any location-specific risk.

While the responses of firm supply chains to climate risk have received little attention in the literature, closely related is ongoing work by Balboni et al. (2023) and Blaum et al. (2024), who study supply chain responses to floods in Pakistan, and U.S. importer responses to shipping-time volatility, respectively. These papers provide rich empirical evidence of varied aspects of firm responses to supply chain risk. Our empirical evidence is complementary, but our focus here is on the quantitative model studying the spatial general equilibrium implications of supply chain adaptation to climate risk. At the micro level, our firm problem is similar to Blaum et al. (2024), but our model delivers strong implications for how wages across space are shaped by regional risk in general equilibrium, and can be used to infer the risk that firms assign to different sourcing locations.

Our theoretical and quantitative results are also related to the insights in Kopytov et al. (2021), who study supply chain adaptation to supplier volatility, and to Pellet and Tahbaz-Salehi (2023), who study the implications of rigidities in supply chains that arise due to incomplete information. Caselli et al. (2019) show that diversification across sectors can lower aggregate volatility in a quantitative trade model. Similar to the rigid inputs in Pellet and Tahbaz-Salehi (2023), firms in our model place orders for intermediate inputs prior to the realization of shocks, and cannot adjust their orders ex-post. In contrast to these papers, our model features households in multiple regions who cannot trade shares of the different firms, and the incentive to mitigate volatility arises from the concavity of firm profits. As a result, in our framework, aggregate volatility decreases in trade openness, as firms mitigate risk. However, expected real wages can be lower under costly trade compared to autarky. This parallels the results in these papers that aggregate output is also lower due to diversification away from volatile suppliers. We show, however, that eliminating trade barriers permits both expected real wages and aggregate volatility to be lower, maximizing the benefits of diversification.

Supply chain fragility and resilience have received increased attention in the literature following the Covid-19 pandemic (Goldberg and Reed, 2023; Grossman et al., 2023, 2024; Khanna et al., 2022), and recent global disruptions (Korovkin et al., 2024). Our firm-to-firm data are similar to Khanna et al. (2022), but our identification strategy uses extreme weather events, and we emphasize the adaptation of supply chains to climate risk and the general equilibrium consequences, which are not studied in that paper. Our empirical evidence indeed suggests that firm supply chain responses to climate-related risk vary qualitatively and quantitatively from their responses to an unanticipated, temporary shock like Covid-19.

Additionally, we also build on a growing research agenda on how production networks respond to shocks. A long literature documents the importance of international trade in inputs and studies the macroeconomic consequences of such trade (Antràs et al., 2017; Caliendo and Parro, 2015; Hummels et al., 2001; Huo et al., 2024; Johnson and Noguera, 2012, 2017; Yi, 2003). A strand of this literature has emphasized the transmission of natural disasters through trade and supply chain links (Barrot and Sauvagnat, 2016; Boehm et al., 2019; Carvalho et al., 2021). In contrast to studying the responses of firms or sectors to the incidence of shocks, we quantify the general equilibrium economy-wide consequences of firm supply chain adaption to the (changing) probability of disruptions.

Finally, our paper contributes to research studying trade under risk (e.g. Helpman and Razin (1978), Esposito (2022), Allen and Atkin (2022), Adamopoulos and Leibovici (2024), among others), albeit without an emphasis on supply chains and climate risk.

The rest of our paper is structured as follows. Section 2 outlines our data, shows descriptive patterns, and contains our event study analysis around flood events. Section 3 sets up the model, derives some analytical results, and performs comparative statics. Section 4 calibrates and quantifies the model, while 4.4 contains the climate change counterfactuals, and Section 5 concludes.

2 Empirical Approach

2.1 Data

Firm-to-firm trade. Our primary data source is daily establishment-level transactions (while we use the term "firm", the data are at the granular establishment level). These data are from the tax authority of a large Indian state with a fairly diversified production structure, roughly 50% urbanization, and high population density. Comparing this context to others with firm-to-firm transaction data, we observe that the state has roughly three times Belgium's population, seven times Costa Rica's, and double Chile's.

The data contain daily transactions from April 2018 to October 2020 between all registered establishments within the state, and all transactions where one node of the transaction (either buyer or seller) is in the state. All transactions have unique tax identifiers for both the selling and buying establishments, which include the value of the whole transaction, the value of the items being traded by 8-digit HSN code, the quantity of each item, its unit, and transportation mode.

Each transaction also reports the zip code location of both the selling and buying establishments, which we merge with other geographic data. By law, any goods transaction with value over Rs.50,000 ($700) has to generate eway-bills, which populate our data.

Figure 1: Monsoonal rain floods, 2018-2020

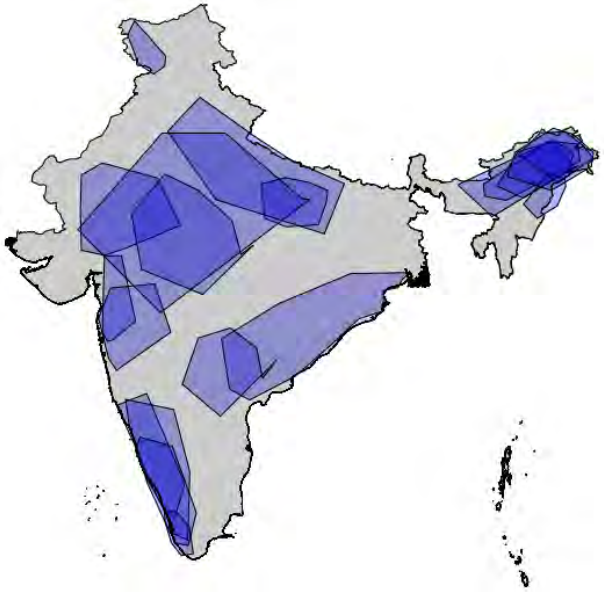

Note: The figure plots the geographic coverage of all large floods that occurred between 2018 and 2020, as described in the Dartmouth Flood Observatory.

Transactions with values lower than $700 can also optionally be registered. As such, our network is representative of relatively larger firms, but the threshold is sufficiently low to capture small firms as well. More information is in Appendix D.1, with summary statistics in Table A1. The distribution of customers and suppliers each firm has is very similar to that documented by Alfaro Ureña et al. (2018) for Costa Rica.

We use the data to construct the buyer-supplier network every period and the total value of inputs purchased and output sold by firms. To obtain a measure of real inputs and output, we use the reported quantity of each transaction to calculate unit values for each product, construct a price index, and deflate the total firm-level input purchases and sales. Our output measure is noisier than inputs, given that we do not observe direct-to-consumer sales. Therefore, when using output as an outcome, we restrict the sample to firms with positive sales every period before the flooding event began.

Climate data. We use data from the Dartmouth Flood Observatory to identify geocoded flooding events throughout India for our event study analysis. As shown in Figure 1, we identify 19 events of large monsoonal floods throughout India between 2018 and 2021. For our event study analysis, we limit the set of floods to those that occurred outside of our state, for which we have at least 3 months of data before and after the flood, and that caused at least 100 individuals to be displaced by the flood. These restrictions leave us with seven large flood events, which we use in our analysis in Section 2.3. We complement the climate-related datasets with information on district-level historical and projected daily rainfall, coastal flooding, riverine flooding, and average temperatures.

Details on this data can be found in Appendix D.1.

2.2 Descriptive Analysis

To begin our analysis, we document three facts related to supplier diversification and climate risk to motivate the key features of our model.

Fact 1: A significant mass of firms source the same product from multiple regions.

We leverage the detailed product information in our transaction data and compute the number of districts a firm sources a given product from. As shown in Table 1 Column 1, 62% of the firms in our data buy from more than one district. In columns 2 to 4, we show that a significant fraction of firms also multisource the same product across regions. We compute the number of districts a firm-by-HSN product code pair sources from. In Column 2, we use 2-digit product codes; in Column 3, we use 4-digit product codes; and in Column 4, 8-digit product codes. Even with the narrowest product definition available in our data, 14.4% of firms source the same product from more than one district. This is evidence that a significant fraction of firms multisource their products. In Appendix Table A3, we show that the distribution of the number of supplier districts is very similar when we exclude likely wholesalers and likely retailers from the analysis.

Table 1: Share of firms that source from multiple districts

Number of supplier districts	Share of buyers	Share of buyers x HSN 2	Share of buyers x HSN 4	Share of buyers x HSN 8
1	37.9%	67.7%	77.1%	85.6%
2	20.6%	16.8%	13.8%	10.1%
3	12.2%	6.7%	4.5%	2.5%
4	7.7%	3.3%	1.9%	0.9%
5	5.3%	1.8%	1.0%	0.4%
6	3.7%	1.1%	0.5%	0.2%
7	2.7%	0.7%	0.3%	0.1%
8	2.0%	0.5%	0.2%	0.1%
9	1.5%	0.3%	0.1%	0.0%
+10	6.4%	1.1%	0.4%	0.1%

Note. Column 1 aggregates the data at the firm level and computes the share of firms that source from a certain number of districts. Column 2 aggregates the data at the firm-by-2-digit product level, Column 3 at the firm-by-4-digit product level, and Column 4 at the firm-by-8-digit product level.

Fact 2: Firms that multisource more, buy products from farther distances, dryer regions, and pay higher input prices.

For this analysis, we focus on firm-product pairs using the 8-digit product classification. In Figure 2a, we show that firms that source the same product from more regions tend to buy from suppliers that are farther away. For instance, firm-product pairs that source

from one district have an average distance of 350km to suppliers. On the other hand, firm-product pairs with five suppliers per product have an average distance of more than double, at 711km.

In Figure 2b, we also show that firm-product pairs with more suppliers also seem to source from lower rainfall districts. For firm-product pairs that source from one district, such districts have, on average, a 6.5mm daily rainfall. On the other hand, for firm-product pairs that source from five districts, such districts have, on average, 5.4mm of daily rainfall. The 1.1mm difference in rainfall between one and five source districts, is 17% with respect to the mean. In Appendix Table A4, we show that such patterns are also prevalent for other measures of climate risk, such as historical riverine flooding.

Finally, in Figure 2c, we show that firms that source from more districts also tend to pay higher prices for their inputs.[3] As shown in Figure 2c, firms that source from five districts pay an average price that is almost one standard deviation higher than firms that source from only one district. The average price paid monotonically increases with the number of districts sourced from.[4]

Figure 2: Supplier characteristics by number of districts sourced from

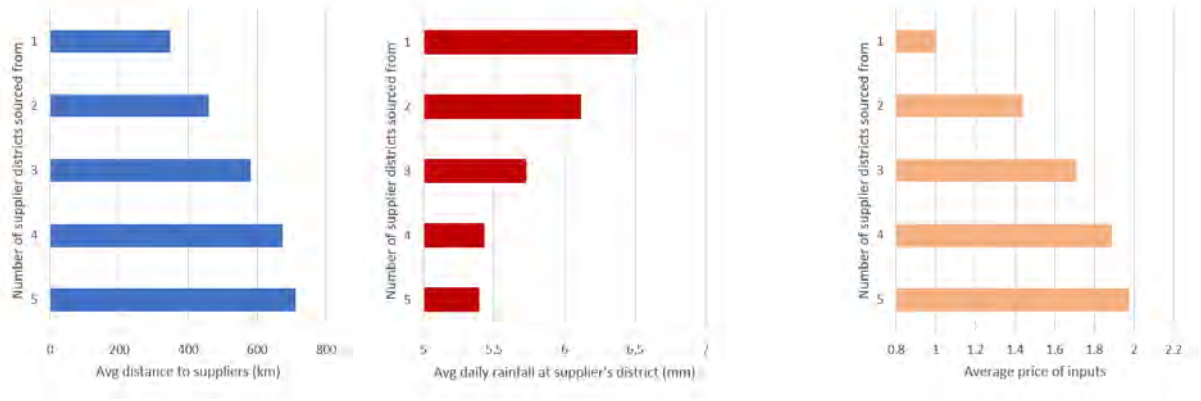

(a) Distance to suppliers (b) Average rainfall (c) Average price of inputs

Note. In the left panel, we compute the average distance between the firm and each of its suppliers from our transaction data. We then compute the average distance across firm-product pairs sourcing from 1 to 5 districts. In the middle panel, for each firm-product pair, we compute the average daily rainfall at each of the districts the firm sources from. Daily rainfall comes from the India Meteorological Department. We then compute the average across all firm-product pairs sourcing from 1 to 5 districts. In the right panel, we compute the average price paid for inputs for firm-product pairs sourcing from 1 to 5 districts. To construct our price index, we first run a regression of log prices on product fixed effects and take the residual. We standardize the residual and normalize it to 1 for firm-product pairs that source from only one district.

[3]To compute average prices, we first estimate a regression of log price on product fixed effects, and standardize the residual of such regression to construct our residual price index. We then normalize the average price for those firms that source from only one region to one.

[4]In Appendix Table A4, we show that these patterns are statistically significant, and remain so within product and controlling for buyer size and supplier size. In other words, the patterns are not driven by specific products, or by larger buyers, or by supplier capacity.

Fact 3: Supplier districts that face higher climate risk charge lower prices.

Figures 2b and 2c suggest that as buyers purchase from more suppliers, they source from regions with lower climate risk and pay higher prices. The flip side of this pattern is that suppliers in riskier areas might charge lower prices. To investigate this relationship further, we estimate a regression at the buyer (j) - supplier district (d) - product (p) level as in equation 1.

$$\begin{aligned}\log(\text{Price})_{j,d,p} = \alpha_1 \log(\text{Climate risk})_d + \alpha_2 \log(\text{Distance})_{j,d} + \alpha_3 \mathbb{1}(j \text{ in } d) + \\ \alpha_4 \mathbb{1}(j, d \text{ in same state}) + \gamma X_{d,p} + \delta_j + \delta_p + \epsilon_{j,d,p} ,\end{aligned} \tag{1}$$

where $\log(\text{Price})_{j,d,p}$ is the log of the average price charged to buyer j for product p by suppliers in district d. We control for the distance between j and d, indicators on whether the buyer is in district d or the same state as district d, and a set of controls at the product-supplier district level ($X_{d,p}$) such as the log size of all supplier sales from that district-product pair, and the log of the total sales from that district. We also include buyer and product fixed effects, so the identification of the climate variables comes from firms that buy from multiple districts. Additionally, we include covariates that aim to capture market power at the supplier district, such as the log of the total number of suppliers for a given product in the district, and the log of the largest supplier market share for that product in the district.

We consider two climate risk measures: the average daily rainfall for each district in 2019 and the historical river flooding in each district. Details on how these climate variables are computed can be found in Appendix D.1. As shown in Table 2, both climate measures are negatively correlated with prices. The magnitudes are robust to including additional controls at the supplier-district level. A 10% increase in rainfall in a district, is associated with suppliers in those districts charging 0.11% lower prices. Similarly, a 10% increase in riverine flooding levels in a district is associated with 2.55% lower prices charged by suppliers in that district. While these results cannot be interpreted as causal, they are suggestive that riskier areas charge lower prices.

2.3 Motivating Evidence: Event-Study Analysis

Our empirical evidence serves to motivate how firms adapt to varied probabilities of disruptions across space. However, it is also useful to understand how firms react to the *realization* of a disruption, to discipline the appropriate portion of the theory.

We proceed by documenting further motivating evidence on how firms respond to the incidence of climate-driven supply chain disruptions. We leverage the timing of these

Table 2: Correlation between price and supplier district climate risk

	$\text{Log (Price)}_{j,d,p}$	$\text{Log (Price)}_{j,d,p}$		$\text{Log (Price)}_{j,d,p}$	$\text{Log (Price)}_{j,d,p}$
$\text{Log(Avg Rainfall)}_d$	-0.0179***	-0.0112**	$\text{Log(Avg River Flooding)}_d$	-0.381***	-0.255***
	(0.005)	(0.005)		(0.026)	(0.026)
N obs	991,802	991,802	N obs	996,720	996,720
Additional controls	No	Yes	Additional controls	No	Yes

Note. *** $p < 0.01$, ** $p < 0.05$, * $p < 0.1$. We run a cross-sectional regression at the firm (j), supplier district (d), 8-digit product (p) level. The outcome is the log of the average price charged by suppliers in district d, to firm j for product p. The first and third columns control for log average distance between j and suppliers in d, a dummy variable for whether j is in district d, a dummy variable for whether j is in the same state as d, the log of total sales in product p from suppliers in d, the log of total sales of suppliers in d across all products, buyer fixed effects and product fixed effects. Columns 2 and 4 include additional controls for the log number of suppliers for product p in d and the log market share of the highest supplier in product p. Climate variables used are average daily rainfall in district in 2019 (left panel) and historical riverine flooding levels in district (right panel).

unexpected weather shocks to examine how sales and purchases change in the lead-up to and right after the shock. Our goal is to isolate the effect of the shock from other determinants that drive changes in sales and purchases.

Our event-study analysis allows us to examine pre-trends in the lead-up to the shock, and dynamics thereafter. The absence of pre-trends may provide suggestive evidence that our parallel-trends identification assumption is likely to hold, whereas the post-shock dynamics are informative of how long it takes for firms to recover after the flood. The shock responses will aid our quantification exercise in Section 4.2, as we will use the magnitude of the shock response to calibrate a parameter disciplining the severity of the incidence of a disruption.

First, we study how the shock directly affected suppliers in flood-hit regions. Then, we use the existing supplier network (in the pre-shock period) as a measure of the exposure to the shock, to study how buyers were affected when their suppliers were hit. Intuitively, we want to compare two firms that face the same trends in demand and productivity and only differ in the location of their suppliers. By comparing the observed disruptions of a firm whose suppliers were more exposed to floods with a similar firm whose suppliers were less exposed, we can isolate the impact driven by supply chain disruptions.

Effects on suppliers in flood-hit regions. We begin with documenting the direct effect on suppliers in flood-hit zones with the specification, where we examine outcomes $y_{j,t,k,\tau}$ for firm j, in period t, and industry k, measured in event-time (since flood) τ:

$$y_{j,t,k,\tau} = \sum_{x=-5}^{x=+5} [\alpha_x \mathbb{1}\left(\text{Exposed to flood}\right)_{j\tau} + \delta_{\tau,x} + \beta_x X_{j,\tau_0-1}] + \delta_j + \delta_{k,t} + \epsilon_{j,t,k,\tau}. \quad (2)$$

Here, the variable "Exposed to flood$_{j\tau}$" takes a value of 1 if firm j was exposed to a particular flood. We include a wide range of high-dimensional fixed effects to account for confounding shocks. These include firm fixed effects δ_j that control for firm-specific time-invariant differences; industry-by-time fixed effects $\delta_{k,t}$ that control for industry-specific shocks; and flood event-time since flood fixed effects $\delta_{\tau,x}$ that control for aggregate trends around the flood event that affect all firms (including those not in the flood-exposed areas). We also control for firm size-specific shocks, by controlling for purchases in the pre-period X_{j,τ_0-1}, interacted with time-since flood indicators. The sample consists of firms that had positive sales in the month before a flood.

Figure 3 plots α_x, which are time dummies that capture the differential impacts on firms that were directly exposed to the flood, relative to other (non-flood-hit) firms that had positive sales in the month before a flood. The figure shows a lack of meaningful pre-trends in the lead-up to the flood. After the flood, there is an immediate decline in sales of 0.11 log points, which worsens until two months after the flood. About two months after the flood, sales are about 0.25 log points lower than baseline sales. After the two-month slump in sales, there is a quick recovery, and four months after the flood, sales recover to what they were in the pre-period.

Figure 3: Sales of affected suppliers

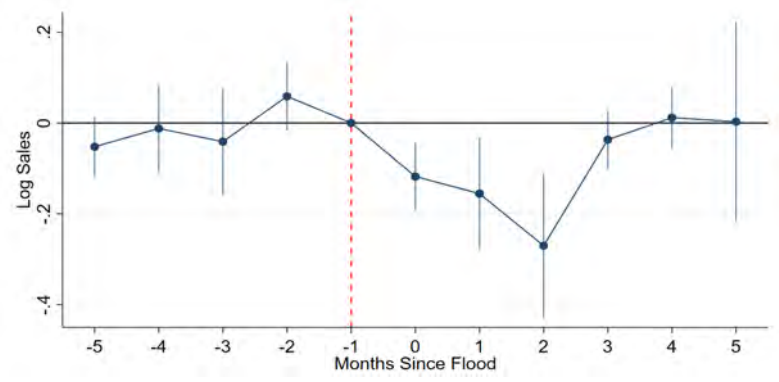

Note. Event-study specification documenting sales of firms that were exposed to floods in month= 0. The specification includes firm, time, event-time, and industry-real time fixed effects, and log pre-period sales-time controls. Standard errors clustered at the district level.

Effects on downstream firms. To examine how buyers are affected, we need to first define a buyer's exposure to the floods. We define a firm j's supplier exposure to be how exposed its suppliers were to the flood:

$$(\text{Supplier Exposure})_{j\tau} = \sum_{i}^{N} s_{i,j,\tau_0-1} \times \mathbb{1}\left(\text{Supplier } i \text{ exposed to flood in } \tau\right) \ ,$$

where s_{i,j,τ_0-1} is the value of purchases that firm j buys from firm i, relative to firm j's total purchases, just before the flood. The index, essentially, calculates the weighted average of the flood exposure of firm j's sellers. A higher value of the index implies firm j faces a higher "supplier-exposure," as a larger share of its purchases were coming from firms exposed to the flood. The exposure measure has a mean of 0.018 and standard deviation of 0.1.

With the help of this variable, we can now study the outcomes $y_{j,t,k,\tau}$ of downstream firms j in period t, industry k, and time-since flood τ:

$$y_{j,t,k,\tau} = \sum_{x=-5}^{x=+5} [\gamma_x \left(\text{Supplier Exposure}\right)_{j\tau} + \delta_{\tau,x} + \beta_x X_{j,\tau_0-1}] + \delta_j + \delta_{r,k,t} + \epsilon_{j,t,k,\tau}. \quad (3)$$

Once again, we control for firm-specific time-invariant factors δ_j; industry-by-district-by-time fixed effects $\delta_{k,r,t}$ that control for industry-by-region specific shocks; and flood event-time since flood fixed effects $\delta_{\tau,x}$ that control for aggregate trends around the flood event that affect all firms. X_{j,τ_0-1}, interacted with time-since flood indicators, controls for firm size-specific shocks.

Figure 4: Purchases and sales of downstream firms

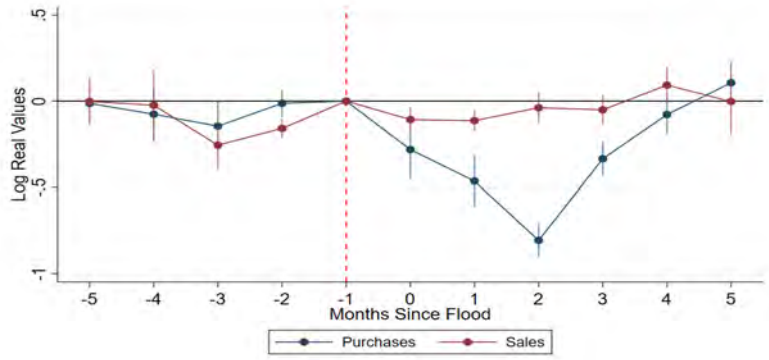

Note. Event-study specification documenting sales and purchases of downstream firms that were exposed to floods in month= 0. The specification includes firm, time, event-time, and industry-district-real time fixed effects, and log pre-period sales-time controls. Standard errors clustered at the district level.

Figure 4 plots coefficients γ_x, which are time indicators that capture the differential outcomes (sales or purchases) of downstream firms with higher supplier risk. Once again, the coefficients in the pre-periods do not display any meaningful trends, suggesting that perhaps high- and low-exposed firms had similar trends, at least in the pre-flood period.

Consistent with Figure 3, we find that purchases decline sharply for the first few months, and then start to recover. Purchases are the lowest at two months after the flood, dropping by 0.078 log points with respect to the baseline period, for every one standard deviation increase in the supplier exposure (SD of exposure is 0.1). Purchases recover to the pre-

period levels by four months after the flood. This pattern follows closely with what happens to sales for directly affected suppliers in Figure 3. We later revisit this estimate to set the parameters of the shock distribution in our model quantification, to generate the same response to the incidence of a disruption in the model that we estimate here.

Interestingly, however, Figure 4 also shows that the sales of downstream firms are relatively modestly affected and only decrease by 0.009 log points the month following the flood, for a 1SD increase in exposure. This rebounds quickly. Inventories of output or intermediate inputs could explain this divergence in the effects on output relative to inputs. Unfortunately, our data do not contain information on inventories, so we cannot empirically assess their role here. We develop a model extension in Appendix C.3, illustrating how intermediate input inventories can generate a divergence in the response of sales and inputs following a shock, consistent with the patterns here. Importantly, whether or not firms hold inventories matters for the sales impact of disruptions, but not for their incentives to diversify risk ex-ante, and therefore for the general equilibrium consequences of such diversification.

New suppliers vs. existing suppliers. Suppliers that are hit by temporary shocks may induce buyers to seek out new suppliers. We compare what happens to purchases from new suppliers and existing suppliers (traded in the last 3 months) in Figure 5 to examine this switching behavior. The blue line shows that, if anything, there is a temporary fall in purchases from new suppliers as well. There is, as expected, a meaningful fall in purchases from existing suppliers, which recovers strongly eventually. In general, buyers are unlikely to create new links, and they instead revert back to their existing suppliers after the shock abates. These patterns are consistent with evidence from the same context that highlights how buyer-supplier relationships are personalized as relationship-capital is important (Cevallos Fujiy et al., 2023), and as a result, firms are unlikely to switch to other suppliers in the face of temporary shocks (Cevallos Fujiy et al., 2021).

Products and prices. An advantage of our version of the firm-to-firm trade data is that it has detailed product codes and unit values. This allows us to examine product-specific trades and changes in prices as a result of upstream suppliers being exposed to a shock. We first transform the data to the buyer-by-product-by-time level. Figure 6a shows the results of shocks to upstream suppliers on the sales and purchases of downstream buyers. Our specification is similar to Equation 3, but with a product dimension that allows us to include event-time, industry-district-product-time, and firm-by-product fixed effects, along with controls for pre-period firm-by-product sales interacted with time indicators. Figure 6a shows similar patterns to before: downstream purchases fall, even as sales of downstream firms do not change substantially.

Figure 5: Purchases from existing or new suppliers

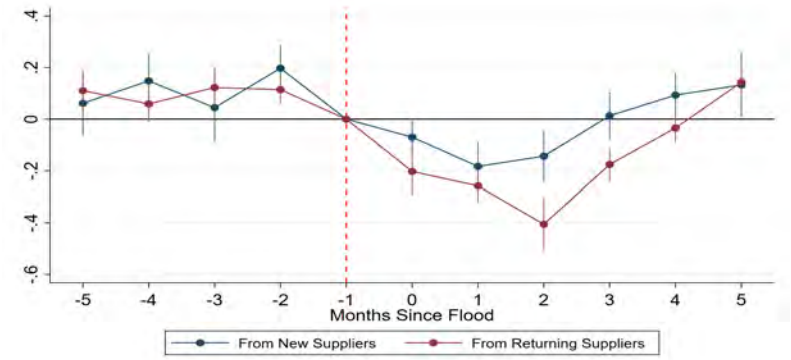

Note. Figures include firm, time, event-time, and industry-district-real time fixed effects, and demand controls and log pre-period purchases-time controls. Standard errors clustered at the district level.

Figure 6: Product-level trade and prices

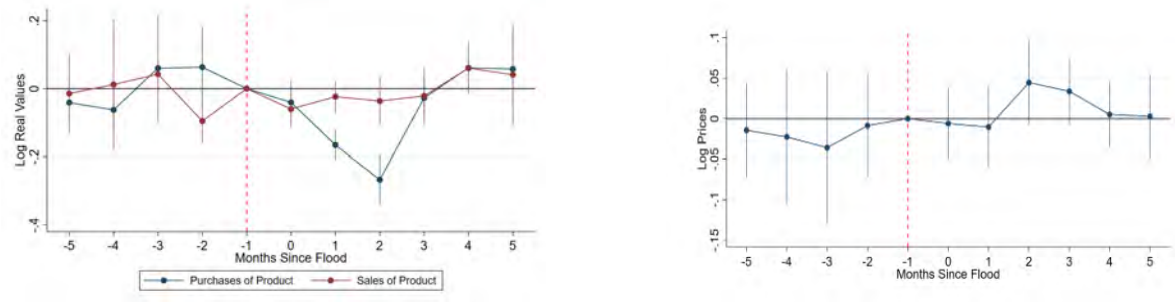

(a) Product-Level Purchases and Sales (b) Changes in Prices

Note. Figure 6a includes event-time, industry-district-product-time, and firm-by-product fixed effects, along with controls for pre-period firm-by-product sales interacted with time indicators. Figure 6b includes product-time, firm-product, and event-time fixed effects. Standard errors clustered at the district level.

In Figure 6b, we study the evolution of product-specific prices for transactions that occur around the flood. While noisier, there seems to be an increase in price levels two months after the flood, but they recover and return to the baseline levels four months since the flood event.

New advances in two-way fixed effects methods. Recent econometric advancements in two-way fixed effects methods point out that staggered treatment can lead to the negative weighting of certain disaggregated treatment effects (Goodman-Bacon, 2018). New methods developed by Borusyak et al. (2021); Callaway and Sant'Anna (2020); Sun and Abraham (2020) provide consistent and interpretable estimates. Yet, our setting offers some further challenges. Our "treatment" (index) is continuous, turns "off" and "on" and perhaps "on" again, and our specifications control for various time-varying covariates, and a wide variety of other fixed effects, making some of these new advances challenging to apply in our setting. A new Local Projections Difference-in-Differences (LP-DID) es-

timator developed by Dube et al. (2023) allows us to recover interpretable estimates in a flexible and efficient manner.

Figure 7: Linear Projection DID: Purchases for Buyers

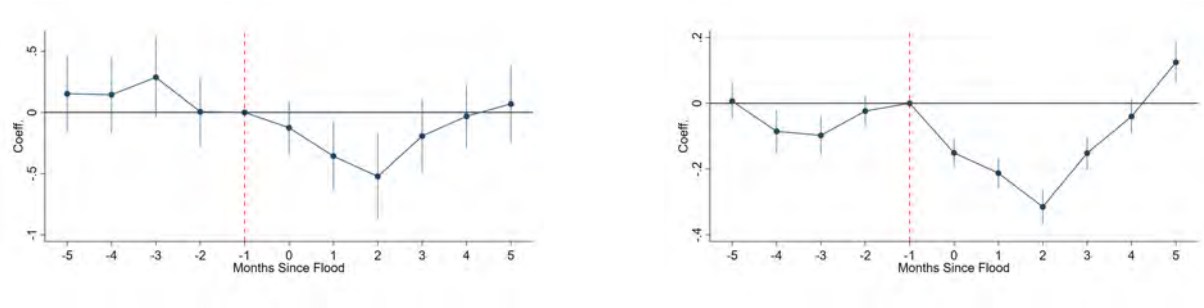

(a) LP-DID Continuous (b) LP-DID Discrete

Note. Specification includes firm, flood, and industry-district-month fixed effects. Controls include log pre-period purchases interacted with time indicators. Figure 7b discretizes the treatment variable, by being equal to 1 if more than 5% of weighted purchases were from affected suppliers. Standard errors clustered at the district level.

We present the results from this LP-DID estimator, which show similar patterns. In implementing this method, we need to take a stand on using the continuous treatment variable, or a more conventional discretized one. We first study purchases for buyers in Figure 7a using the continuous treatment variable. In Figure 7b, we discretize the treatment variable, and once again reproduce the same pattern as before: purchases fall for the first few months, and thereafter recover by month 4.

Figure 8: Linear projection DID: other outcomes

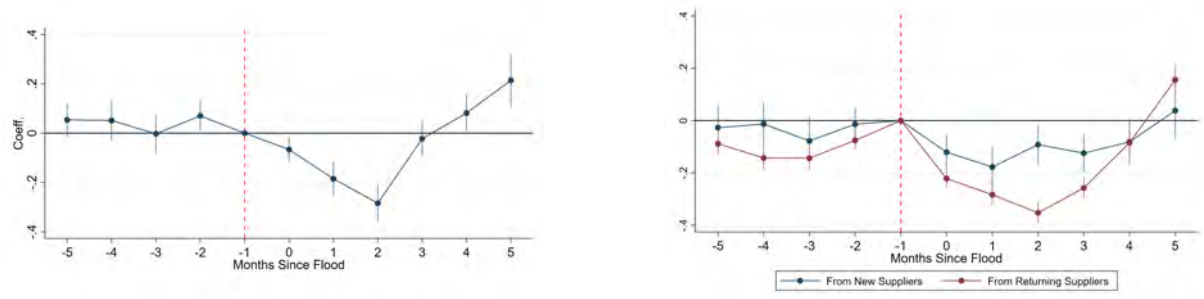

(a) Sales of Affected Suppliers (b) Buyer Purchases from Suppliers

Note. Figure 8a includes firm, flood, and month-by-industry fixed effects. Figure 8b includes firm, flood, and industry-district-month fixed effects. Controls include log pre-period purchases interacted with time indicators. Figures discretizes the treatment variable by being equal to 1 if more than 5% of weighted purchases were from affected suppliers. Standard errors clustered at the district level.

The results from the LP-DID method qualitatively resemble our main results for all other outcomes as well. Figure 8a shows the sales of affected suppliers, and Figure 8b contrasts existing vs. new suppliers. These patterns once again show that sales of affected suppliers fall, and that purchases from buyers decrease from both new and existing suppliers.

3 Model

This section develops a spatial general equilibrium model of firm sourcing under risk and performs comparative statics. Section 4 calibrates and quantifies the model. The model is static, as the rich geographic variation and a large number of locations is necessary for illustrating the diversification mechanism.[5]

3.1 Setting

The economy consists of I regions. Each region is endowed with L_i workers, a unit continuum of final goods producers who produce nontraded final goods, and competitive intermediate goods producers.

Timing. The model is static and consists of two stages. In the first stage, final goods producers in each location i place their orders for intermediate inputs from location j, M_{ji}. In the second stage, inputs are produced, sourcing disruption shocks are realized, and then inputs are delivered. Final goods firms choose their labor inputs and produce, households supply labor and consume, and all markets clear at equilibrium prices.

Households. The household in region i supplies labor L_i inelastically to firms in i and consumes a CES aggregate of the non-traded regional final goods q_i with elasticity of substitution $\sigma > 1$. It solves

$$\max_{q_i(\omega)} \left(\int_{\omega \in [0,1]} q_i(\omega)^{\frac{\sigma-1}{\sigma}} d\omega \right)^{\frac{\sigma}{\sigma-1}}$$

such that

$$\int_{\omega \in [0,1]} p_i(\omega) q_i(\omega) = Y_i \ , \tag{4}$$

where $p_i(\omega)$ is the price of final good $q_i(\omega)$, and Y_i is total income in region i. Our baseline model assumes labor is immobile across regions.

Intermediate goods producers. In each region, there are a continuum of competitive suppliers of tradable intermediate inputs M_i with production function $M_i = z_i \ell_i^M$, where z_i is their productivity. The price of intermediates in i is equal to their constant marginal cost, $p_i^M = \frac{w_i}{z_i}$, where w_i corresponds to the wages in that region.

[5] While the event studies illustrated short-lived dynamic responses to the incidence of shocks, a dynamic model with sufficiently rich geographic/locational variation is not currently tractable. Our emphasis is on understanding the steady state general equilibrium consequences of a distribution of risk across space, not on the reaction to the incidence of a disruption. That said, our model can be used to study the immediate ex-post response to the incidence of a disruption, as we do in Section 4.4. Given the short-lived responses in the data, we would not expect a significant role for additional dynamics here.

Let p_{ji}^M denote the price of intermediates from j used in i. We assume iceberg trade costs τ_{ji} between regions. No arbitrage in shipping implies that the price "at the factory gate" and the price at the time of intermediate usage are related by: $p_{ji}^M = \tau_{ji} p_j^M$.

Final goods firms. Each region i contains a unit continuum of homogenous final goods producers that produce differentiated varieties ω. Final goods are not tradable across regions. The constant returns to scale production function of the firms is

$$q_i(\omega) = \phi_i \ell_i(\omega)^{\beta} x_i(\omega)^{1-\beta} , \tag{5}$$

where ϕ_i is the productivity of final goods' producers in location i, $\ell_i(\omega)$ is the firm's labor input, and intermediates $x_i(\omega)$ can be sourced from each region $j \in I$ as perfect substitutes:[6]

$$x_i(\omega) = \sum_{j \in I} x_{ji}(\omega) . \tag{6}$$

Second stage. In the second stage, final goods firms have already placed their orders of intermediates $M_{ji}(\omega)$, shocks have been realized, and production takes place. The profit maximization problem of a final goods firm in i in the second stage is

$$\max_{q_i, \{x_{ji}\}_{j=1}^I, \ell_i} \left[Y_i \mathbb{P}_i^{\sigma-1} \right]^{\frac{1}{\sigma}} q_i(\omega)^{\frac{\sigma-1}{\sigma}} - w_i \ell_i(\omega) \tag{7}$$

$$\text{such that} \quad x_i(\omega) = \sum_{j \in I} x_{ji}(\omega) \tag{8}$$

$$x_{ji}(\omega) \leq \chi_j M_{ji}(\omega) \quad \forall\, j , \tag{9}$$

and the production function (5). Here, Y_i is income, and $\mathbb{P}_i$ is the price index in region i. $\chi_j \leq 1, j \in I$ are the shock realizations. We assume the shocks destroy some of the orders of inputs M_{ji} that have been placed in the region in the first stage, and so if a shock materializes, the firm receives fewer inputs than its order. This captures the notion of climate-associated shocks such as rainfall or floods, and we will calibrate the shock size to match our event study estimates in Section 2.3. We assume the stochastic shocks are origin-specific, and so they affect orders of inputs from all buying regions. As the shocks are not idiosyncratic, they will potentially affect aggregate outcomes.

Note that as second-stage profits (7) are monotonically increasing in input usage $x_i(\omega)$, the firm will always optimally use all available inputs that are delivered of its orders

[6] Alternatively, we could also use an aggregator of K varieties of inputs, where inputs of the different regions are perfect substitutes within a variety. For simplicity, our baseline model uses a single "variety" of input that can be sourced from multiple regions. Appendix F considers a CES aggregate of inputs.

$M_{ji}(\omega)$. In other words, Equation (9) will always hold with equality.

The first order conditions of the firm's second stage problem (7) pin down a firm's optimal choices of labor l_i, as well as its price p_i, quantity q_i, and profits π_i as a function of the vectors of first stage orders $\boldsymbol{M_i} = \{M_{ji}\}_{j=1}^{I}$ and origin-specific shocks, $\boldsymbol{\chi} = \{\chi_j\}_{j=1}^{I}$. In particular, the expression of profits for a firm in region i, suppressing the variety index ω for concise exposition, is:

$$\pi_i(\boldsymbol{M_i};\boldsymbol{\chi}) = \left[\frac{\sigma(1-\beta)+\beta}{\beta(\sigma-1)}\right]\left[\frac{\beta(\sigma-1)}{\sigma}\right]^{\frac{\sigma}{\beta+\sigma(1-\beta)}} w_i^{\frac{\beta(1-\sigma)}{\beta+\sigma(1-\beta)}} \left[\left[Y_i\mathbb{P}_i^{\sigma-1}\right]\phi_i^{\sigma-1}\left(\sum_{j\in I}\chi_j M_{ji}\right)^{(1-\beta)(\sigma-1)}\right]^{\frac{1}{\beta+\sigma(1-\beta)}}. \tag{10}$$

First stage. In the first stage, prior to the realization of shocks, final goods producers in all locations choose their orders M_{ji} of inputs to maximize expected profits. Firms have rational expectations and make their input sourcing decisions based on the true joint distribution of origin-specific disruption shocks, $G(\boldsymbol{\chi})$.[7] The firm's problem in stage one is

$$\max_{M_i\geq 0} \mathbb{E}_\chi\left(\pi_i(\boldsymbol{M_i};\boldsymbol{\chi})\right) - \sum_{j\in I} p_j^i M_{ji}\ , \tag{11}$$

where p_j^i is the order cost of inputs from j in i, and $\pi_i(\boldsymbol{M_i};\boldsymbol{\chi})$ is as in Equation 10. The first order conditions of this problem are

$$\mathbb{E}_\chi\left(\chi_j\Theta_i\left[\sum_{j\in I}\chi_j M_{ji}\right]^{\frac{-1}{\beta+\sigma(1-\beta)}}\right) \leq p_j^I \ \ \forall\ j\ , \tag{12}$$

where $\Theta_i = \left[\frac{(1-\beta)}{\beta}\right]\left[\frac{\beta(\sigma-1)}{\sigma}\right]^{\frac{\sigma}{\beta+\sigma(1-\beta)}} w_i^{\frac{\beta(1-\sigma)}{\beta+\sigma(1-\beta)}} \left[\left[Y_i\mathbb{P}_i^{\sigma-1}\right]\phi_i^{\sigma-1}\right]^{\frac{1}{\beta+\sigma(1-\beta)}}$ is a function of equilibrium aggregates that are potentially stochastic, as Y_i, w_i, and $\mathbb{P}_i$ might depend on the shock realizations across regions.

These first order conditions highlight that when placing an order for intermediate inputs of a given origin j, firms equate marginal benefits and marginal costs. Moreover, this optimality condition elucidates under which circumstances the firm does not source from a particular location. This occurs if the expected marginal benefit from placing an infinitesimal order in location j, with optimal orders elsewhere, is strictly smaller than its price, p_j^I.

[7] In our empirical implementation of the model, we assume that these shocks are binary, occurring with probability ρ_i in each location i. In our quantification of the model we permit spatially-correlated shocks. Note that we impose rational expectations. This is only necessary for our solution approach, the model can accommodate alternative belief structures.

Proposition 1 *Ex-ante profits are concave in orders of inputs M_{ji}.*

Proof. See Appendix C. ■

This property of the firm's problem is important for the firm's optimal sourcing strategy. Interestingly, it implies that the firms behave as if they are risk averse, even without explicit risk aversion in consumer or managerial preferences. In fact, firms are fundamentally risk-neutral. As a result, the "risk-aversion" through the concavity in profits will imply firms will optimally diversify sourcing locations.

Appendix F shows that the concavity of firm profits continues to hold with a CES aggregator of inputs.[8]

3.2 General Equilibrium

In the second stage, shocks are realized, inputs are delivered across regions, and all goods and labor markets clear. The labor market clearing condition for each region i is

$$\underbrace{L_i - \frac{\bar{M}_i}{z_i}}_{\tilde{L}_i,\text{ Final goods labor}} = \left[\frac{\beta(\sigma-1)}{\sigma}\frac{1}{w_i}\left[Y_i\mathbb{P}_i^{\sigma-1}\right]^{\frac{1}{\sigma}}\left(\phi_i\left(\sum_{j\in I}\chi_j M_{ij}\right)^{1-\beta}\right)^{\frac{\sigma-1}{\sigma}}\right]^{\frac{\sigma}{\beta+\sigma(1-\beta)}}, \tag{13}$$

where $\tilde{L}_i$ is the labor used in the production of final goods in i, and $\frac{\bar{M}_i}{z_i}$ is the labor used in the production of $\bar{M}_i = \sum_{j=1}^{J}\tau_{ij}M_{ij}$ intermediates to ship to all regions $j \in I$ from region i.

Goods markets clear in each region, implying that the region's income is equal to its expenditure

$$Y_i = w_i L_i + \hat{\Pi}_i\ , \tag{14}$$

where $\hat{\Pi}_i$ are the aggregate profits in i of the final goods firms as in Equation (7) less their intermediate goods order costs

$$\hat{\Pi}_i = \int \pi_i(\omega)d\omega - \int \sum_j p_{ij}^I M_{ij}(\omega)d\omega. \tag{15}$$

[8] With a finite elasticity of substitution, firms would choose to source from all locations, inconsistent with the data on sourcing shares. Here, the diversification motive would imply they source more at the intensive margin from each region. While our assumption of perfect substitutes in the input bundle is analytically convenient, estimates of input substitution elasticities are often low. With a low substitution elasticity, the CES aggregator features "dislike-for-variety." Allowing for an extensive margin of choosing the number of sourcing locations would imply that firms in a low-elasticity world would choose few sourcing locations. Observed multisourcing would then be driven by the diversification motive.

Notice that we assume firms pay for their orders of intermediate inputs, not for the fraction they receive after the shock. Additionally, Equation (13) implies that the full quantity of intermediates ordered in stage 1 is produced. This implies that the shocks "destroy" a fraction of produced inputs.[9]

Features of the equilibrium. As all firms in a region are homogeneous, under the unit mass of firms assumption, the regional price index $\mathbb{P}_i = p_i$, and aggregate profits $\hat{\Pi}_i = \hat{\pi}_i$. We can then characterize several features of the equilibrium.

Lemma 1 *Aggregate profits are a constant fraction of labor income* $\hat{\Pi}_i = \frac{1}{\sigma-1} w_i L_i$. *Further, aggregate expenditure on materials in* i *is given by*

$$\sum_j p_{ij}^I M_{ij} = \frac{(1-\beta)(\sigma-1)}{\sigma} Y_i. \tag{16}$$

Proof. See Appendix C. ■

These properties imply that aggregate income in location i is given by

$$Y_i = \frac{\sigma}{\sigma-1} w_i L_i, \tag{17}$$

and that the share of labor used in producing final goods in region i is constant

$$\frac{\tilde{L}_i}{L_i} = \beta. \tag{18}$$

Equation (18) has strong implications for equilibrium wages. In particular, equilibrium wages need to be such that the remaining workers are allocated to the intermediate inputs sector in stage 1.

Lemma 2 *Equilibrium wages* w_i *are deterministic.*

Proof. See Appendix C. ■

In the ex-post general equilibrium, the expression for Θ_i which is part of the marginal contribution to profits of a marginal unit of M_{ij} (Equation 7) is given by the following

[9] We do not observe actual contracts between firms in the data, so we have to make an assumption regarding what fraction of the orders of inputs are paid for. Our setup would remain tractable under alternative assumptions, e.g. only a fraction of the order is paid for upfront. While that would change the input costs entering Equation (11), it would not change the concavity of first stage profits in order costs, which is the key mechanism for firm input diversification in this framework.

expression

$$\Theta_i = (1-\beta) w_i L_i \left(\sum_{j \in I} \chi_j M_{ji} \right)^{-\frac{(1-\beta)(\sigma-1)}{\beta+\sigma(1-\beta)}}.$$

This implies that Θ_i is stochastic from the perspective of firms in stage 1. The only aggregate variable that is stochastic, varying with the realization of shocks, is the ideal price index, $\mathbb{P}_i$.

Ex-Ante General Equilibrium As pointed out above, the vector of nominal wages in each location is deterministic and determined at the first stage. Since aggregate labor demand by final goods' producers is a constant fraction of the labor endowment, $\tilde{L}_i = \beta L_i$, wages must be such that intermediate goods producers employ $(1-\beta)L_i$ workers in input production. In turn, due to the linear technology assumption, it must be the case that in equilibrium, the production of intermediates in each location is equal to $M_i = (1-\beta) z_i L_i$. In the equilibrium of this economy, the vector of wages,$\{w_i\}_{i=1}^I$, must be such that total demand from intermediate goods producers in each region exactly equals this amount.

From re-arranging the trade balance and the optimal total intermediates expenditure conditions, one can derive the following equilibrium system, which generates the equilibrium vector of wages,

$$w_j L_j = \sum_i w_i L_i s_{ji}(\{w_i\}_{i=1}^I) \;\; ; \;\; s_{ji}(\{w_i\}_{i=1}^I) = \frac{\frac{w_j \tau_{ji}}{z_j} M_{ji}(\{w_i\}_{i=1}^I)}{\sum_\ell \frac{w_\ell \tau_{\ell i}}{z_j} M_{\ell i}(\{w_i\}_{i=1}^I)} \;\; \forall \; j \in I,$$

where crucially, the matrix of sourcing shares defined by $\left\{ s_{ji}(\{w_i\}_{i=1}^I) \right\}_{i=1,j=1}^I$ is a function of the vector of wages, the parameters of the model and the probability distribution of the shocks.[10] This completes the description of the economy.

Welfare Agents' welfare is given by their expected consumption, which, is equal to the output of the final goods' producers and varies by region. In general equilibrium, the aggregate output of the final sector in region i, conditional on the available inputs, is given by

$$Q_i\left(\boldsymbol{M_i}; \boldsymbol{\chi}\right) = \phi_i \beta^\beta L_i^\beta \left(\sum_j \chi_j M_{ji} \right)^{1-\beta},$$

[10] Similar non-linear systems of equations in wages appear in several static trade models. Note that here, the system includes orders of intermediates M_{ij} which are also equilibrium objects and do not have a closed form solution.

and expected welfare becomes

$$\mathcal{W}_i = \mathbb{E}_{\boldsymbol{\chi}}\left[Q_i\left(\boldsymbol{M_i};\boldsymbol{\chi}\right)\right] = \phi_i \beta^{\beta} L_i^{\beta} \mathbb{E}_{\boldsymbol{\chi}}\left[\left(\sum_j \chi_j M_{ji}\right)^{1-\beta}\right]. \tag{19}$$

As it is clear from this expression for welfare, even though consumers are risk neutral, the sourcing strategy selected by the final goods producers has effects on their welfare. Consumer also benefit from some diversification in the firms' sourcing strategies. However, as this expression also shows, the curvature of this function with respect to the amount of inputs differs from the curvature in the firms' profit function, which was given by $\frac{(1-\beta)(\sigma-1)}{\beta+\sigma(1-\beta)}$. This discrepancy in curvatures causes a disagreement between consumers and firms in the optimal diversification. In particular, as we discuss in the next proposition, under the empirically relevant values for β and σ, the profit function is more concave than the welfare function.

Proposition 2 *If $\beta(\sigma-1) < 1$, expected welfare is less concave in the realizations of the disruptions, χ_j, than firms' profits.*

Proof. See Appendix C. ■

An implication of this difference of the concavity of welfare and of profits in terms of input orders is that consumers value that firms diversify when this diversification is cheap, in particular, when firms can import inputs from other regions at a low cost. However, when trade costs increase, consumers would prefer to have less costly goods than less volatility, although firms still have incentives to source from other regions. In terms of welfare, this makes consumers prefer autarky when trade costs increase, rather than having the likelihood of trading. We provide numerical evidence in a simplified setting for these countervailing forces in Appendix Figures A7 and A8.

3.3 A Two Location Example

To gain intuition, consider a simple case with two locations. Region 1 is risky and receives a shock $\chi_1 < 1$, with probability ρ, and region 2 is a safe location.[11] Additionally, there are no trade costs, and therefore, the optimal intermediate bundle chosen by firms is the same in both locations.

Notice that in equilibrium it must be that $p_1^I < p_2^I$, because otherwise, the safe location's input is unambiguously better than the input from the risky location, and the labor market will not clear in the risky location.[12]

[11] That is, $\mathbb{E}_{\chi}^1 = \rho\chi_1 + (1-\rho)$ and $\mathbb{E}_{\chi}^2 = 1$.

[12] The fact that in this simple case, we have an interior solution for firms in both locations does not

The optimal stage 1 sourcing choices of firms for firms from both regions $i \in 1, 2$ is

$$M_{1i} : \rho\chi_1\Theta_i^S \left[\chi_1 M_{1i} + M_{2i}\right]^{\frac{-1}{\beta+\sigma(1-\beta)}} + (1-\rho)\Theta_i^{NS}\left[M_{1i} + M_{2i}\right]^{\frac{-1}{\beta+\sigma(1-\beta)}} = p_1^I \tag{20}$$

$$M_{2i} : \rho\Theta_i^S \left[\chi_1 M_{1i} + M_{2i}\right]^{\frac{-1}{\beta+\sigma(1-\beta)}} + (1-\rho)\Theta_i^{NS}\left[M_{1i} + M_{2i}\right]^{\frac{-1}{\beta+\sigma(1-\beta)}} = p_2^I\,, \tag{21}$$

where $\Theta_i^S = \frac{(1-\beta)(\sigma-1)}{\sigma} Y_i \left(\chi_1 M_{1i} + M_{2i}\right)^{-\frac{(1-\beta)(\sigma-1)}{\beta+\sigma(1-\beta)}}$ and $\Theta_i^{NS} = \frac{(1-\beta)(\sigma-1)}{\sigma} Y_i \left(M_{1i} + M_{2i}\right)^{-\frac{(1-\beta)(\sigma-1)}{\beta+\sigma(1-\beta)}}$. As discussed above, Θ_i is stochastic, and depends on whether or not the shock materializes in region 1. Under the monopolistic competition assumption, all firms take these aggregates as given. Entering these shifters into the first order conditions of the firms, we can solve for optimal orders as a function of wages:

$$M_{1i} = \frac{(1-\beta)(\sigma-1)}{\sigma} Y_i \left[\frac{1-\rho}{p_1^I - \chi_1 p_2^I} - \frac{\rho}{p_2^I - p_1^I}\right] \tag{22}$$

$$M_{2i} = \frac{(1-\beta)(\sigma-1)}{\sigma} Y_i \left[\frac{\rho}{p_2^I - p_1^I} - \frac{(1-\rho)\chi_1}{p_1^I - \chi_1 p_2^I}\right]. \tag{23}$$

Let wages in the less risky region 2 be the numeraire. As intermediates are priced at marginal cost and from the labor market clearing condition (Equation 13), a constant fraction of labor is used in the production of intermediates, we can show that equilibrium wages in the risky region 1 are given by

$$w_1 = \frac{z_1}{z_2} \frac{z_1 L_1 \chi_1 + z_2 L_2 (1 - \rho(1-\chi_1))}{z_1 L_1 (\rho + \chi_1(1-\rho)) + z_2 L_2}. \tag{24}$$

Equation 24 shows that the nominal wage in the risky location relative to the safe one is a function of relative productivities, relative sizes, and the probability and magnitude of the shock. This wage is increasing in relative productivity and decreasing in relative population of location 1, and particularly relevant to our application, decreasing in both the probability and the magnitude of the sourcing disruption.

3.4 Comparative Statics

For a larger number of regions, the model does not have an analytical solution. Prior to a full calibration to districts in India in Section 4.2, we first illustrate the model's properties in a stylized 3-region setting.

To narrow the focus to the role of varied risk across space in firm sourcing decisions, we assume the regions are homogeneous in the productivity of their firms ϕ_i, their labor endowment L_i, and the productivity of their intermediate goods producers z_i. Trade is

need to hold in general when there are multiple locations and trade costs.

costly between regions and increasing in distance with elasticity 0.5. Finally, we assume that if a shock occurs, 90% of the inputs ordered are destroyed ($\chi = 0.1$).

We consider two situations. First, we look into the case where the three locations are equidistant from each other. Second, we allow for regions to also vary in their distance to each other. The results for the first scenario highlight how firms diversify their suppliers without the feature that some suppliers are closer than others. The second adds geography as an additional margin that affects input sourcing choices. For stark comparative statics, we place the three regions on a straight line. This allows for a possible trade-off between the diversification motive and higher trade costs of sourcing from farther regions. In some experiments, we also vary the probabilities of shocks across regions.

We consider five experiments. In the first, "no risk" experiment, we assume $\rho_i = 0$ for all regions. In the second, "homogeneous risk" case, we assume a constant shock probability across space. That is, we assume $\rho_i = 0.5$ for all i. In the third, "heterogeneous risk" scenario, we assume the shock probability varies across space, with the mean shock probability the same as the homogeneous risk case ($\frac{1}{I}\sum_{i=1}^{3}\rho_i = 0.5$). In the fourth, "heterogeneous risk in autarky" case, we raise trade costs to infinity, effectively prohibiting interregional input sourcing. In the fifth, "heterogeneous risk with free trade" case, we set trade costs to 0 across regions. The probabilities of shocks in cases four and five are the same as in the baseline heterogeneous risk case 3.

Case 1: No Risk. Figure 9 illustrates the sourcing shares and expected real wages when $\rho = 0$ for all regions. With identical fundamentals and positive trade costs, it is optimal for every firm to source all inputs domestically within its own region. This is true regardless of geography. Figure 9a illustrates the diagonal terms are 1, i.e., within-region sourcing shares are 1 for all regions, and cross-region sourcing shares are zero. The figure also makes clear that expected real wages are equalized across all regions under both geographies. This setting benchmarks our model relative to typical trade and spatial models where there is no sourcing risk. As all regions are identical and inputs are perfectly substitutable, there are no gains from trade, and the equilibrium is regional autarky. In particular, the contrast between equidistant regions and regions on a line does not change either sourcing shares or regional real wages. There is no role for geography in the equilibrium with no risk and positive trade costs.

Case 2: Homogeneous Risk. Figure 10 illustrates the bilateral sourcing shares when the risk of shocks in each region is $\rho = 0.5$. Firms now face a trade-off: as shocks are independent across regions, they can reduce the probability of input disruptions by sourcing from multiple regions. On the other hand, sourcing from other regions is costly, given trade costs. As a result, firms still largely source inputs from their own regions, but also

Figure 9: Scenario with no risk

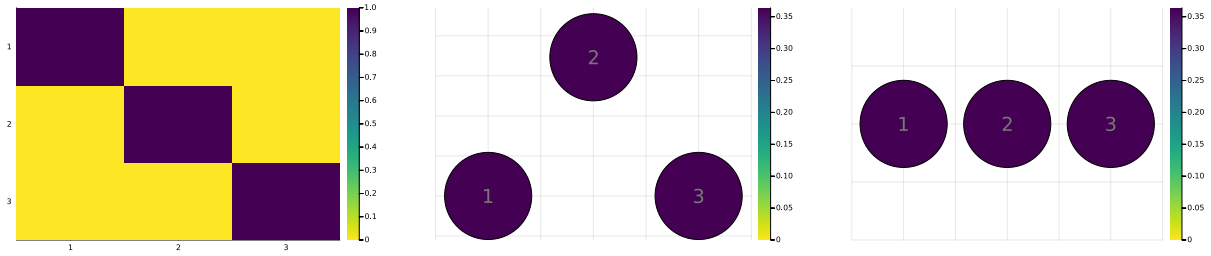

(a) Bilateral Sourcing Shares (b) Real Wages (c) Real Wages

Note. Panel A shows the 3x3 input-output matrix where the buying regions are in the vertical axis and the supplying regions are in the horizontal axis. Each row represents the share of inputs purchased by a buying region from each (column) supplying region. In the scenario with no risk, the sourcing shares in Panel A are the sourcing shares for the geographies in Panels B and C. Panels B and C present the real wages for each region, as well as a visual representation of the geographical location of regions in space. In Panel B, regions are equidistant from each other. In Panel C, regions are in a straight line, implying that the regions have different distances from each other.

diversify by sourcing some inputs from geographically closer regions where trade costs are lower. Panel B illustrates that this higher demand for inputs from more central regions in equilibrium results in higher expected real wages in these regions. These more central regions also diversify their risk the most by participating in interregional sourcing. Note that the expected price index in more central regions is therefore lower in equilibrium, as firms from these regions pay less in trade costs for inputs and better diversify risk. In contrast, Panel A shows that while firms diversify risk with some interregional sourcing, there is no geographic variation in expected real wages or in sourcing patterns with equidistant regions.

Case 3: Heterogeneous Risk. The left panels of Figure 11 illustrate the regional maps and the shock probabilities of each region in the heterogeneous risk case under both equidistant regions and heterogeneous distance. The middle panels show the bilateral sourcing shares between regions. The diagonal is again the darkest: in the presence of trade costs, all regions source most of their inputs from their own region despite heterogeneous risk. However, there is clear variation. Regions 1 and 3 (the safest regions), see the most "own sourcing." The riskiest region 2 diversifies the most, particularly when it is more geographically central. All regions source inputs from other regions, with relatively larger shares from those with low risk. Geography plays an important role too, with relatively more sourcing from risky region 2 when it is more central.

The right panels show that expected real wages across regions are negatively correlated with the risk of shocks, and are highest in safest locations despite identical regional fundamentals. The underlying mechanisms at work are that safer regions experience higher labor demand for their intermediate inputs from all regions, pushing up nominal

Figure 10: Scenario with homogeneous risk

Panel A: Same distance between regions

(a) Bilateral Sourcing Shares

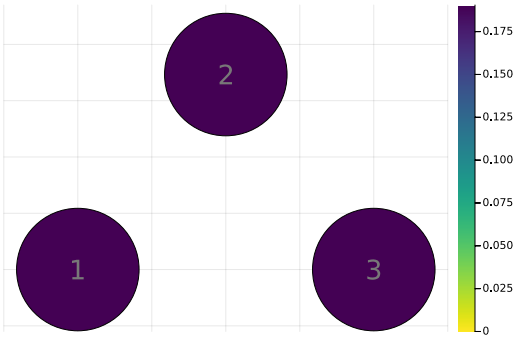

(b) Real Wages

Panel B: Different distance between regions

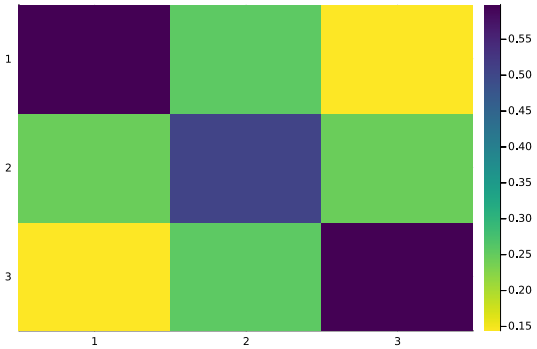

(c) Bilateral Sourcing Shares

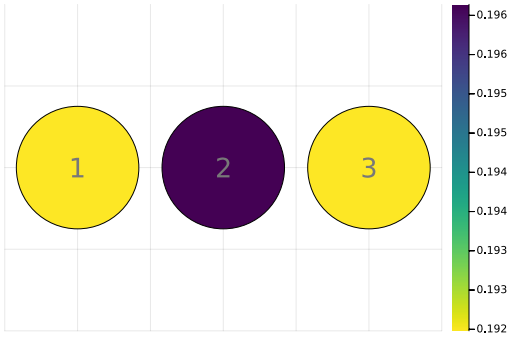

(d) Real Wages

Note. The figures in the left panel consist of a 3x3 input-output matrix where the buying regions are in the vertical axis and the supplying regions are in the horizontal axis. Each line represents the share of inputs purchased by a buying region from each supplying region (column). The figures in the right panels present the real wages for each region, as well as a visual representation of the geographical location of regions in space. In Panel A, regions are equidistant from each other. In Panel B, regions are in a straight line, such that the regions have different distances between each other. The scales are shown to the right of each figure.

wages. They also face a lower price index of their final goods, as they can source safer "domestic" inputs without paying trade costs. Notice that in general equilibrium, the wage impacts on riskier regions will modulate sourcing from them. As a result, when the regions are on a line and trade costs to the risky region are low, its equilibrium real wages are slightly higher than in the equidistant setting.

Importantly, under our assumption that inputs are perfect substitutes, and that regions have identical fundamentals, there is no source of traditional gains from trade either through comparative advantage or increasing varieties. The incentives for trade here arise entirely to mitigate risk, with strong spatial general equilibrium implications for wages and prices. We will return to this point below, when evaluating the welfare gains

Figure 11: Scenario with heterogeneous risk

Same distance between regions

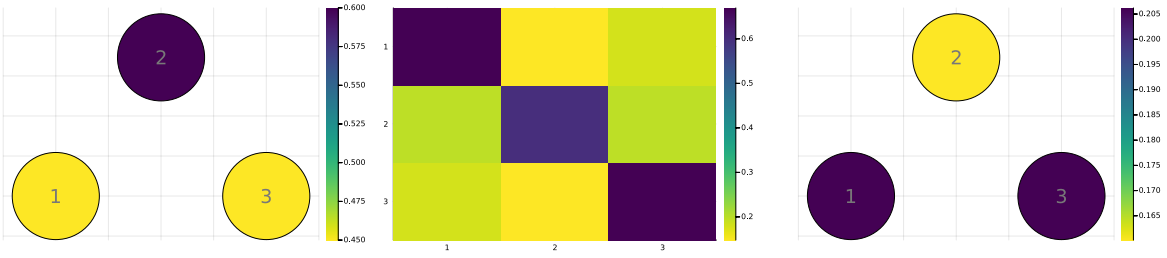

(a) Shock Probabilities (b) Bilateral Sourcing Shares (c) Real Wages

Different distance between regions

(d) Shock Probabilities (e) Bilateral Sourcing Shares (f) Real Wages

Note. The figures in the left panel show the probability that each region is hit by a shock, as well as a visual representation of the geographical location of regions in space. The figures in the middle panel consist of a 3x3 input-output matrix where the buying regions are in the vertical axis and the supplying regions are in the horizontal axis. Each line represents the share of inputs purchased by a buying regions from each supplying region. The right panels present the real wages for each region. For the top panels, regions are equidistant from each other. In the bottom panels, regions are in a straight line, such that the regions have different distances between each other. The scales are shown to the right of each figure.

from supplier diversification.

Comparison between homogeneous and heterogeneous risk cases. Figure 12 compares the expected real wages and their variance between the homogeneous and heterogeneous risk cases. The left panels show the ratio of expected real wages, and the right panels show the ratio of their variance. As is immediately clear, the riskiest region 2 has the largest declines in its expected real wages as we move from homogeneous to heterogeneous risk under both geographies, while the safest regions 1 and 3 have lower expected real wages under homogeneous risk. The right panels of the figure show that the safer regions see an increase in the variance of their expected real wages in the heterogeneous risk case relative to the homogeneous risk. This is despite their disruption probability decreasing when moving to heterogeneous risk. While they face less volatility from their own shocks, they diversify when risk is heterogeneous and source more from relatively riskier regions. The riskiest region 2 sees an decline in the variance of real wages when moving to heterogeneous risk, because it mitigates volatility by sourcing from safer regions. This decline is larger when region 2 is more central, and faces lower trade costs

for diversification.

Figure 12: Comparison between homogeneous and heterogeneous risk cases

Same distance between regions

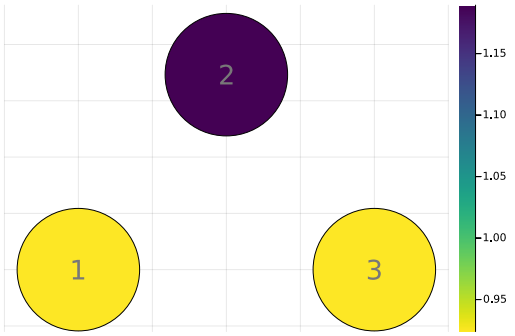

(a) Expected Real Wages Ratio

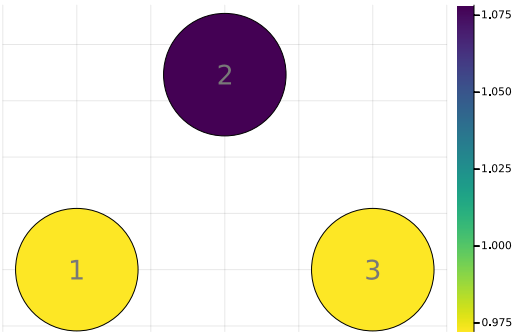

(b) Variance of Real Wages Ratio

Different distance between regions

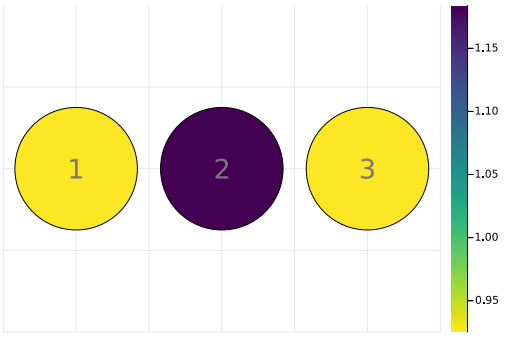

(c) Expected Real Wages Ratio

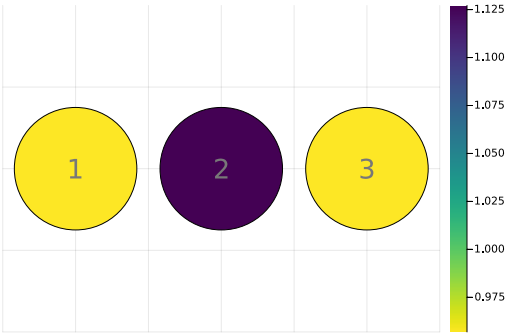

(d) Variance of Real Wages Ratio

Note. In this figure we plot the expected real wages (left panel) and variance of real wages (right panel) for the homogeneous case shown in Figure 10 relative to the heterogeneous case shown in Figure 11. The variance of real wages is computed across potential states of the world. For the top panels, regions are equidistant from each other. In the bottom panels, regions are in a straight line, such that the regions have different distances between each other. The scales are shown to the right of each figure.

Case 4: Heterogeneous Risk and Autarky. We next maintain the heterogeneous risk across regions but raise trade costs to infinity, shutting down inter-regional input sourcing. Figure 13 illustrates that while the probabilities of shocks remain the same as Case 3 above (left panel), bilateral sourcing mimics the no-risk Case 1 (middle panel). However, the impact on expected real wages is very different in both Case 1 and Case 3 (right panel). The riskiest region sees the lowest expected real wages, while the safest regions see the highest expected real wages, as they have the lowest expected prices due to the lowest shock probabilities and fully domestic sourcing. In Appendix C, we show that the expected real wage patterns are similar for equidistant regions, as with autarky, regional geography has no impact on regional outcomes.

Figure 13: Scenario with heterogeneous risk and infinite trade costs

Different distance between regions

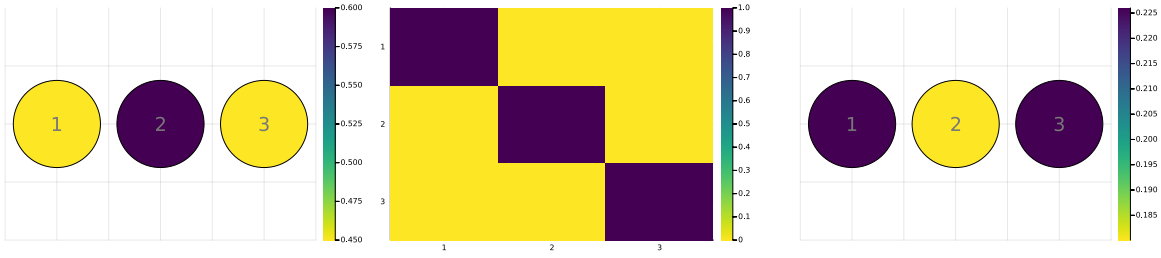

(a) Shock probabilities (b) Bilateral Sourcing Shares (c) Real Wages

Note. This figure presents the case where trade costs are set to infinity. The figures in the left panel show the probability that each region is hit by a shock, as well as a visual representation of the geographical location of regions in space. The figures in the middle panel consist of a 3x3 input-output matrix where the buying regions are in the vertical axis and the supplying regions are in the horizontal axis. Each line represents the share of inputs purchased by a buying regions from each supplying region. The right panel presents the expected real wages for each region. The scales are shown to the right of each figure. In this scenario, regions vary in their distance and are located on a line. The case with equidistant regions is shown in Figure A3.

Welfare comparison between costly trade and autarky with heterogeneous risk cases. We next consider how expected real wages change across regions moving from costly trade to autarky in Panel A, Figure 14. Interestingly, all regions see a decline in expected real wages moving to trade from autarky. The intuition is that in this setting, there are no "conventional" gains from trade, as there is no comparative advantage or gains from variety. The primary reason for trade here is for risk diversification. However, trade is costly, so the benefits of diversification are obtained at a higher average input price, raising regional price indices and lowering expected real wages under costly trade. The smallest decline in real wages is for the central high-risk region 2, which pays the least in trade costs for diversification. It also has the lowest expected real wages in both the costly trade scenario and autarky scenarios.

Notice that this stark example is dependent on the assumed distribution of disruption risk and trade costs. In Appendix Figures A7 and A8, we show that for low enough trade costs, trade can be welfare-improving relative to autarky. When disruption probabilities are higher, the range of trade costs for which trade is welfare improving relative to autarky increases. However, in general, costly trade, particularly with relatively high trade costs, is not always Pareto-improving relative to autarky, as was discussed in Section 3.

While the diversification motive for trade does not improve welfare as measured by the expected real wage in this comparative static, Panel B of the figure illustrates that the variance in real wages increases sharply, moving to costly trade from autarky for all regions. Supply chain diversification lowers the variance in final goods prices across all regions, insuring against shocks and real wage volatility. Again, the riskiest region 2

sees the largest increase in the variance of expected real wages when trade is barred. Appendix Figure A4 shows the same insight holds with equidistant regions: regional geography primarily modulates sourcing patterns via trade, but does not otherwise play a role in the mechanisms underlying the relative decline in real wages, given the disruption probabilities and trade costs, and increase in their variance moving from costly trade to autarky.

Figure 14: Comparison between heterogeneous risk under costly trade and autarky

Different distance between regions

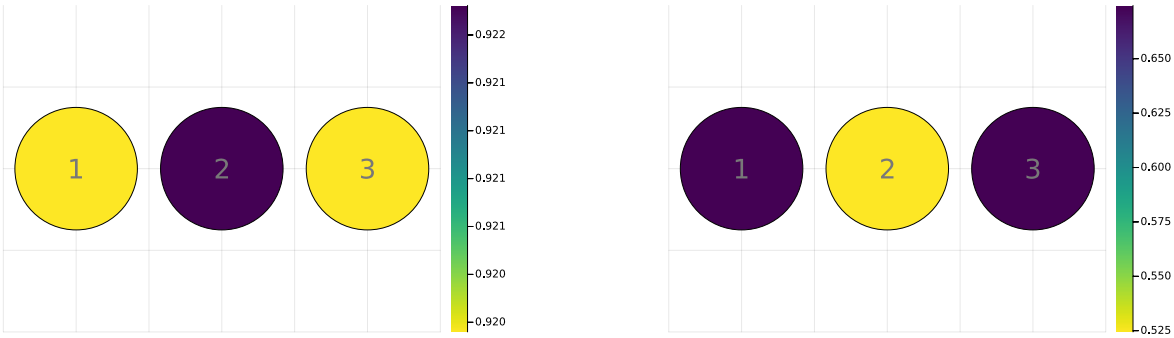

(a) Expected Real Wages Ratio (b) Variance of Real Wages Ratio

Note. In this figure we plot the expected real wages (left panel) and variance of real wages (right panel) for the scenario with heterogeneous risk and costly trade shown in Figure 11 relative to the scenario with heterogeneous risk and trade autarky shown in Figure 13. The variance of real wages is computed across potential states of the world. Here, regions are in a straight line, such that the regions have different distances between each other. The scales are shown to the right of each figure. The case with equidistant regions is shown in Figure A4.

Case 5: Heterogeneous Risk and Free Trade. Under free trade, firms can diversify their input risk at lower costs – the trade-off is only that inputs in lower-risk regions will be more costly in equilibrium as those regions will see higher expected real wages. With the same fundamentals across regions and free trade, in equilibrium, every firm in every region has the same optimal sourcing strategy. The middle panel of Figure 15 illustrates these sourcing shares. The left panel illustrates that sourcing concentrates in the safest location, regions 1 and 3, pushing up real wages there. Under free trade, regional geography plays no role in these patterns, and sourcing shares and expected real wages are the same as in this case when regions are equidistant (Figure A5).

Welfare comparison between costly and free trade with heterogeneous risk. Panel A of Figure 16 illustrates that in contrast to costly trade, all regions see higher expected real wages under free trade. This is due to the lower costs of inputs, both from risk diversification and the lack of trade costs. The largest increases in expected real wages moving from costly to free trade are in the risky region 2. This region sees

Figure 15: Scenario with heterogeneous risk and free trade

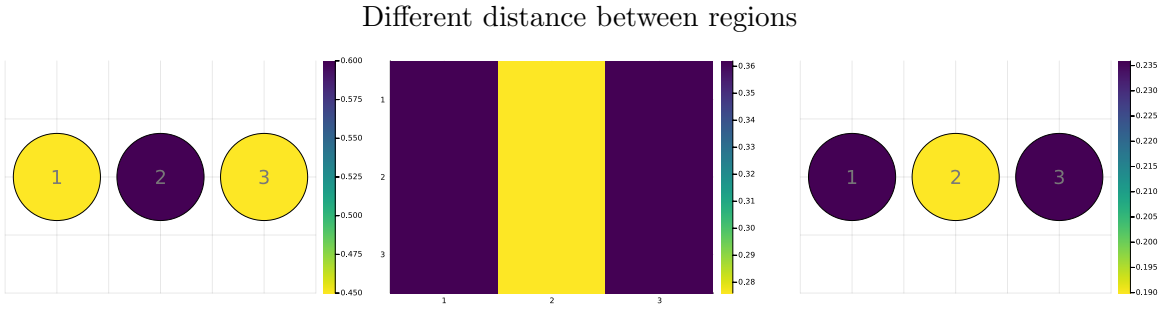

(a) Shock Probabilities (b) Bilateral Sourcing Shares (c) Real Wages

Note. This figure presents the case where there are no trade costs. The figure in the left panel shows the probability that each region is hit by a shock, as well as a visual representation of the geographical location of regions in space. The figure in the middle panel consists of a 3x3 input-output matrix where the buying regions are in the vertical axis and the supplying regions are in the horizontal axis. Each line represents the share of inputs purchased by a buying regions from each supplying region. The right panes present the real wages for each region. The scales are shown to the right of each figure. Figure A5 illustrates the case when regions are equidistant from each other.

increases in sourcing from all regions as firms no longer face high trade costs to access the region's higher risk inputs, and so its equilibrium wage does not need to decline as much as the case with costly trade. Panel B illustrates that moving from costly to free trade also lowers the variance of expected real wages across all regions. Thus, under free trade, there is no trade-off between higher expected real wages and lower volatility. Similar insights hold when regions are equidistant (Figure A6).

Figure 16: Comparison between costly and free trade

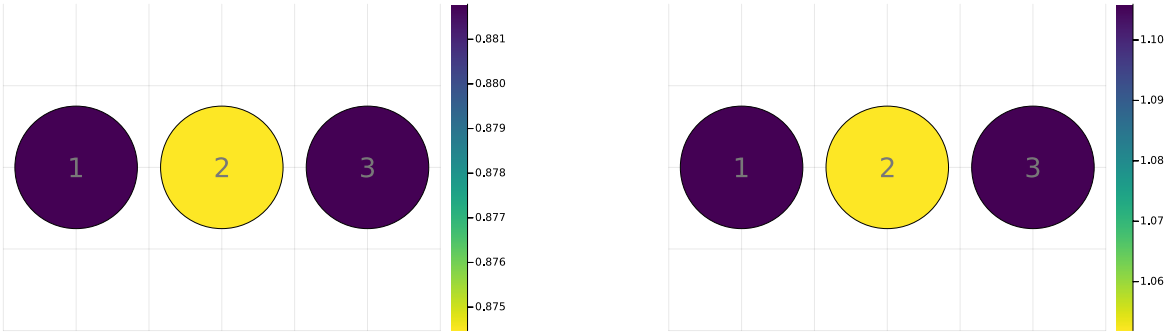

(a) Expected Real Wages Ratio (b) Variance of Real Wages Ratio

Note. In this figure we plot the expected real wages (left panel) and variance of real wages (right panel) for the scenario with heterogeneous risk and costly trade shown in Figure 11 relative to the scenario with heterogeneous risk and free trade shown in Figure 15. The variance of real wages is computed across potential states of the world. Here, regions are in a straight line, such that the regions have different distances between each other. The case with equidistant regions is in Figure A6. The scales are shown to the right of each figure.

4 Quantification

4.1 Solution Approach

The solution to the quantitative model introduced in Section 3 requires overcoming three computational challenges. First, the perfect substitutability across intermediate inputs from different origins, combined with the existence of trade costs, implies that the solution to the firms' sourcing problem may not necessarily be interior; that is, firms in some regions might find it optimal not to source intermediates from certain origins. Second, finding the solution to the firms' optimal sourcing problem involves computing a high-dimensional expectation over 2^I states of the world.[13] Third, the two challenges mentioned above are compounded by the need to find the equilibrium of the model, which essentially surmounts to finding the vector of wages for which all markets clear.

Given a vector of wages, $\{w_i\}_{i=1}^I$, and shock probabilities, $\{\rho_i\}_{i=1}^I$, we leverage the structure of the model to solve it efficiently. The first property of the problem described in Equation 11 is that the objective function is concave, and that the constraints are linear. Thus, any locally optimal point is also globally optimal, i.e., the Karush-Kuhn-Tucker (KKT) conditions are both necessary and sufficient for global optimality. These allow us to solve the firm's problem by combining the stationarity and complementary slackness conditions to find that at the optimum, the following condition:

$$\mathbb{E}\left(\chi_i \Theta_j \left[\sum_{i=1}^{I} \chi_i M_{ij}\right]^{\frac{-1}{\beta+\sigma(1-\beta)}}\right) M_{ij} = \frac{w_i \tau_{ij}}{z_i} M_{ij} \quad \forall\, i \in I,$$

which results from multiplying the first order condition in Equation 12 by M_{ji}. Then, we substitute for the general equilibrium object, Θ_j, to derive the following simplified expression:

$$(1-\beta) w_j L_j M_{ij} \mathbb{E}\left[\chi_i \left(\sum_{i=1}^{I} \chi_i M_{ij}\right)^{-1}\right] = \frac{w_i \tau_{ij}}{z_i} M_{ij} \quad \forall\, i \in I.$$

This system of I equations in I unknowns defines a nonlinear complementarity problem for which efficient numerical optimization routines exist.[14] Finally, we approximate the high-dimensional expectation by using simulations, effectively solving the following system

[13] There are more than 600 districts in India, but we group small contiguous districts to create 271 super-districts. We implement our model for the 271 super-districts, so that involves computing expectations over $2^{271} \approx 10^{82}$ states of the world.

[14] We solve this problem using the optimizer `PATH` implemented on `Julia` through the optimization modeling language `JuMP` (see, respectively, Ferris and Munson 1999, Bezanson et al. 2017 and Lubin et al. 2023).

of equations for each region:[15]

$$(1-\beta)w_j L_j M_{ij} \frac{1}{S}\sum_{s=1}^{S}\left[\chi_i^{(s)}\left(\sum_{i=1}^{I}\chi_i^{(s)}M_{ij}\right)^{-1}\right] = \frac{w_i\tau_{ij}}{z_i}M_{ij} \quad \forall\, i \in I.$$

The procedure described above yields a solution to the firms' sourcing problem given a vector of wages, $\{w_i\}_{i=1}^{I}$. To find the equilibrium wages, we manipulate the trade balance and the optimal total intermediates expenditure conditions to derive the following equilibrium system,

$$w_j L_j = \sum_i w_i L_i s_{ji}(\{w_i\}_{i=1}^{I}) \quad ; \quad s_{ji}(\{w_i\}_{i=1}^{I}) = \frac{\frac{w_j\tau_{ji}}{z_j}M_{ji}(\{w_i\}_{i=1}^{I})}{\sum_\ell \frac{w_\ell\tau_{\ell i}}{z_\ell}M_{\ell i}(\{w_i\}_{i=1}^{I})} \quad \forall\, j \in I,$$

where, the matrix of sourcing shares defined by $\left\{s_{ji}(\{w_i\}_{i=1}^{I})\right\}_{i=1,j=1}^{I}$ is a function of the vector of wages and the parameters of the model. The solution to the system of equilibrium conditions above finds the equilibrium wages conditional on a vector of probabilities, $\{\rho_i\}_{i=1}^{I}$. We describe how we calibrate these probabilities in the next subsection.

4.2 Calibration

We group the 600 districts in India into 271 super-districts by grouping contiguous low-population districts.[16] We calibrate our model to these 271 districts. To calibrate the model for India as a whole, we complement our transaction data with the Annual Survey of Industries (ASI), which is a nationally representative survey of manufacturing plants in India with more than ten employees. We primarily use the wave of 2006-7 since it is the latest year for which the ASI has publicly available data at the district level.

We need to calibrate the following parameters and moments: the demand elasticity (σ), the input disruption due to the shock (χ_j), labor endowments by district (L_i), regional productivities (ϕ_i), the labor share in the production function (β), iceberg trade costs (τ_{ij}), and flood probabilities (ρ_i).

First, we set the demand elasticity $\sigma = 2$ following Boehm et al. (2023) and choose the input disruption parameter χ_j to match the drop of 0.77 log points in buyer purchases as supplier exposure goes from 0 to 1, as estimated in our event study (Figure 4). Second, we use the ASI to obtain employment by district, which is our labor endowments L_i.

[15] In our estimation procedure and in the computation of counterfactuals, we use 10.000 simulations.

[16] We aggregate districts with fewer than 10000 manufacturing workers to a single district within a state, or merge them to neighboring larger districts in their own state. We present results with all districts in Appendix D.

To estimate productivities by district, ϕ_i, and the labor share β, we follow the literature on production function estimation and use the Ackerberg, Caves, and Frazer (2015) approach (henceforth ACF).[17] We use revenues as the dependent variable and labor, materials, and capital as the production function inputs. We implement the ACF procedure to estimate the production function parameters and the productivities.[18]

Panel A of Figure 17 illustrates the estimated variation in district-level productivities. From the ACF procedure, we also get the corresponding coefficients for labor, materials, and capital. The results are shown in the left panel of Table 3, where the materials share is 0.81, the labor share 0.17, and the capital share 0.08. We compute the labor share as $\beta = 1 - 0.81 = 0.19$. Since we do not have capital in the model, we think of the labor share as the share of capital-augmented labor, so we include both capital and wage expenses into the calculations.

Figure 17: Estimated productivities and disruption probabilities

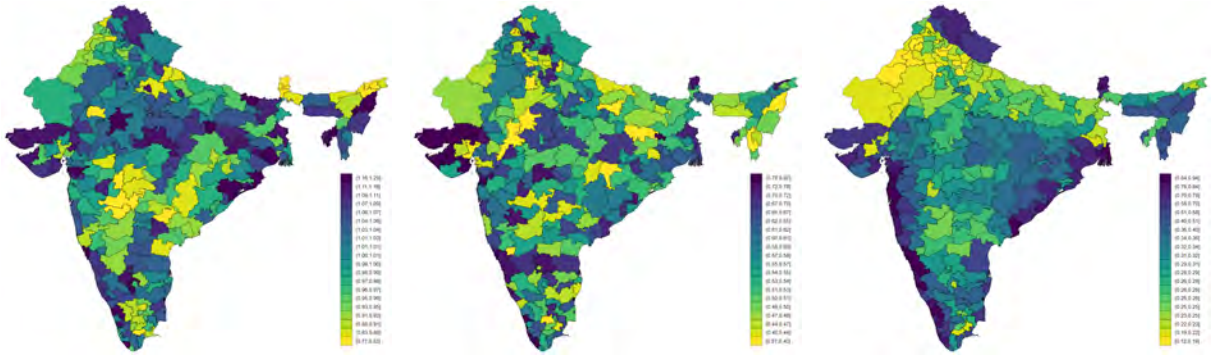

(a) Productivity (b) Model-Implied Risk Profile (c) Parameterized Risk Profile

Note. In this figure, we plot the estimated district-level productivities (left panel) and the model-implied district-level disruption probabilities (central panel). Productivities are estimated using the ACF procedure as described in the text. Baseline disruption probabilities are obtained by matching model-implied sourcing shares to the data as described in the text. The right panel plots the district-level disruption probabilities implied by the parameterized approach outlined in the text. The scales are shown to the right of each figure.

The iceberg trade costs τ_{ij} are estimated using our transaction data, leveraging our information on transaction-level prices. Our data is only available if one node of the transaction lies in one particular state, but we need to back out trade costs for each bilateral pair of districts throughout India. To address this, we proceed in two steps. First, we use our

[17] This approach requires lagged values of labor and materials as instruments, and we need a panel of firms. However, the public version of the ASI is a cross-section of plants which prevents constructing a firm-level panel. As a solution, we use the waves for 2004-05, 2005-06, and 2006-07 to construct a synthetic panel at the industry-district level. We then treat each industry-district pair as a "firm" for the purposes of estimation.

[18] Once we back out the ACF productivity for each industry-district pair, we aggregate at the district level by using weights based on the relative importance of each industry in each district. In the few cases where productivity cannot be estimated due to missing data for smaller districts, we assign those regions the average productivity of their closest neighbors.

transaction data, focus on firms in our state that sell their goods, and aggregate the data at the seller-buyer-product-time level. We then estimate Equation 25.

$$\log(p_{s,b,t,q}) = \gamma_1 \log(\text{distance from } s \text{ to } b)_{s,b} + \gamma_2 \mathbb{1}(b \text{ in same state as } s)_{s,b} + \gamma_{s,q,t} + \epsilon_{s,b,t,q}, \tag{25}$$

where $p_{s,b,t,q}$ is the price charged by seller s to buyer b for product q at time t. For each buyer-supplier pair, we compute the log distance between them as reported in our transaction data. We also include a dummy variable on whether the buyer (b) is in our state. The coefficient on distance captures how prices charged change as distance increases. Importantly, we add seller-product-time fixed effects, so effectively, the coefficients γ_1 and γ_2 are being identified by sellers that sell the same product to multiple buyers in a given time period. Since we are doing this within seller-product-time, the estimates are not driven by firm-level shocks such as productivity that might also affect prices. The results of this regression can be found in the right panel of Table 3.

Table 3: Estimation results

Panel A: Production Function Estimation		**Panel B:** Trade Costs Estimation	
	log(Sales)		log(Price$_{s,b,t,q}$)
log(Materials)	0.81***	log(distance from s to b)	0.0174***
	(0.076)		(0.0001)
log(Workers)	0.17***	$\mathbb{1}(b$ in same state as $s)$	-0.086***
	(0.061)		(0.0001)
log(Fixed Capital)	0.08		
	(0.063)		
Number of Observations	9128	Number of Observations	65,477,898

Note. *** $p < 0.01$, ** $p < 0.05$, * $p < 0.1$ Panel A presents the results of the production function estimation using the ACF procedure. The reported coefficients are for log materials, log number of workers, and log fixed capital as calculated from the ASI. Panel B presents the results for the trade costs estimation using our transaction data. The outcome is the log price charged by a seller in our state (s), for a given product (q), to a buyer (b) in a given month-year period (t). The main regressors are log distance from buyer to seller and a dummy that takes the value of 1 if the buyer is in the same state as the seller. We control for seller-product-time fixed effects.

Second, we use the estimated coefficient to predict trade costs for the rest of India. We compute bilateral distances between the centroid of each district and use those distances to predict trade costs between regions using the estimated coefficients $\hat{\gamma}_1$ and $\hat{\gamma}_2$. We assume that the border effect estimated through coefficient $\hat{\gamma}_2$ is the same for all states.

Disruption probabilities. Our model implies that bilateral sourcing shares are pinned down by district fundamentals like productivities and labor force, and bilateral trade costs, in addition to the vector of district-level shock probabilities. Therefore, we can obtain the vector of shock probabilities, ρ_i, by minimizing the distance between the observed

sourcing shares in the data with those implied by the model. Importantly, in estimating the probabilities, we allow for spatial correlation in the realization of disruptions, as floods or other disruptions might affect more than one district.[19]

The intuition of the exercise is as follows: conditional on the rest of the parameters and moments of the model, we pick the shock probabilities of each district to minimize the distance between the model-implied shares with the observed shares of purchases from every district in our state to each other district in India. This is our baseline approach, as it allows us to remain agnostic on the sources of risk in the model. Instead, we can validate our model by projecting the shock probabilities on plausible sources of risk. Panel B of Figure 17 plots the baseline disruption probabilities by district. To illustrate the spatial correlation in disruption probabilities, Figure 18 illustrates the likelihood of disruptions in other districts when either Ahmadabad (Panel A) or Kolkata (Panel B) sees the incidence of a shock. As an alternative approach, we also parameterize regional risk as a function of observables, and estimate the parameters of this function, as described below.

Figure 18: Correlation in Disruption Realizations: Ahmadabad and Kolkata

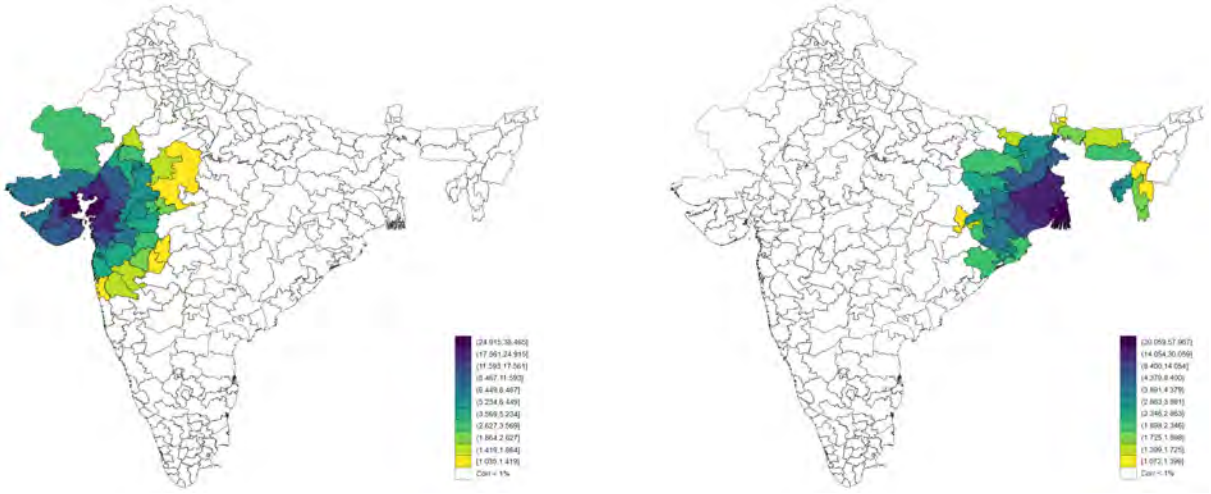

The underlying assumption of our baseline approach is that anything that is not captured by the district-level productivities and trade costs is part of the risk of the district. Of course, in practice, such residuals do not only include flooding risk, but also many other risk components. However, in Figure 19 and Appendix Figure A11, we show that our estimated probabilities are significantly correlated with observables related to historical and projected flood risk such as average rainfall, coastal flooding, and riverine flooding,

[19] We assume that these disruptions are generated by a binary random variable that is equal to 1 whenever a Normal latent variable with mean 0 and standard deviation 1 is below a threshold equal to $\Phi^{-1}(\rho_i)$, where Φ^{-1} is the standard normal inverse CDF. We allow these latent variables to be correlated across regions where the correlation in the realizations between region i and region j is equal to $e^{-\zeta Dist_{ij}}$, where ζ is a measure of spatial decay in this correlation. We estimate ζ in the same routine as the probabilities, ρ_i.

as well as with average temperature.

In Table 4, we run pairwise regressions of the model probabilities on the climate variables (historical and projected 2050) as well as other variables that could also be related to risk. Interestingly, besides the climate variables, a few other variables are significantly correlated with the risk probabilities. We also consider court congestion, terrain elevation and ruggedness, and nightlights luminosity as alternative measures. Court congestion and ruggedness are associated with increased disruption probability, while nightlights are uncorrelated with the estimated probabilities. In Appendix Table A5, we present the full regression of probabilities on all observables. Finally, in Figure A10, we show that these probabilities do not show a strong correlation with either productivities, nor the average distance to the state of our study.

Figure 19: Model probabilities and Historical Observables

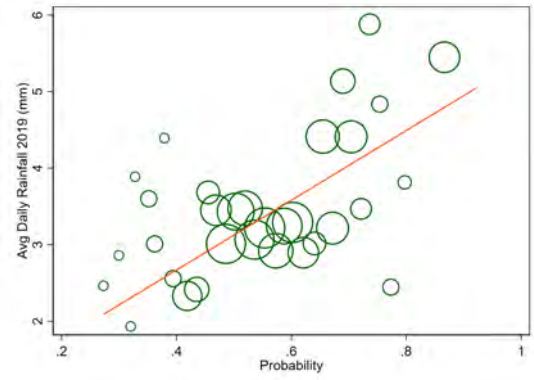

(a) Daily Rainfall - Historical

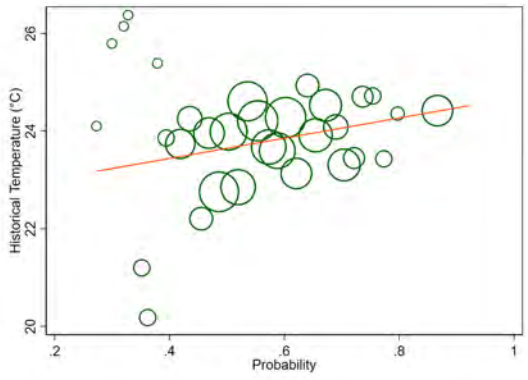

(b) Average Temperature - Historical

.

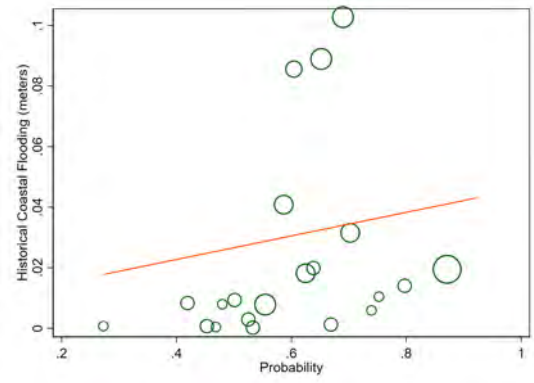

(c) Coastal Flooding - Historical

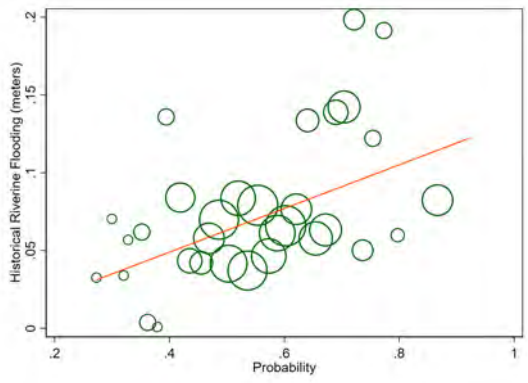

(d) Riverine Flooding - Historical

Note. In this figure, we plot the estimated probabilities against climate observables. In Figure 19a, we correlate the probabilities with the average daily rainfall in 2019. In Figure 19b, we correlate the probabilities with average temperature. Figures 19c use historical coastal flooding, while Figure 19d correlate the probabilities with historical riverine flooding, respectively. A more detailed definition of each of the variables can be found in Appendix D.2.

Table 4: Pairwise regressions between model probabilities and observables

	Log daily rainfall (historical)	Log daily rainfall (projected 2050)	Log coastal flooding (historical)	Log coastal flooding (projected)	Log riverine flooding (historical)	Log riverine flooding (projected 2050)
Log(Probabilities)	0.0298***	0.0140***	0.0096*	0.0097**	0.0069**	0.0067**
	(0.0081)	(0.0047)	(0.0018)	(0.0018)	(0.0031)	(0.0026)
N obs	271	271	271	271	271	271
R2	0.048	0.032	0.098	0.101	0.018	0.024

	Log avg temperature (historical)	Log avg temperature (projected 2050)	Log avg nightlights luminosity	Log avg elevation	Log avg ruggedness	Log avg court congestion
Log(Probabilities)	0.0585*	0.0543*	-0.0003	-0.0105**	0.0139*	0.0709*
	(0.0332)	(0.0316)	(0.0041)	(0.0042)	(0.0079)	(0.0368)
N obs	271	271	271	271	271	271
R2	0.011	0.011	0.000	0.023	0.011	0.014

Note. *** $p < 0.01$, ** $p < 0.05$, * $p < 0.1$ We run pairwise regressions of the model probabilities on observables. Each of the columns in the table shows the regression coefficient of the different variables. Probabilities and observables are logged. A more detailed definition of each of the variables can be found in Appendix D.2.

Notice that this exercise requires solving jointly for the vector of district-level risk that minimizes the gap between model-implied sourcing shares and data, as all bilateral sourcing shares are equilibrium objects that depend on the fundamentals and risk of all other districts. Further, we cannot exactly match all bilateral sourcing shares in the data, as we choose a single shock probability for each district, but we observe multiple sourcing shares for that district from all districts in our state. We, therefore, set up a Minimum Distance Estimator, which aims to match the average sourcing shares for each origin district observed across all destination districts in our data. In practice, we also are able to match all the bilateral sourcing shares in the data well, as Figure 20 shows. As external validation, the right panel of Figure 20 shows that our model also matches the data on sales shares well, which are untargeted moments.[20]

Robustness Our baseline approach has the benefit of remaining agnostic about the sources of disruptions firms face. However, it requires estimating a disruption probability for each district, which is a large number of parameters. As an alternative, we assume that the disruption risk in each district is a function of observables, including the climate and alternative variables in Table 4. We then estimate the coefficients of this function to minimize the distance between model-implied and observed sourcing shares. This has the advantage that we restrict the number of parameters to be estimated to 10. However, as we do not observe all sources of disruptions, there will be more unexplained variation. Panel C of Figure 17 illustrates district-level disruption risk implied by this approach. Unsurprisingly, as the observable risk measures were correlated with the "agnostic" risk from

[20]While our estimated probabilities might seem high, as discussed above, they capture several sources of risk. Further, available evidence from Indian businesses suggests that supply chain disruptions are a key concern. For instance, PwC's 26th Annual Global CEO Survey in late 2022 found that 50% of India CEOs were concerned about supply chain disruptions (https://www.pwc.in/assets/pdfs/research-insights-hub/immersive-outlook-3/paradigm-shift-in-supply-chain-management.pdf).

our baseline approach, the results of the parameterized approach are also correlated with our baseline. Appendix E outlines this approach in more detail, provides the estimated coefficients, and presents all our quantitative results under this alternative approach. Our main conclusions remain unchanged.

Table 5 summarizes our model calibration.

Table 5: Calibrated moments

Parameter	**Source**
L_i: Labor endowments	Annual Survey of Industries (ASI), 2019-20
ϕ_i: Region productivities	Ackerberg et al. (2015) estimation (ASI, 2004-2007)
τ_{ij}: Iceberg trade costs	Regression of within firm-product price on distance between buyer and seller (Transaction data)
ρ_i: Flood probabilities	Model inversion using sourcing shares across districts (Transaction data)
χ_i: Flood shock	Match drop in buyer purchases from event study (Transaction data)
β: Labor share	0.19: Ackerberg et al. (2015) estimation (ASI, 2004-2007)
σ: Demand elasticity	2: Based on (Boehm et al., 2023)

Figure 20: Sourcing shares: Model vs. Data

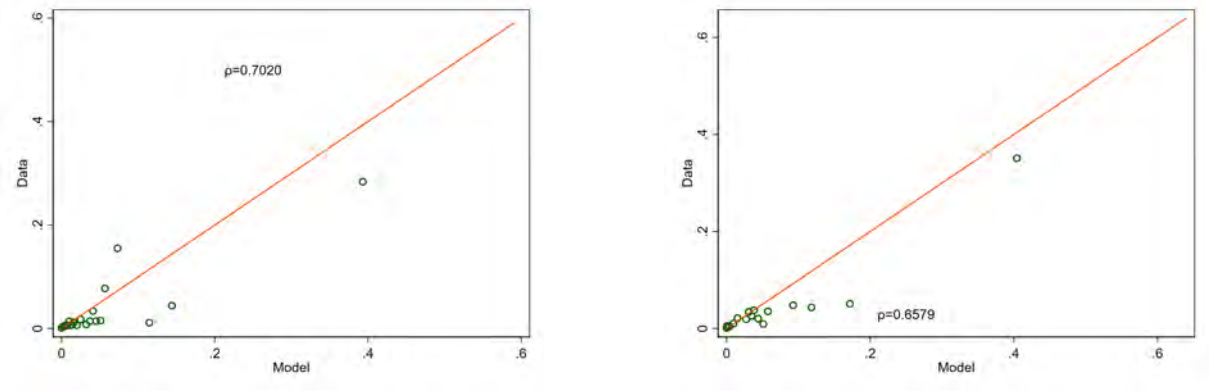

(a) Input Shares (b) Output Shares

Note. In this figure, we plot the sourcing shares in the data against the model. The red line is a 45-degree line. In the left panel we plot the input sourcing shares. We target average sourcing probabilities from our state's districts to the rest of the districts, but we do not force anything to match the particular sourcing shares of each district. The left panel plots each individual district's input shares. The right panel shows sales shares, which are entirely untargeted.

4.3 Quantitative Results

We begin by showing that the model delivers a strong negative relationship between shock probabilities and relative nominal wages (and real wages) in the cross-section. Figure 21 shows that both nominal and real wages are negatively correlated with shock probabilities, as we would expect. In Figure A12, we also show that the price index and the variance in real wages are negatively correlated with the shock probabilities.

Figure 21: Shock probabilities and wages

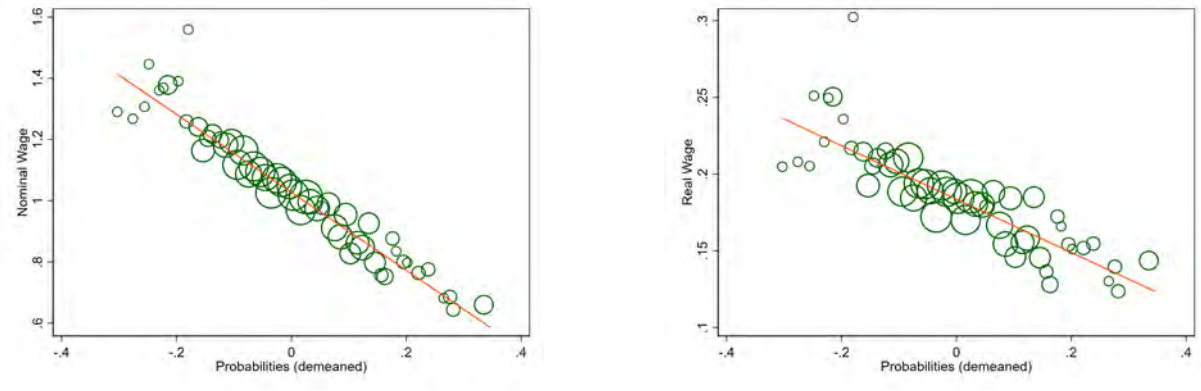

(a) Nominal Wages (b) Real Wages

Note. In this figure, we plot model-derived nominal (left panel) and real wages (right panel) against the estimated shock probabilities. Figure A12 further plots the price index and the variance in real wages against the shock probabilities.

Probabilities and sourcing shares. To illustrate the rich heterogeneity in bilateral sourcing patterns in the quantitative model, we show the sourcing choices of two districts in Figure 22. The left panel illustrates the sourcing patterns of Ahmadabad, a relatively low-risk district. The right panel shows the sourcing shares chosen by Kolkata, a high-risk district. In both districts, firms diversify, but sourcing strategies depend on geography – they source more from relatively geographically closer areas than, say, the far south of India. Diversification also depends on the risk profile of the origin district – for Kolkata, the model implies the district's firms choose more interdistrict sourcing to mitigate risk. In fact, Ahmadabad's own-district sourcing share is 42.8%, while Kolkata's largest sourcing share is own-district sourcing of 29.8%. Sourcing is not purely determined by proximity, and also depends on the spatial correlation of disruptions with the own district. Comparing these patterns to Figure 18, both districts clearly source from districts less spatially correlated with themselves as well. Notice that the sourcing patterns for both districts imply several zeros (our solution algorithm permits zero sourcing shares in equilibrium, as discussed in Section 4.1). In Appendix Figure A13, we show that under free trade, the sourcing patterns for all regions are identical, and each region sources from districts all over the country.

Figure 22: Ahmadabad sourcing, Kolkata sourcing

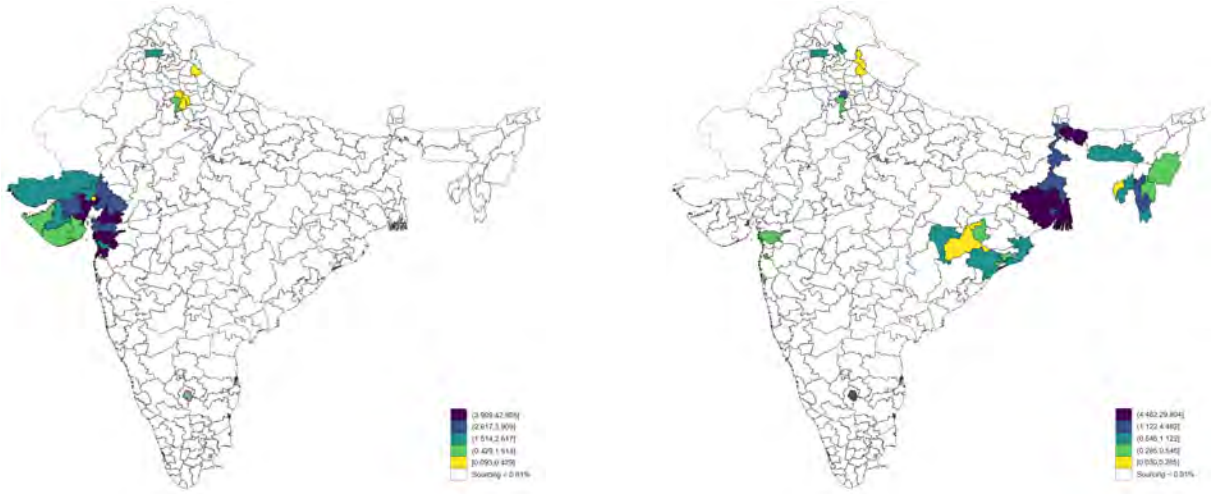

Expected real wages under baseline and autarky. The comparative statics in Section 3 show that with identical regional fundamentals, calibrated trade costs, and independent disruption probabilities, expected real wages are lower for all regions with costly trade than in autarky. To assess whether this mechanism is quantitatively relevant in the calibrated model with varying regional fundamentals, estimated trade costs, and disruption probabilities that are spatially correlated, we compute the difference in expected real wages in the baseline model with the model-implied expected real wages given the same regional fundamentals, disruption probabilities and infinite trade costs.

Figure 23 illustrates the spatial variation of expected real wages in the baseline model and in the autarky counterfactual. On average, expected real wages are 3.22% higher in autarky than in the baseline model. However, 1.12% of districts have lower expected real wages. The variance of real wages is 113.02% higher in autarky than in the baseline model, validating the quantitative relevance of the main comparative statics exercises.

The quantification clarifies where the deviation from the stark comparative statics result with identical fundamentals arises. The regions that see welfare gains in autarky relative to costly trade are those that have relatively lower risk and high productivity, leading to high equilibrium expected real wages under both trade and autarky. These regions do not benefit much from diversification of their own risk, as they are lower risk.

With costly trade, there are two opposing effects. Diversification by riskier districts pushes up the nominal wages in these districts, as their fundamentals make them attractive sourcing locations. On the other hand, the prices of their final goods also go up as their "own" input costs increase through the wage effects. They also diversify and source relatively higher-cost traded inputs. For these regions, the increase in final goods prices more than offsets the nominal wage increase, and they see a decline in expected real wages

under costly trade.

Overall, our quantitative results suggest that estimated trade costs are relatively high, and given the disruption probability distribution, they are in the region where moving to autarky can be beneficial to some regions (see Appendix Figure A7).

Expected real wages under baseline and free trade. In contrast, Figure 23 shows that expected real wages are higher for all regions under a free trade counterfactual. To implement free trade in our quantitative exercise, we set the iceberg trade costs to 1 between all districts. Under free trade, expected real wages are, on average, 6.5% higher than in the baseline, whereas the variance of real wages is 62.7% lower.

Figure 23: Quantitative results

Panel A: Expected real wages

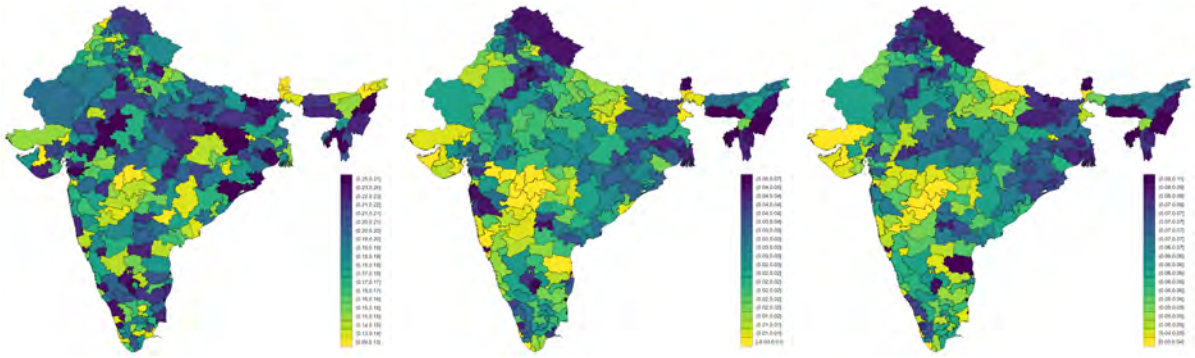

(a) Baseline (b) % Δ in Autarky (c) % Δ in Free Trade

Panel B: Variance of real wages

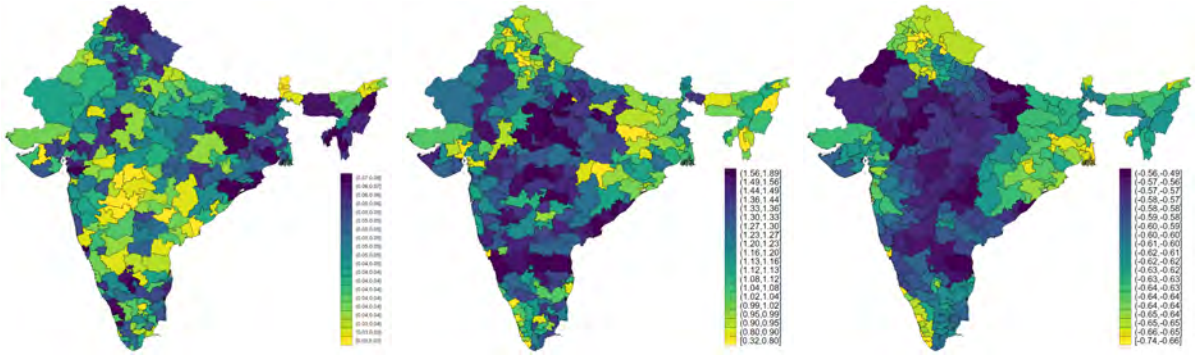

(d) Baseline (e) % Δ in Autarky (f) % Δ in Free Trade

Note. This figure shows expected real wages (Panel A) and their variance (Panel B). The left column shows expected real wages and their variance in the baseline calibrated model. In the middle and right columns, the figure shows the percentage changes in expected real wages under the autarky and the free trade counterfactuals relative to the baseline scenario. In the bottom panel, the middle and right figures show the percentage changes in the variance of real wages under the autarky and the free trade counterfactuals relative to the baseline scenario.

Shock propagation Our framework can also be used to assess the effect of disruptions ex-post for aggregate welfare. In Panel A of Figure 24, we show, for each origin district, what is the impact of a disruption in that district on the real wages of all other districts (including itself). We use the size of the labor force in each district to compute the weighted average of the effect. The impact of a realized disruption in a district on the rest depends on how large is the affected district as a supplier to the rest. The effects vary widely by district, with shocks that materialize in lower-risk or more productive districts that are more important as sourcing locations in equilibrium having larger welfare consequences. While the "own" effect of the shock is important, a large component (-23.64% on average) of the aggregate welfare changes happens through the propagation of the shock, as Panel B of the figure illustrates. Here, we plot the aggregate welfare changes caused by the incidence of a disruption in each origin district, excluding the own effect. Finally, Panel C illustrates the number of districts that experience a welfare decline when an origin district experiences a disruption.

Figure 24: Shock Propagation

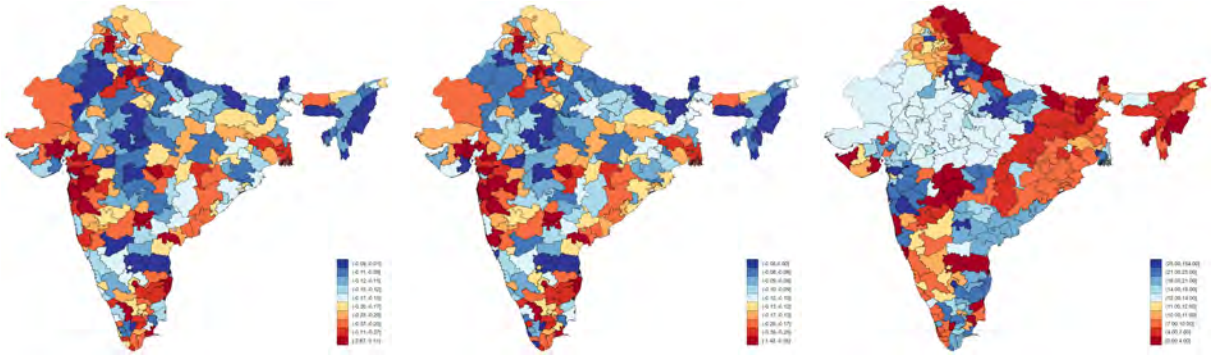

(a) Weighted Average Welfare Change (b) Weighted Average Welfare Change in Other Regions (c) Number of regions with Welfare Decline $> 1\%$

Note. In Panel A, for each district, we compute the impact a materialized disruption has on the real wages of all other districts (including itself). We then use the labor force in each district to calculate the weighted average of the impact. Panel B, removes the own impact in real wages of a disruption, to isolate the "propagation" effect to other districts. Panel C, reports the number of districts that experience a welfare decline, when the district experiences a disruption.

Inventories. In Appendix C.3, we develop an extension of our model to a setting with intermediate input inventories. While we lack detailed inventory data to quantify this extension, we show that the model can qualitatively generate a pattern similar to that in Figure 4, with a larger decline in inputs than in sales following a shock. The extension makes clear the ability to hold inventories does not change a firm's diversification motives ex-ante, as the firm's expected profit function remains convex in input orders. However, existing inventories do shift the level of inputs available within a period for production, which mitigates the short-run effects of a shock on output should one occur.

4.4 Climate Change Counterfactuals

While the previous section explored several counterfactuals, such as autarky or free trade, we next study the implications of varying climate risk in our model. We estimate the share of our model-implied shock probabilities that can be explained by climate-risk-related variables such as rainfall or flooding events. Through the lens of our model, these probabilities capture the risk firms assign to each district. However, as discussed above, the risk associated with each region can be due to climate risk, but also other regional characteristics such as infrastructure or governance. In this section, to highlight the implications of changing climate risk, we hold all other sources of risk constant and double the climate risk of each region relative to the baseline.

We proceed as follows: First, we regress the inverse logit transformation of our probabilities on the historical measures of rainfall, coastal flooding, and riverine flooding presented in Figure 19. Second, we use the estimated coefficients to predict the value of the probabilities in 2050 using the projected values for rainfall, coastal flooding, and riverine flooding, presented in Appendix Figure A11. This method yields how the probabilities would change if climate variables evolve as predicted.

Panel A of Figure 25 illustrates how these probabilities change across space in our main counterfactual. As the figure makes clear, there is wide variation in the changes in climate risk, with the northeast and parts of the west coast seeing large increases in risk, while the central part of the country sees decreases in risk. On average, risk increases by 0.38 percentage points. Panel B illustrates the change in supplier input prices across the country in this counterfactual. There is less variation in the supplier input price changes, but the regions that see the highest climate risk increases see decreases in the input prices their intermediate producers offer.[21]

Panel C illustrates changes in expected real wages. The riskiest regions see the largest declines in expected real wages, while regions that get safer see increases. On average, there is nearly a 2% decline in expected real wages, and a 1.2% decrease in their volatility. Thus, while increased climate risk has negative implications for expected real wages, diversification by firms mitigates the impact on their volatility. Nearly 44% of districts see expected real wage gains, however, reflecting that many districts see lower climate risk in the counterfactual.

Climate change has implications for spatial inequality. While the average region will see a real wage decline, the range of expected real wage changes is 4.18pp, implying large spatial variation. It will adversely affect regions in the North East, which already have low

[21] Recall input prices $p_i = \frac{w_i}{z_i}$. Effectively, the nominal wages in risky regions are decreasing, although by less than the increase in their risk due to general equilibrium effects of sourcing diversification.

wages. Climate risk will not only subject them to increased flooding, but also a decrease in real wages as supply chains become less reliant on this region. Table 6 summarizes the quantitative results across all counterfactuals. In Appendix Figures A14, A15 and A16, we show results where only precipitation, expected floods or temperature, respectively, change, while holding the others constant. Appendix Table A7 summarizes the results under the alternative estimation approach for the disruption probabilities.

Figure 25: Counterfactuals: Climate Risk Increase

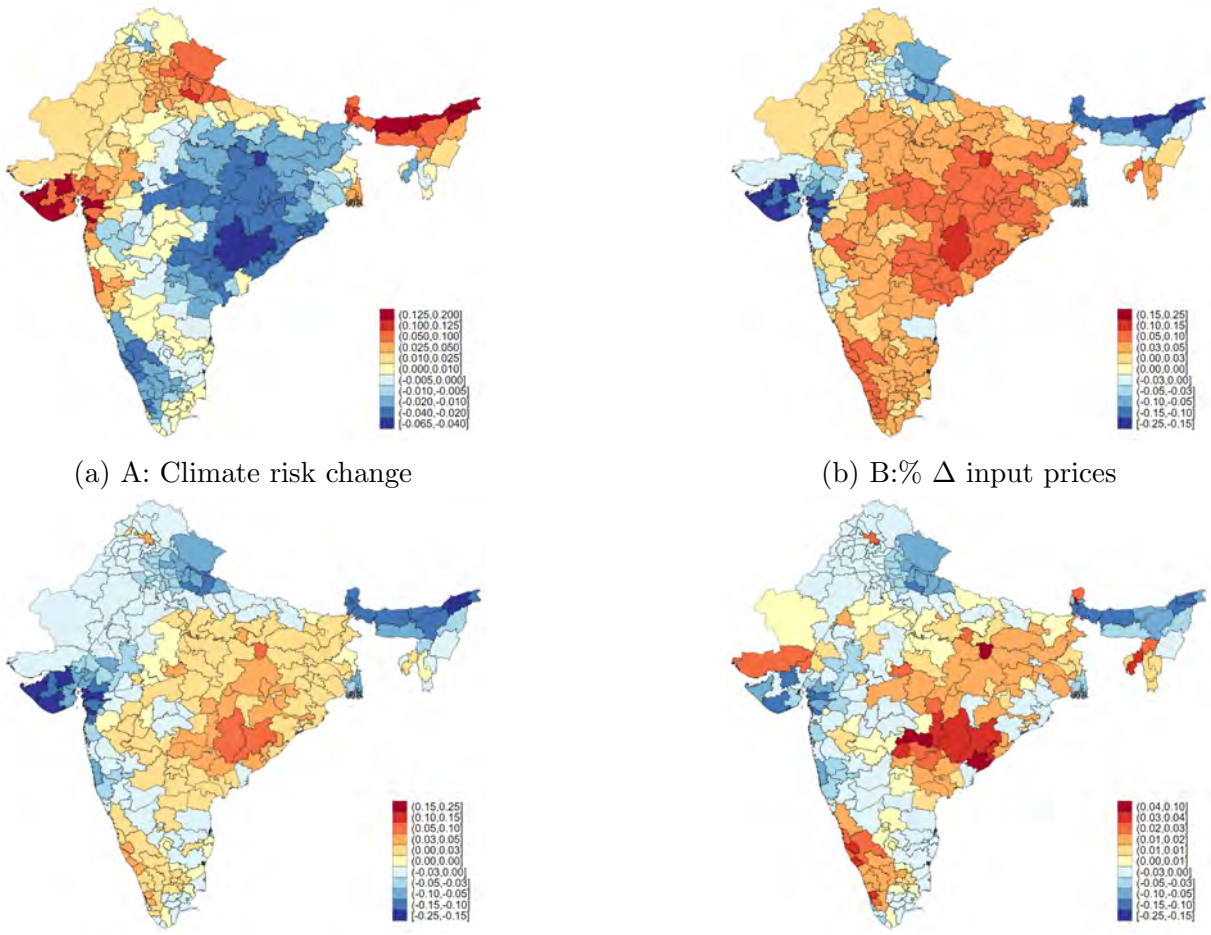

(a) A: Climate risk change

(b) B:% Δ input prices

(c) C:% Δ Expected Real Wages

(d) D: % Δ Volatility

Note. In this figure, we plot the change in probabilities of climate risk (panel A), the change in district input prices (panel B) the change in expected real wages (panel C) and the change in the volatility of real wages (Panel D) as climate risk increases as described in Section 4.4.

5 Conclusion

Climate risk is an increasingly important concern worldwide, with large projected economic impacts. Adaptation of firm supply chains to perceived climate risk is a crucial channel through which economies might adjust to climate risk. Such adaptation has implications for the spatial concentration of economic activity and regional income. Re-

Table 6: Model Counterfactuals: Summary

Counterfactual	Expected Real Wages		Real Wage Volatility		% districts
	Avg. change	Range	Avg. change	Range	Real wage declines
Baseline risk					
Autarky	3.22%	2.07 p.p	113.02%	28.72 p.p	1.12%
Free Trade	6.51%	1.68 p.p	-62.68%	4.33 p.p	0.00%
Alternative risk					
Climate change	-1.99%	4.18 p.p	-1.18%	2.82 p.p	56.09%
Only Rainfall Risk	-0.35%	3.44 p.p	-0.35%	2.43 p.p	39.48%
Only Flood Risk	-1.36%	0.1 p.p	-0.85%	1.00 p.p	98.15%
Only Temperature Risk	-0.36%	0.90 p.p	-0.39%	1.02 p.p	50.55%

Note. This table shows statistics of the distribution of percentage changes between the baseline scenario with current climate risk and costly trade and other scenarios, weighted by district population. Range refers to the interquartile range.

gions that are low-risk but less productive might see increases in their real wages as firms diversify their supply chains.

This paper provides empirical evidence suggesting firm supply chains are structured taking climate risk into account. Our new model of firm supply chain decisions under risk incorporates key patterns we see in the data: firms source the same inputs from multiple locations and seek drier regions to source inputs even when they are farther away. The model results suggest that, on the one hand, input sourcing decisions mitigate climate risk as firms diversify their sources. Yet, on the other hand, they amplify the distributional effects, as regions that face adverse climate shocks will also suffer lower real wages.

Our quantification exercise infers that the impact of climate risk on firm sourcing delivers important implications for economic activity across space. In particular, expected real wages are higher for regions that are less risky. Further, for some regions, expected real wages decrease under costly trade compared to autarky, as firms diversify their climate exposure by sourcing inputs from less productive and more costly producers. However, the volatility of real wages is unambiguously lower with the possibility of diversification through supply chains.

References

Ackerberg, D. A., K. Caves, and G. Frazer (2015, November). Identification Properties of Recent Production Function Estimators. *Econometrica 83*(6), 2411–2451.

Adamopoulos, T. and F. Leibovici (2024). Trade Risk and Food Security. *Working paper*.

Alfaro Ureña, A., M. Fuentes Fuentes, I. Manelici, and J. P. Vasquez (2018). Costa Rican Production Network: Stylized Facts. *Working paper*.

Allen, T. and D. Atkin (2022). Volatility and the Gains from Trade. *Econometrica 90*(5), 2053–2092.

Antràs, P., T. C. Fort, and F. Tintelnot (2017, September). The Margins of Global Sourcing: Theory and Evidence from US Firms. *American Economic Review 107*(9), 2514–64.

Balboni, C. (2021, October). In Harm's Way? Infrastructure Investments and the Persistence of Coastal Cities. *Mimeo*.

Balboni, C., J. Boehm, and M. Waseem (2023). Firm Adaptation and Production Networks: Structural Evidence from Extreme Weather Events in Pakistan. *Mimeo*.

Barrot, J.-N. and J. Sauvagnat (2016). Input Specificity and the Propagation of Idiosyncratic Shocks in Production Networks. *Quarterly Journal of Economics 131*(3), 1543–1592.

Bezanson, J., A. Edelman, S. Karpinski, and V. B. Shah (2017). Julia: A Fresh Approach to Numerical Computing. *SIAM Review 59*(1), 65–98.

Bilal, A. and E. Rossi-Hansberg (2023, June). Anticipating Climate Change Across the United States. Working Paper 31323, National Bureau of Economic Research.

Blaum, J., F. Esposito, and S. Heise (2024). Input Sourcing Under Risk: Evidence from U.S. Manufacturing Firms. *Mimeo*.

Boehm, C. E., A. Flaaen, and N. Pandalai-Nayar (2019, March). Input Linkages and the Transmission of Shocks: Firm-Level Evidence from the 2011 Tōhoku Earthquake. *The Review of Economics and Statistics 101*(1), 60–75.

Boehm, C. E., A. A. Levchenko, and N. Pandalai-Nayar (2023, April). The Long and Short (Run) of Trade Elasticities. *American Economic Review 113*(4), 861–905.

Borusyak, K., X. Jaravel, and J. Spiess (2021). Revisiting Event Study Designs: Robust and Efficient Estimation. *Working paper*.

Caliendo, L. and F. Parro (2015, 11). Estimates of the Trade and Welfare Effects of NAFTA. *The Review of Economic Studies 82*(1), 1–44.

Callaway, B. and P. H. C. Sant'Anna (2020). Difference-in-Differences with Multiple Time Periods. *Journal of Econometrics*.

Carvalho, V. M., M. Nirei, Y. U. Saito, and A. Tahbaz-Salehi (2021, May). Supply Chain Disruptions: Evidence from the Great East Japan Earthquake. *Quarterly Journal of Economics 136*(2), 1255–1321.

Caselli, F., M. Koren, M. Lisicky, and S. Tenreyro (2019, 09). Diversification Through Trade. *The Quarterly Journal of Economics 135*(1), 449–502.

Castro-Vincenzi, J. (2024, February). Climate Hazards and Resilience in the Global Car Industry. *mimeo*.

Cevallos Fujiy, B., D. Ghose, and G. Khanna (2021). Production Networks and Firm-level Elasticities of Substitution. *Working Paper*.

Cevallos Fujiy, B., G. Khanna, and H. Toma (2023). Cultural Proximity and Production Networks. *Working Paper*.

Cruz, J.-L. and E. Rossi-Hansberg (2023). The Economic Geography of Global Warming. Technical report.

Desmet, K., R. E. Kopp, S. A. Kulp, D. K. Nagy, M. Oppenheimer, E. Rossi-Hansberg, and B. H. Strauss (2021, April). Evaluating the Economic Cost of Coastal Flooding. *American Economic Journal: Macroeconomics 13*(2), 444–86.

Dube, A., D. Girardi, O. Jorda, and A. Taylor (2023). A Local Projections Approach to Difference-in-Differences Event Studies. *NBER Working Paper 31184*.

Esposito, F. (2022). Demand risk and diversification through international trade. *Journal of International Economics 135*(103562).

Farrokhi, F. and A. Lashkaripour (2024). Can Trade Policy Mitigate Climate Change? . Working Paper.

Ferris, M. C. and T. S. Munson (1999). Interfaces to PATH 3.0: Design, Implementation and Usage. *Computational Optimization and Applications 12*(1), 207–227.

Goldberg, P. K. and T. Reed (2023, April). Is the Global Economy Deglobalizing? And If So, Why? And What Is Next? Working Paper 31115, National Bureau of Economic Research.

Goodman-Bacon, A. (2018, September). Difference-in-Differences with Variation in Treatment Timing. NBER Working Papers 25018, National Bureau of Economic Research, Inc.

Grossman, G., E. Helpman, and H. Lhuillier (2023). Supply Chain Resilience: Should Policy Promote Diversification or Reshoring? *Journal of Political Economy 131*.

Grossman, G., E. Helpman, and A. Sabal (2024). Resilience in vertical supply chains. *Mimeo*.

Gu, G. and G. Hale (2022). Climate Risks and FDI. *Mimeo*.

Helpman, E. and A. Razin (1978, August). Welfare Aspects of International Trade in Goods and Securities. *The Quarterly Journal of Economics 92*(3), 489–508.

Hsiao, A. (2023). Sea Level Rise and Urban Adaptation in Jakarta. *Mimeo*.

Hummels, D., J. Ishii, and K.-M. Yi (2001, June). The Nature and Growth of Vertical Specialization in World Trade. *Journal of International Economics 54*, 75–96.

Huo, Z., A. A. Levchenko, and N. Pandalai-Nayar (2024, 03). International Comovement in the Global Production Network. *The Review of Economic Studies*.

Indaco, A., F. Ortega, Taspınar, and Süleyman (2020, 11). Hurricanes, Flood Risk and the Economic Adaptation of Businesses. *Journal of Economic Geography 21*(4), 557–591.

Jia, R., X. Ma, and V. W. Xie (2022, July). Expecting Floods: Firm Entry, Employment, and Aggregate Implications. Working Paper 30250, National Bureau of Economic Research.

Johnson, R. C. and G. Noguera (2012). Accounting for Intermediates: Production Sharing and Trade in Value Added. *Journal of International Economics 86*(2), 224 – 236.

Johnson, R. C. and G. Noguera (2017). A Portrait of Trade in Value-Added over Four Decades. *The Review of Economics and Statistics 99*(5), 896–911.

Khanna, G., N. Morales, and N. Pandalai-Nayar (2022). Supply Chain Resilience: Evidence from Indian Firms. NBER Working Papers 30689, National Bureau of Economic Research, Inc.

Kopytov, A., B. Mishra, K. Nimark, and M. Taschereau-Dumouchel (2021, October). Endogenous Production Networks under Supply Chain Uncertainty. *mimeo*.

Korovkin, V., A. Makarin, and Y. Miyauchi (2024). Supply Chain Disruption and Reorganization: Theory and Evidence From Ukraine's War. Working Paper.

Lubin, M., O. Dowson, J. Dias Garcia, J. Huchette, B. Legat, and J. P. Vielma (2023). JuMP 1.0: Recent Improvements to a Modeling Language for Mathematical Optimization. *Mathematical Programming Computation*.

Nath, I. (2022). Climate Change, the Food Problem, and the Challenge of Adaptation through Sectoral Reallocation. *Mimeo*.

Pankratz, N. and C. Schiller (2021). Climate Change and Adaptation in Global Supply-Chain Networks. *Mimeo*.

Pellet, T. and A. Tahbaz-Salehi (2023). Rigid Production Networks. *Journal of Monetary Economics 137*(C), 86–102.

Sun, L. and S. Abraham (2020). Estimating Dynamic Treatment Effects in Event Studies with Heterogeneous Treatment Effects. Working Paper.

Yi, K.-M. (2003, February). Can Vertical Specialization Explain the Growth of World Trade? *Journal of Political Economy 111*(1), 52–102.

Appendix for online publication only

A Details on the Firm-to-Firm Data

We illustrate a stylized example of our establishment-level networks data in Figure A1. As the diagram shows, we observe all transactions where one node of the transaction is within the state. This includes all transactions between establishments within the state (the yellow lines), any inflows from or outflows to the rest of the country (the blue lines), and all international imports and exports (the green lines).

Figure A1: Stylized Example of Establishment-Level Network

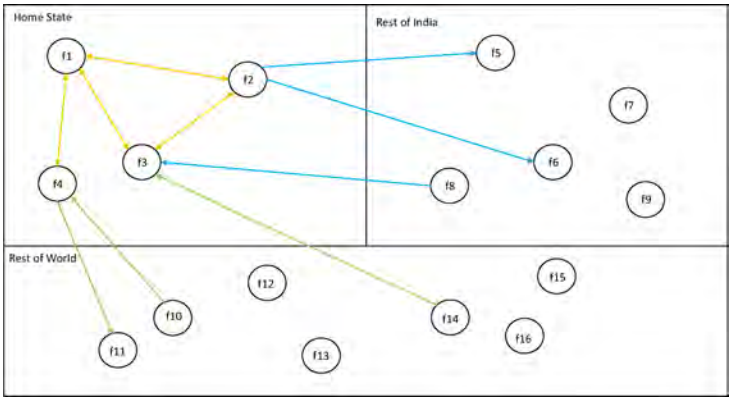

Notes: Stylized example of establishment-level data. The upper half represents the country, and the upper left quadrant represents the state in question. The data includes all transactions within the state, and all transactions where one node of the transaction (either buyer or seller) is in the state.

The data report value and quantity of traded items, so we can construct unit values. To do this, we aggregate values and quantities at the four-digit HSN/month/transaction level, and then construct implied unit values. We can then collapse the data at the 4-digit HSN/month level to construct average unit values, the number of transactions between each seller and buyer pair, and total value of the goods transacted. This is the foundation of the firm-to-firm dataset we use in the analysis. Additionally, we can aggregate these data to the buyer level, which we use in our reduced-form section. Table A1 summarizes our primary variables of interest using this dataset. In Table A2 we present statistics on the number of buyers per supplier and suppliers per buyer. Despite differences in region sizes, the distribution of firms follows closely the one documented by Alfaro Ureña et al. (2018) for Costa Rica.

Table A1: Summary Statistics for Main Variables

Outcome	Mean	p25	p50	p75
Separation Rate (%)	30.9	0	16.67	52.78
Entry Rate (%)	74.06	0	50	106.67
Net Separations (%)	-43.12	-70	0	0
Real Input Value (log)	14.91	12.48	14.55	16.96
Real Sales (log)	16.33	13.57	16.05	18.66
Avg. Supplier Size (millions of rupees)	106.42	9.65	34.04	127.49
Avg. Supplier Outdegree	43.04	3.3	10.97	31.99
Share Purch. Lgst. Supplier (%)	52.39	31.06	47.84	71.82
Number Products	12.05	3	7	14
Share Purch. Diff. Prod. (%)	60.19	21.25	72.78	97.81
Supply Chain Depth	32.32	28.15	31.46	36.35
Number Suppliers	12.35	3	7	14
Avg. Distance (km)	486.71	97.13	251.65	712.75
Share Purch. Non-Home State (%)	38.54	0	24.42	78.48

Note. We calculate summary statistics for key outcomes to describe the network. Summary statistics calculated in December 2019-February 2020. Number of firms included in calculations: 136,562.

Table A2: Distribution of buyers and suppliers

	Mean	SD	10th	25th	50th	75th	90th	95th	99th
N suppliers per buyer	8.0	23.6	1	1	3	8	18	29	72
N of buyers per supplier	16.3	55.3	1	1	4	12	36	65	194
N supplier districts per buyer	3.5	4.4	1	1	2	4	7	11	21
N buyer districts per supplier	3.1	3.0	1	1	2	4	7	10	14

Note. We calculate network characteristics for the year 2019. The top two rows compute the number of buyers per supplier and suppliers per buyer. The bottom rows compute the number of supplier districts per buyer and number of buyer districts per supplier.

B Empirical Facts Appendix

In Table 1 we show that firms seem to multi-source products even within detailed product categories. We proceed to show that such results is not driven by retailers and wholesalers. While we cannot directly identify retailers and wholesalers in our data, we can use the pattern of their transactions to infer firms that likely belong to those industries. For retailers, we expect that they would sell their goods predominantly to final consumers instead of shipping their goods to other firms, hence they should show up as having zero sales in our data. For wholesalers, we expect that they would not transform the products they buy in order to sell them. Hence, we identify as wholesaler firms that buy and sell the same HSN-4 products. Of course, these classifications will be overestimating retailers and wholesalers, as manufacturing firms might buy and sell the same 4-digit product or not ship goods to other firms. However, we want to corroborate that our results are robust to excluding these firms.

From our sample in 2019, we have a total of 195,872 firms. Of those, 7,867 fall under our classification of wholesalers and 137,574 fall under our classification of retailer. As shown in Table A3, the distributions of regions sourced from stay fairly constant when excluding such firms.

Table A3: Share of firms that source from multiple districts (excluding wholesale and retail)

Number of supplier districts	Share of buyers	Share of buyers x HSN 2	Share of buyers x HSN 4	Share of buyers x HSN 8
1	12.0%	56.2%	69.4%	80.9%
2	13.4%	19.0%	16.4%	12.6%
3	12.4%	9.1%	6.4%	3.5%
4	10.6%	5.1%	3.0%	1.4%
5	8.9%	3.1%	1.6%	0.6%
6	7.3%	2.1%	1.0%	0.3%
7	6.0%	1.4%	0.6%	0.2%
8	5.0%	1.0%	0.4%	0.1%
9	4.1%	0.7%	0.3%	0.1%
+10	20.3%	2.4%	0.9%	0.2%

Note. Column 1 aggregates the data at the firm level and computes the share of firms that source from a certain number of districts. Column 2 aggregates the data at the firm-by-2-digit product level, Column 3 at the firm-by-4-digit product level, and Column 4 at the firm-by-8-digit product level. We exclude likely-retailers and likely-wholesalers from the analysis.

Next, we show that firms that have larger purchases of a given product are more likely to source from multiple regions. To see this, we rank all firm-by-8-digit HSN pairs into percentiles, based on total purchases, where the higher percentiles include the firm-product pairs with the higher purchase volume. As shown in Figure A2, the smallest firm-product pairs tend to only source from a single supplier. However, towards the end of the distribution, the largest firm-product pairs source, on average, from more than one region. Firms above the 95th percentile source, on average, from two districts, and firms in the top percentile source from four. This suggests that larger, more productive firms are more likely to multisource.

However, firm size does not drive the descriptive patterns shown in Figures 2a-2c. In Table A4, we document that our descriptive patterns under Fact 2 are not driven by firm size, product composition or capacity of suppliers. We run a regression at the product-firm level as shown in equation 26.

$$\log y_{j,p} = \beta \mathbb{1}(\text{Firm } j \text{ multisources } p) + \gamma X_j + \delta_p + \epsilon_{j,p} \tag{26}$$

Where $\log y_{j,p}$ is the log of the average characteristic of a firm's suppliers such as average distance to suppliers, average rainfall of supplier districts, average riverine flooding of

Figure A2: Number of supplier districts by total purchases

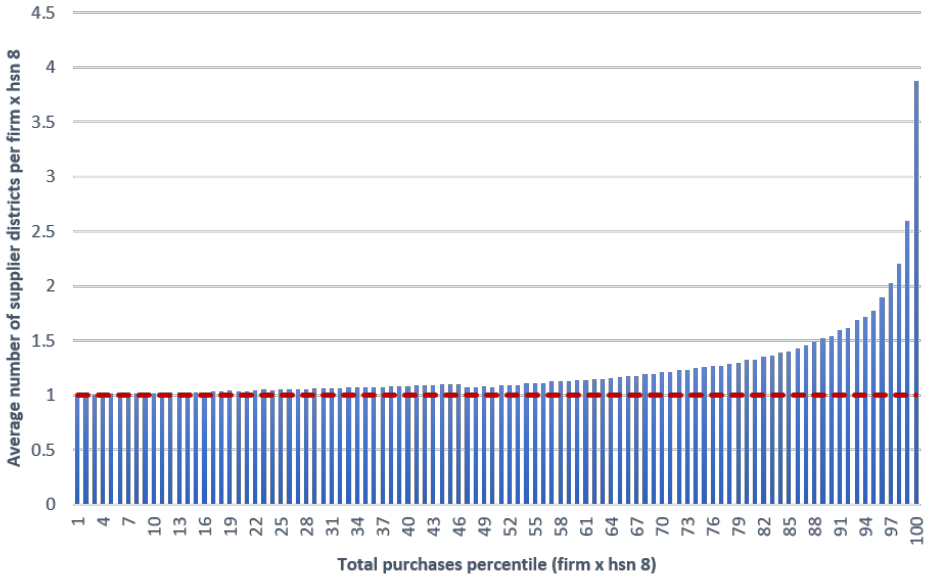

Note. We rank all firm-product pairs into percentiles (1-100) based on the volume of total purchases in 2019. For each percentile (in the horizontal axis), we compute the average number of districts the firm-product pairs source from.

supplier districts and average prices paid to suppliers. The key explanatory variable is $\mathbb{1}$(Firm j multisources p) which is a dummy that indicates whether the firm sources product p from more than one district. Importantly, we control for product fixed effects, the log of total purchases by firm j, and log average sales of suppliers.

As shown in Table A4, our descriptive patterns are robust to adding these controls. Multi-sourcers buy products from distances 76% farther than single-sourcers. They also source from districts with 2.3% lower rainfall and 1.4 % lower river flooding levels. Finally, they pay 44% higher input prices than single sourcers. The product fixed effects help us rule out that the differences between single sourcers and multisourcers are driven by differences in product quality. The own purchases control rules out that the patterns are just driven by differences in firm size (e.g. large firms multisource more and also pay higher prices). Finally, the control for supplier size helps us rule out that the reason for multisourcing is that their suppliers don't have enough capacity to meet demand.

Table A4: Supplier characteristics by number of districts sourced from

	Log (Distance to suppliers)	Log(Daily Rainfall)	Log(Historical riverine flooding)	Log(Price of inputs)
$\mathbb{1}$(Multisourcer)	0.760***	-0.0229***	-0.0140***	0.441***
N	739,520	739,520	739,520	739,520
R-sq	0.327	0.271	0.124	0.545

Note. *** $p < 0.01$, ** $p < 0.05$, * $p < 0.1$. We run a cross-sectional regression at the firm (j), 8-digit product (p) level. The outcome is the log average distance to suppliers (column 1), log average daily rainfall at suppliers' district (column 2), log average riverine flooding at suppliers' district (column 3) and log average price of inputs (column 4). The main regressor is a dummy variable on whether the firm sources the HSN-8 product from more than one district. All regressions include HSN-8 product fixed effects and controls for log size of the firm and log average size of suppliers.

C Theory Appendix

C.1 Proofs

Proposition 1: Proof. Since the cost of materials is linear in M_{ij} and the constraints are conventional (linear) non-negativity constraints, it suffices to show that the expected operating profits function $\mathbb{E}_\chi\left(\pi(\boldsymbol{M};\boldsymbol{\chi})\right)$ is concave in the vector $\boldsymbol{M}$. The expectation operator preserves the concavity of $\pi(\boldsymbol{M};\boldsymbol{\chi})$ which is the only thing required to prove. The concavity of ex-post profits, $\pi(\boldsymbol{M};\boldsymbol{\chi})$, follows from the parametric restriction, $\frac{(1-\beta)(\sigma-1)}{\beta+\sigma(1-\beta)} < 1$. ■

Lemma 1: Proof. Notice that, conditional on some state of the world, $\boldsymbol{\chi}$, ex-post aggregate profits are given by,

$$\int_{\omega\in[0,1]} \pi_i(\omega;\boldsymbol{\chi})d\omega = \int_{\omega\in[0,1]} \left(p_i(\omega;\boldsymbol{\chi})q_i(\omega;\boldsymbol{\chi}) - w_i\ell_i(\omega;\boldsymbol{\chi}) - \sum_j p^I_{ji}M_{ji}(\omega) \right) d\omega.$$

Using the assumption of a unit mass of homogenous firms in a region, ex-post aggregate profits are then

$$\pi_i(\boldsymbol{\chi}) = p_i(\boldsymbol{\chi})q_i(\boldsymbol{\chi}) - w_i(\boldsymbol{\chi})\bar{L}_i - \sum_j p^I_{ji}M_{ji}.$$

where $p_i(\boldsymbol{\chi})q_i(\boldsymbol{\chi})$ corresponds to aggregate revenues from the final goods sector, $w_i(\boldsymbol{\chi})\bar{L}_i$ are payments to residual labor, and $\sum_j p^I_{ji}M_{ji}$ is total expenditure on intermediate inputs. As final goods firms are monopolistically competitive and the final goods aggregator is CES, standard algebra shows that profits are a constant fraction of revenues:

$$\pi_i(\boldsymbol{\chi}) = \frac{p_i(\boldsymbol{\chi})q_i(\boldsymbol{\chi})}{\sigma}.$$

The budget constraint implies equilibrium revenues are simply labor income plus profits $p_i(\boldsymbol{\chi})q_i(\boldsymbol{\chi}) = Y_i(\boldsymbol{\chi}) = w_i(\boldsymbol{\chi})L_i + \pi_i(\boldsymbol{\chi})$. Combining these expressions, we can show

that

$$\pi_i(\boldsymbol{\chi}) = \frac{w_i(\boldsymbol{\chi})L_i}{\sigma - 1} \;\; ; \;\; Y_i(\boldsymbol{\chi}) = \frac{\sigma}{\sigma - 1} w_i(\boldsymbol{\chi})L_i$$

This further implies that aggregate costs of firms are $\frac{(\sigma-1)}{\sigma}Y_i$ and aggregate expenditure on materials is then $\sum_j p_{ij}^I M_{ij} = \frac{(1-\beta)(\sigma-1)}{\sigma}Y_i$. ■

Lemma 2: Proof. We prove that wages in each location i, w_i, are deterministic by showing that labor market clearing must occur at the time of producing intermediates.

By backward induction, after intermediate inputs have been produced, final goods producers in each region face an inelastic residual labor supply equal to $\bar{L}_i$. Aggregate labor demand in each region is given by,

$$L_i^D(\boldsymbol{\chi}) = \left[\frac{Y_i(\boldsymbol{\chi})}{\phi_i \left(\sum_{j \in I} \chi_j M_{ij} \right)^{1-\beta} p_i(\boldsymbol{\chi})} \right]^{\frac{1}{\beta}},$$

where final goods' prices can be written as

$$p_i(\boldsymbol{\chi}) = \left[\frac{\beta(\sigma - 1)}{\sigma} \right]^{-\beta} \phi_i^{-1} \left(\sum_{j \in I} \chi_j M_{ij} \right)^{-(1-\beta)} w_i(\boldsymbol{\chi})^{\beta} Y_i(\boldsymbol{\chi})^{1-\beta}.$$

If we plug the expression for prices, in the aggregate labor demand equation, and simplify we get that,

$$L_i^D(\boldsymbol{\chi}) = \beta L_i$$

Crucially, aggregate labor demand by final goods producers does not depend on the realization of the shocks, $\boldsymbol{\chi}$. However to clear the labor market in each location the wage rate needs to be such that the residual labor supply that final goods' producers face, $\bar{L}_i$, is equal to their inelastic labor demand. The wage rate is set ex-ante when intermediate good production takes place and is independent of the realization of the shocks. As a corollary, this implies that the wage rate, $w_i(\boldsymbol{\chi})$, aggregate profits $\pi_i(\boldsymbol{\chi})$ and aggregate income $Y_i(\boldsymbol{\chi})$ are all deterministic. ■

Proposition 2: Proof. Consumers' expected welfare in region i is given by:

$$\mathcal{W}_i = \phi_i \beta^{\beta} L_i^{\beta} \mathbb{E}_{\boldsymbol{\chi}} \left[\left(\sum_j \chi_j M_{ji} \right)^{1-\beta} \right],$$

whereas firms' expected profits are given by,

$$\kappa \mathbb{E}_{\boldsymbol{\chi}} \left[w_i^{\frac{\beta(1-\sigma)}{\beta+\sigma(1-\beta)}} \left[\left[Y_i \mathbb{P}_i^{\sigma-1} \right] \phi_i^{\sigma-1} \right]^{\frac{1}{\beta+\sigma(1-\beta)}} \left(\sum_{j \in I} \chi_j M_{ji} \right)^{\frac{(1-\beta)(\sigma-1)}{\beta+\sigma(1-\beta)}} \right] - \sum_{j \in I} p_j^i M_{ji}$$

From comparing the exponents to effectively delivered orders $\left(\sum_{j \in I} \chi_j M_{ji}\right)$, it is easy to see that

$$\frac{(1-\beta)(\sigma-1)}{\beta+\sigma(1-\beta)} < (1-\beta) \iff \beta(\sigma-1) < 1.$$

The converse holds if $\beta(\sigma-1) \geq 1$ ■

C.2 Additional Results: Comparative Statics

Figure A3: Scenario with heterogeneous risk and infinite trade costs

Same distance between regions

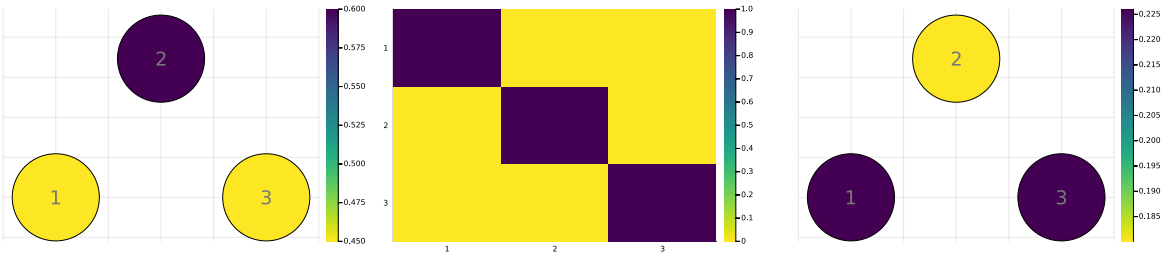

(a) Shock probabilities (b) Bilateral Sourcing Shares (c) Real Wages

Note. This figure presents the case where trade costs are set to infinity and regions are equidistant. The figures in the left panel show the probability that each region is hit by a shock, as well as a visual representation of the geographical location of regions in space. The figures in the middle panel consist of a 3x3 input-output matrix where the buying regions are in the vertical axis and the supplying regions are in the horizontal axis. Each line represents the share of inputs purchased by a buying regions from each supplying region. The right panel present the real wages for each region. The scales are shown to the right of each figure. The case with heterogeneous distance between regions is shown in Figure 13.

Figure A4: Comparison between heterogeneous risk under costly trade and autarky

Equidistant regions

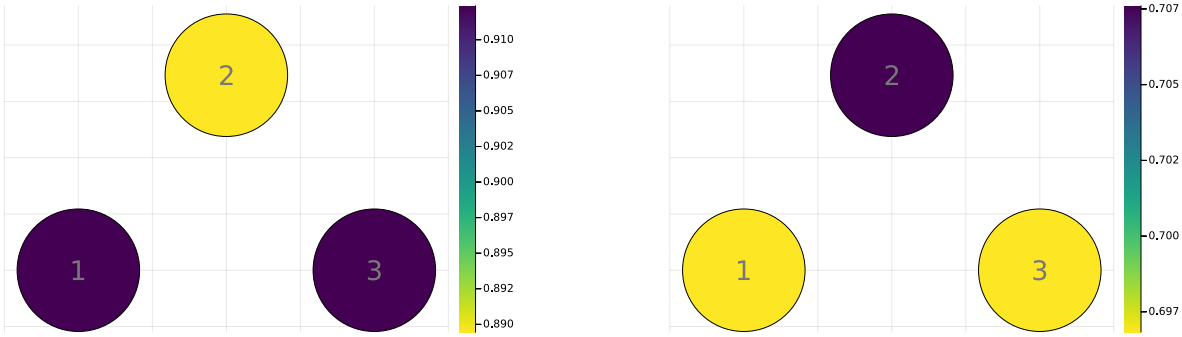

(a) Expected Real Wages Ratio (b) Variance of Real Wages Ratio

Note. In this figure we plot the expected real wages (left panel) and variance of real wages (right panel) for the scenario with heterogeneous risk and costly trade shown in Figure 11 relative to the scenario with heterogeneous risk and trade autarky shown in Figure 13. The variance of real wages is computed across potential states of the world. In this scenario, regions are equidistant from each other. The scales are shown to the right of each figure. The case with regions in a line is discussed in Figure 14.

Figure A5: Scenario with heterogeneous risk and free trade

Same distance between regions

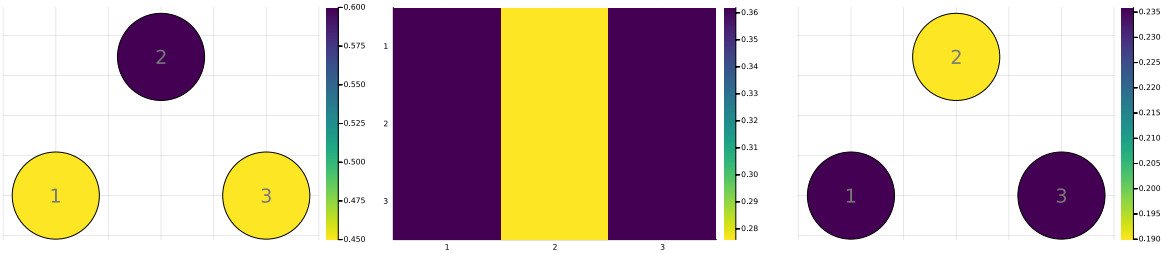

(a) Shock probabilities (b) Bilateral Sourcing Shares (c) Real Wages

Note. This figure presents the case where there are no trade costs. The figure in the left panel show the probability that each region is hit by a shock, as well as a visual representation of the geographical location of regions in space. The figure in the middle panel consist of a 3x3 input-output matrix where the buying regions are in the vertical axis and the supplying regions are in the horizontal axis. Each line represents the share of inputs purchased by a buying regions from each supplying region. The right panels present the real wages for each region. Here, regions are equidistant from each other. The case with heterogeneous distance is in Figure 15. The scales are shown to the right of each figure.

Figure A6: Comparison between costly and free trade

Equidistant regions

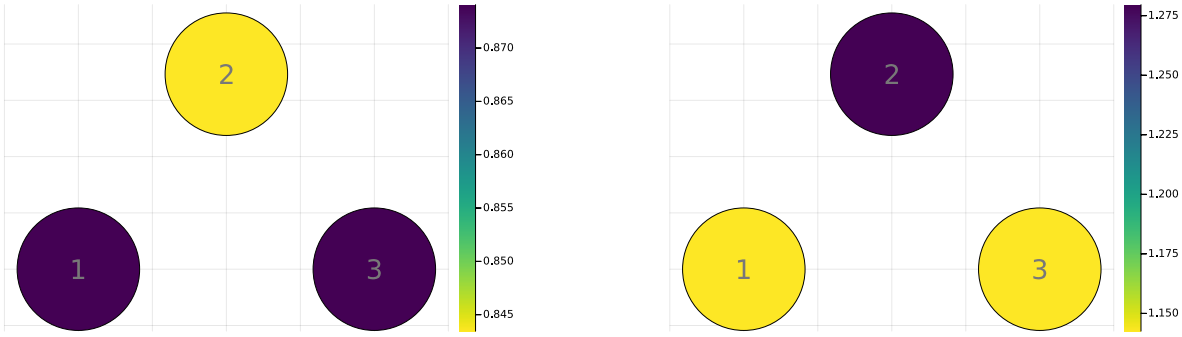

(a) Expected Real Wages Ratio (b) Variance of Real Wages Ratio

Note. In this figure we plot the expected real wages (left panel) and variance of real wages (right panel) for the scenario with heterogeneous risk and costly trade shown in Figure 11 relative to the scenario with heterogeneous risk and free trade shown in Figure 15. The variance of real wages is computed across potential states of the world. Here, regions are equidistant from each other. The case with regions on a line is shown in Figure 16. The scales are shown to the right of each figure.

Figure A7: Comparison between costly and free trade: High shock probability

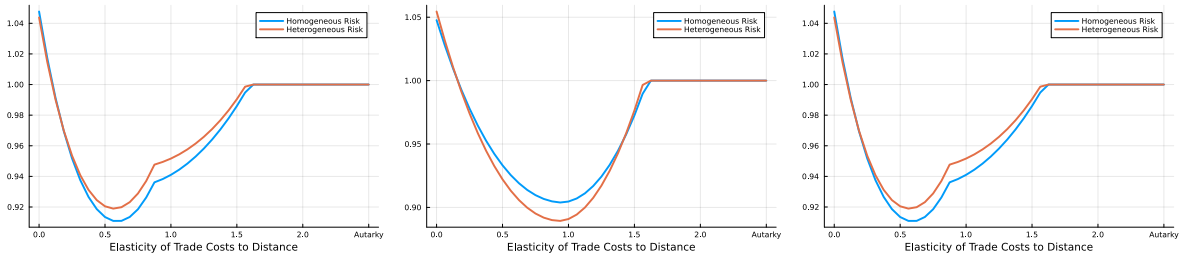

(a) Region 1 (b) Region 2 (c) Region 3

Note. This figure illustrates the welfare in Region 1 (left column), Region 2 (middle column) and Region 3 (right column) relative to autarky, as trade costs increase. The orange curve illustrates relative welfare when risk is heterogeneous, with Regions 1 and 3 having a disruption probability of 0.45 and Region 2 of 0.6. The blue curve illustrates relative welfare when the regions have homogeneous risk of 0.5.

Figure A8: Comparison between costly and free trade: Low shock probability

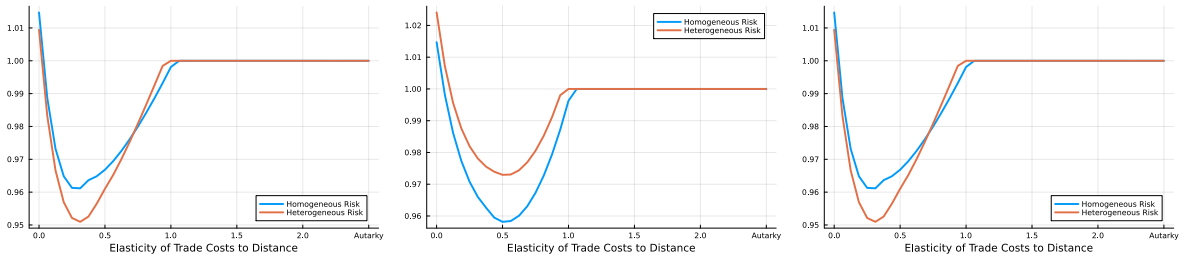

(a) Region 1 (b) Region 2 (c) Region 3

Note. This figure illustrates the welfare in Region 1 (left column), Region 2 (middle column) and Region 3 (right column) relative to autarky, as trade costs increase. The orange curve illustrates relative welfare when risk is heterogeneous, with Regions 1 and 3 having a disruption probability of 0.175 and Region 2 of 0.1. The blue curve illustrates relative welfare when the regions have homogenous risk of 0.15.

C.3 Inventories

We next extend our model to allow firms to hold inventories of their material inputs. We assume inventories accumulated at t can be costlessly stored for one period and used in $t+1$, after which they fully depreciate. The assumption of full depreciation after one period (a quarter) is made for analytical convenience, to curtail the dimension of the state space. However, this setting is sufficient to capture the main motive for firm inventory holdings, as insurance against the i.i.d shocks in this model, and to illustrate that we can qualitatively replicate the pattern in the event studies where shocked buyer output declined less than inputs. Notice that the costs of holding inventories in a country like India are likely higher than the U.S. . However, we lack detailed data on plant or firm inventory holdings to discipline the costs of storage, and so assume costless storage from one quarter to the next (over a total period of 6 months) and full depreciation after.

Timing. At the production stage, firms additionally choose the share of intermediate inputs a_t they want to use to produce in the period. A share $1-a_t$ will then stock inventories, that will carry to the next period.

Firm problem, stage 2. In period t, and after disruptions have taken place, a firm with inventories e_{t-1} solves the following problem:

$$\mathbb{V}^{post}\left(e_{t-1}, \sum_{j\in I}\chi_{jt}M_{ijt}\right) \equiv \max_{a_t} \; C\left[\left(a_t\sum_{j\in I}\chi_{jt}M_{jit}+e_{t-1}\right)^{(1-\beta)(\sigma-1)}\right]^{\frac{1}{\beta+\sigma(1-\beta)}} + \delta\mathbb{V}^{ante}\left(e_t\right) \tag{27}$$

such that

$$e_t = (1-a_t)\sum_{j\in I}\chi_{jt}M_{ijt} \tag{28}$$

$$a_t \in [0,1] \tag{29}$$

$$\mathbb{V}^{ante}\left(e_{t-1}\right) \equiv \max_{M_{ijt}\geq 0} \; \mathbb{E}\left[\mathbb{V}^{post}\left(e_{t-1}, \sum_{j\in I}\chi_{jt}M_{ijt}\right) - \sum_j p_j M_{jit}\right] \tag{30}$$

Here, $\mathbb{V}^{post}(.)$ is the forward looking firm's value function after shocks have materialized in period t and C is a constant. At this point, the firm holds inventories of e_{t-1} stored from the previous period, which is an additional state variable. Equation (27) is the dynamic analog of the firm's ex-ante profit maximization condition in Equation (7). Firms now

have the choice of storing inputs as inventories for period $t+1$, with the constraint that the share of inputs stored as inventories cannot exceed 1. There are no additional storage costs, so the choice of a_t pins down e_t which are available to produce in $t+1$ (Equation (28). At the beginning of a period, the firms' value function is $\mathbb{V}^{ante}$, which is the dynamic analog of Equation (11) given the state variable, the existing inventories, e_{t-1}.

The Euler equation for a_t is:

$$\left[a_t \sum_{j \in I} \chi_{jt} M_{ijt} + e_{t-1}\right]^{\frac{(1-\beta)(\sigma-1)}{\beta+\sigma(1-\beta)}-1} = \delta \mathbb{E}\left(\left[a_{t+1} \sum_{j \in I} \chi_{jt+1} M_{ijt+1} + e_t\right]^{\frac{(1-\beta)(\sigma-1)}{\beta+\sigma(1-\beta)}-1}\right). \quad (31)$$

In other words, a firm in stage 2 chooses inventories for stage 1 of the next period in such a way that it equates the marginal return of materials today with the expected marginal return of those materials tomorrow.

Calibration. We simulate this model in partial equilibrium. Under the assumption of complete discounting ($\delta = 0$) the model collapses to our baseline model. We assume a firm in i's input orders from some location j face an unanticipated shock at $t = 0$ with a magnitude such that available inputs decline by 75% to match the event studies in Section 2.3. Figure A9 illustrates the time path of firm input purchases and sales following the shock, with the inventory mechanism in Panel A and the baseline model with no inventories in Panel B.

Figure A9: Inventory Model: Sales and Inputs

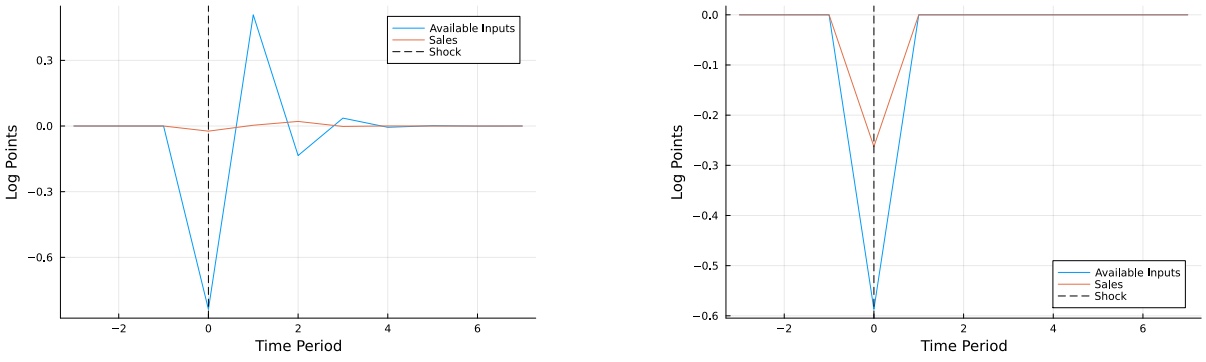

(a) Inventory Model (b) Baseline Model

Note. In this figure, we show the responses of firm sales and input purchases in the model with inventories (left panel) and in the baseline model (right panel).

As is clear from Panel A of Figure A9, adding in the inventory holding mechanism helps firms further smooth sales when they experience a shock to inputs. In fact, the simple

framework here matches the qualitative patterns in the event studies well – inputs decline and then overshoot in the recovery, as firms reaccumulate inventories. Sales in contrast experience a very small decline. Panel B illustrates the responses in our baseline model. Here, for the same decline inputs, sales experience a larger decline relative to Panel A. However, sales fall by less than inputs, illustrating that the diversification across sourcing locations also provides firms an additional means by which to mitigate sales declines when exposed to risk.

Conceptually, inventories and sourcing location diversification are two approaches by which firms can mitigate output volatility. In practice, the trade-off between these two approaches and their relative importance will depend on the relative costs, higher cost inputs vs the costs of inventory storage. As we lack data to discipline inventory holding costs, and the model with inventories is less tractable in general equilibrium, we focus on the sourcing location diversification. Our descriptive evidence suggests that firms are engaging in such diversification, so it is a salient mechanism in practice. Notice that in our model, even given a level of inventories in a period, firm's expected profits remain concave in (residual) input orders, and so firms will continue to diversify across sourcing locations.

D Quantitative Appendix

D.1 Dataset construction

In Section 4.2, we use multiple sources to correlate our model implied probabilities with observables related to supply chain disruption risk. We consider four climate related measures: rainfall, coastal flooding, riverine flooding, and average temperatures. Our climate data is available for grid areas that are much more detailed than our 271 regions. In such cases, we use shape files to overlay our regions to the available maps and calculate the average measure of the climate variables within each of our regions.

Coastal and riverine flooding are taken from the World Resources Institute's Aqueduct Floods Hazard Map. Historical flooding is defined as the present day meters of flooded areas. Projected flooding are the expected meters of increase in flooded areas expected in 2050. We use 10-year floods and the RCP 4.5 as our baseline projection.

Historical and projected temperature data is taken from the IPCC WG1 Interactive Atlas. Historical temperatures are the average daily degrees centigrade in 2005 (the latest year available for historical data). Projected data for 2050 is calculated assuming a risk scenario of RCP 8.5 and using a risk model of NOAA global circulation model and the Swedish Meterological and Hydrological Institute's local circulation model.

Daily rainfall data is taken from the India Meteorological Department and measured in millimeters. We take the average across all days in 2019 for each district. For predicted rainfall, we first extract the average historical (measured in 2005) and predicted 2050 rainfall from the IPCC WG1 Interactive Atlas, using the same settings as for temperature. We then compute the change for each district between 2005 and 2050, and apply the implied yearly change to update the 2019 values to 2050.

The non climate variables mostly come from the Socioeconomic High-resolution Rural-Urban Geographic Platform for India (SHRUG). Elevation is defined as the average elevation in meters of each district while terrain ruggedness is the Terrain Ruggedness Index expressing elevation differences between adjacent pixels. The nightlights luminosity index aims to capture economic activity by detailed regions. Finally, court congestion is taken from the Development Data Lab and measures the average delay in days for the courts in each district.

D.2 Model Probabilities - Additional Analysis

Figure A10: Model probabilities, Productivities and Distance

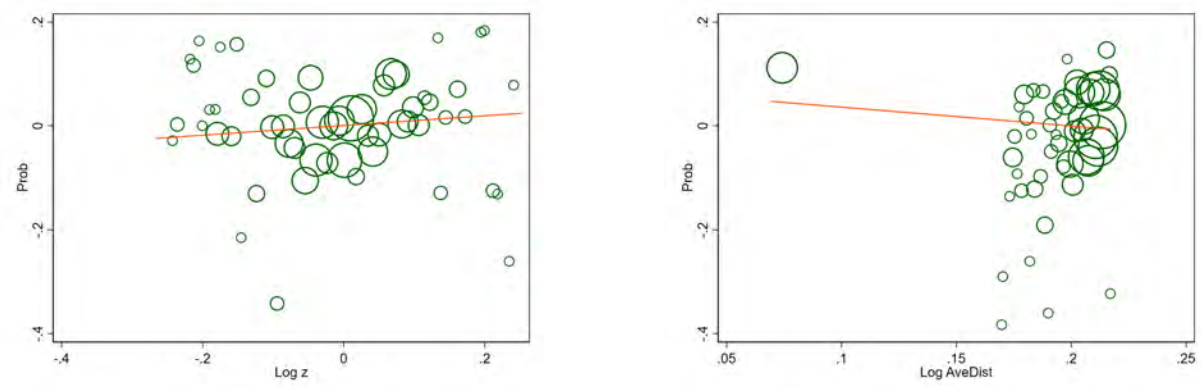

(a) Prob vs Productivities

(b) Prob v Average Distance

Note. In this figure, we plot the estimated probabilities against some observables. In the left panel, we correlate the probabilities with Log(Productivities). In the right panel, we correlate the probabilities with the average distance to the state of our study.

Figure A11: Model probabilities and Projected Observables

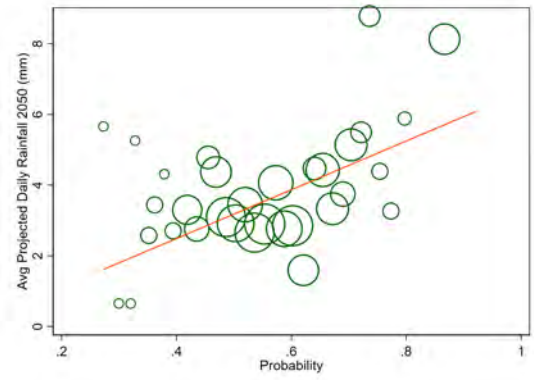

(a) Daily Rainfall - Projected 2050

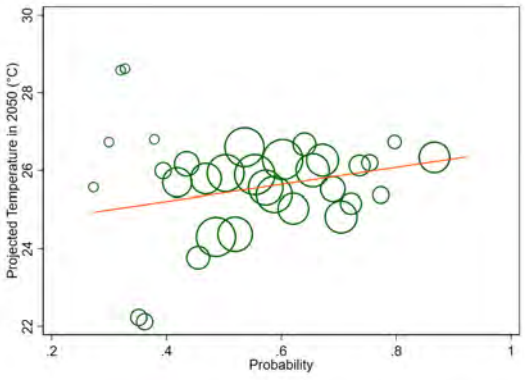

(b) Average Temperature - Projected 2050

.

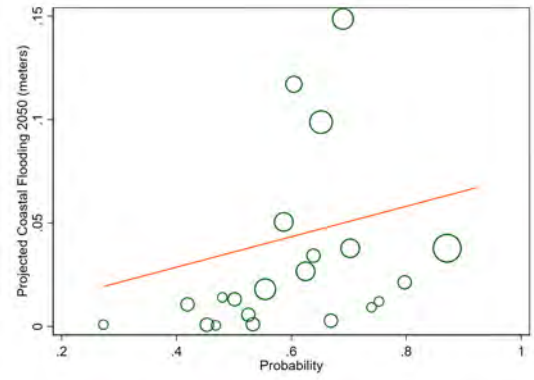

(c) Coastal Flooding - Projected 2050

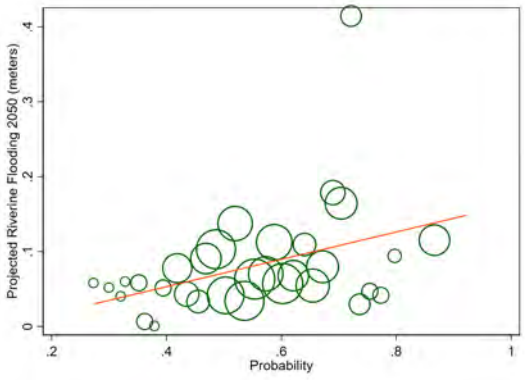

(d) Riverine Flooding - Projected 2050

Note. In this figure, we plot the estimated probabilities against 2050 projections for climate observables. In Figures A11a and A11b, we correlate the rainfall and temperature projections for year 2050 with the recovered probabilities. Figures A11c use the projected coastal flooding, while Figures A11d correlate the probabilities with projected riverine flooding, respectively. A more detailed definition of each of the variables can be found in Appendix D.2.

Figure A12: Model Probabilities, Price Indices and Wages

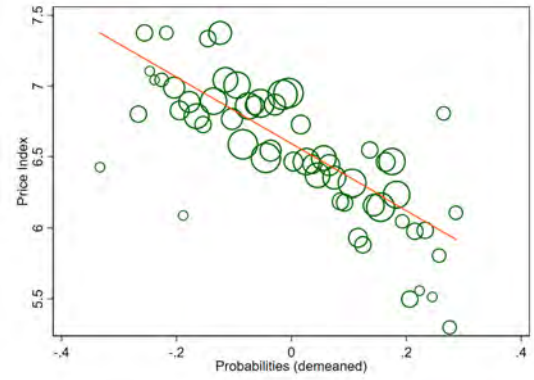

(a) Price Index

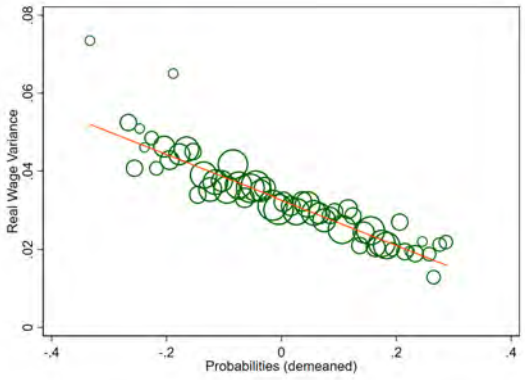

(b) Real Wage Variance

Note. In this figure, we plot the model-derived price index (left panel) and real wage variance (right panel) against the estimated disruption probabilities.

Table A5: Regression of model probabilities on observables

	Historical	Projected (2050)	Historical	Projected (2050)
Daily Rainfall	0.0663***	0.0295***	0.0518***	0.0199**
	(0.0159)	(0.00879)	(0.0189)	(0.00952)
Coastal Flooding	1.378*	1.462**	0.915	1.147*
	(0.813)	(0.576)	(0.853)	(0.601)
Riverine Flooding	0.470	0.220	0.486	0.283
	(0.310)	(0.203)	(0.318)	(0.210)
Avg Temperature	0.0280**	0.0315***	0.0266*	0.0351**
	(0.0125)	(0.0115)	(0.0151)	(0.0137)
Avg Nightlights Luminosity			-0.00508	-0.00410
			(0.00702)	(0.00702)
Avg Elevation			-0.000385**	-0.000462***
			(0.000185)	(0.000177)
Avg Ruggedness			0.0180**	0.0245***
			(0.00877)	(0.00811)
Avg Court Congestion			0.0658*	0.0559
			(0.0341)	(0.0348)
N	271	271	271	271
adj. R-sq	0.095	0.078	0.108	0.102

Note. *** $p < 0.01$, ** $p < 0.05$, * $p < 0.1$. We run regressions of the inverse logit of the estimated model probabilities on observables. In columns 1 and 3, climate variables used are measured with their historical values. In columns 2 and 4, climate variables used are measured with the projected values for 2050. Observables are in levels. A more detailed definition of each of the variables can be found in Appendix D.2.

Figure A13: Ahmadabad sourcing, Kolkata sourcing – Free Trade

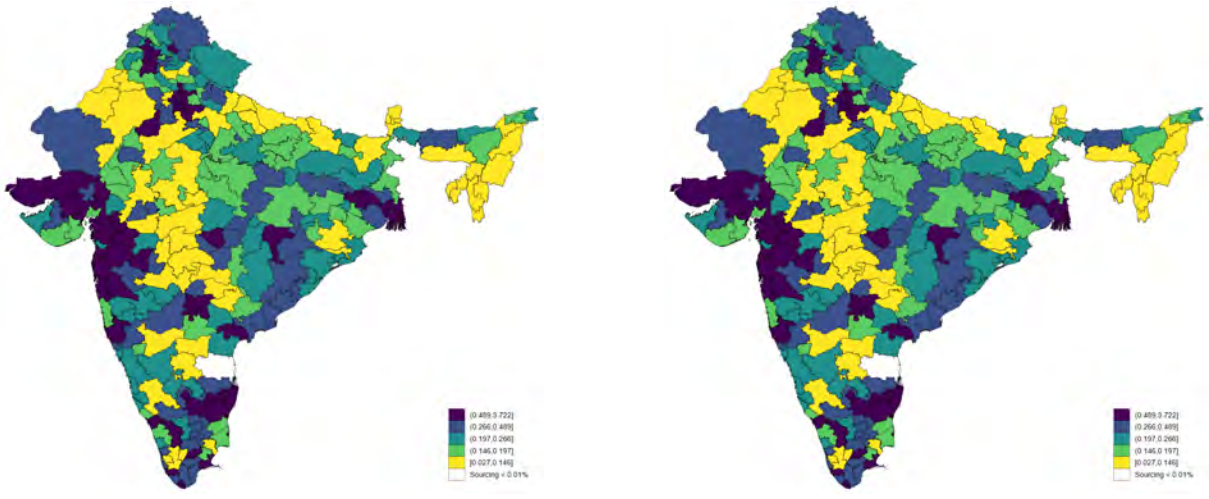

Figure A14: Counterfactuals: Only Precipitation Risk Increase

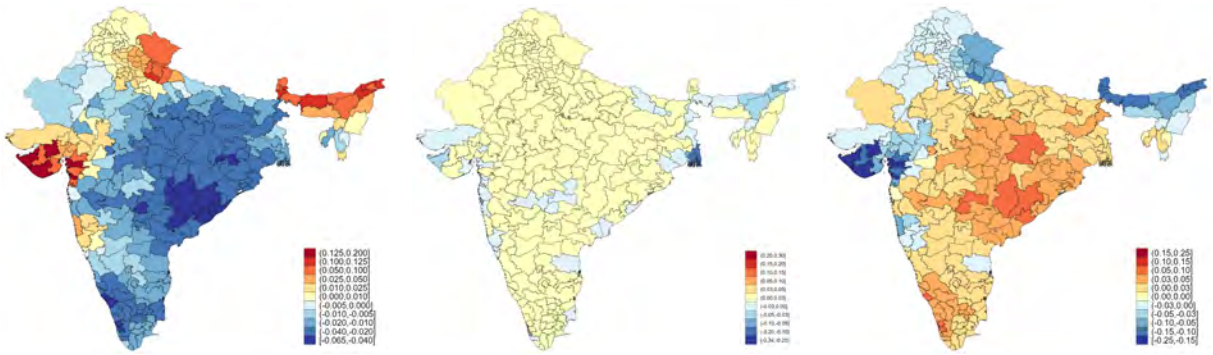

(a) Flood risk change (b) % Δ input prices (c) % Δ Expected Real Wages

Note. In this figure, we plot the change in probabilities due to precipitation (left panel), the change in district input prices (middle panel) and the change in expected real wages (right panel) as precipitation risk increases as described in Section 4.4.

Figure A15: Counterfactuals: Only Flooding Risk Increase

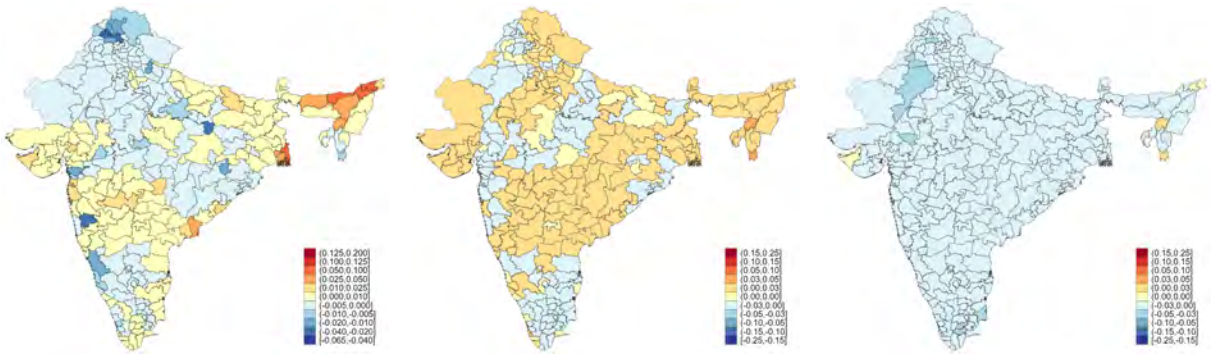

(a) Flood risk change (b) % Δ input prices (c) % Δ Expected Real Wages

Note. In this figure, we plot the change in probabilities due to flooding (left panel), the change in district input prices (middle panel) and the change in expected real wages (right panel) as flood risk increases as described in Section 4.4.

Figure A16: Counterfactuals: Only Temperature Risk Increase

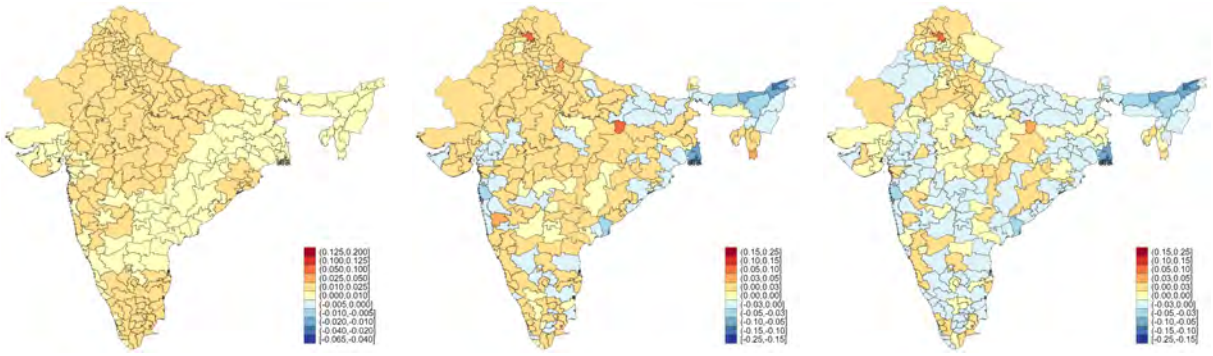

(a) Flood risk change (b) % Δ input prices (c) % Δ Expected Real Wages

Note. In this figure, we plot the change in probabilities due to temperature (left panel), the change in district input prices (middle panel) and the change in expected real wages (right panel) as temperature risk increases as described in Section 4.4.

E Projecting Probabilities on Observables

In this Appendix, we describe an alternative estimation strategy for the disruption probabilities, ρ_i. Instead of computing one parameter per region, we parameterize the vector $\{\rho_i\}_{i=1}^{I}$ on a vector of observable characteristics, Z_i. This vector Z_i includes a constant term, average court delays, ruggedness, elevation, night lights, average rainfall, average coastal flooding, average riverine flooding, and average temperature. We include all of these variables in logs, and we add a dummy for the case in which historical coastal flooding is positive, to allow the function to allow the function to flexibly estimate the asymptotic behavior of the log at 0. Then, we assume that these probabilities have the following functional form,

$$\rho_i = \frac{e^{Z_i'\gamma}}{1 + e^{Z_i'\gamma}},$$

where γ is the vector of parameters that we estimate. We estimate this by minimizing the gap between model-implied and the observed average sourcing shares in the data.

In Table A6, we present the estimates of the vector γ. The resulting probabilities from this approach are shown in Panel (c) of Figure 17.

This estimation approach requires estimating fewer parameters than our baseline, but necessitates that we take a stance on the sources of district-level risk. While the estimation approaches are independent of each other, the estimated coefficients for rainfall and flooding are positive, consistent with the baseline. Nightlights have a zero coefficient, also consistent with the baseline. In contrast to the baseline, however, courts and temperature also contribute positively to risk under this approach.

Table A6: Estimates of the Model for the Probabilities

	Constant	**Courts**	**Ruggedness**	**Elevation**	**Night Lights**	**Rainfall**	**Coastal Flooding**	**Coastal Dummy**	**Riverine Flooding**	**Temperature**
γ	-1.41	0.97	1.02	0.21	0.00	0.21	0.27	0.14	0.07	0.82

Table A7: Model Counterfactuals: Summary – Alternative Model

Counterfactual	Expected Real Wages		Real Wage Volatility		% districts
	Avg. change	Range	Avg. change	Range	Real wage declines
Baseline risk					
Autarky	2.65%	0.89 p.p	120.66%	51.66 p.p	1.85%
Free Trade	4.99%	1.41 p.p	-74.34%	4.59 p.p	0.00%
Alternative risk					
Climate change	-2.00%	13.00 p.p	-0.64%	7.57 p.p	42.07%
Only Rainfall Risk	-0.25%	13.13 p.p	0.15%	8.78 p.p	38.01%
Only Flood Risk	-1.23%	1.12 p.p	0.47%	2.40 p.p	94.83%
Only Temperature Risk	-0.53%	0.85 p.p	0.74%	1.95 p.p	54.24%

Note. This table shows statistics of the distribution of percentage changes between the baseline scenario with current climate risk and costly trade and other scenarios. Range refers to the interquartile range.

Figure A17: Quantitative results - Projected Probabilities

Panel A: Expected real wages

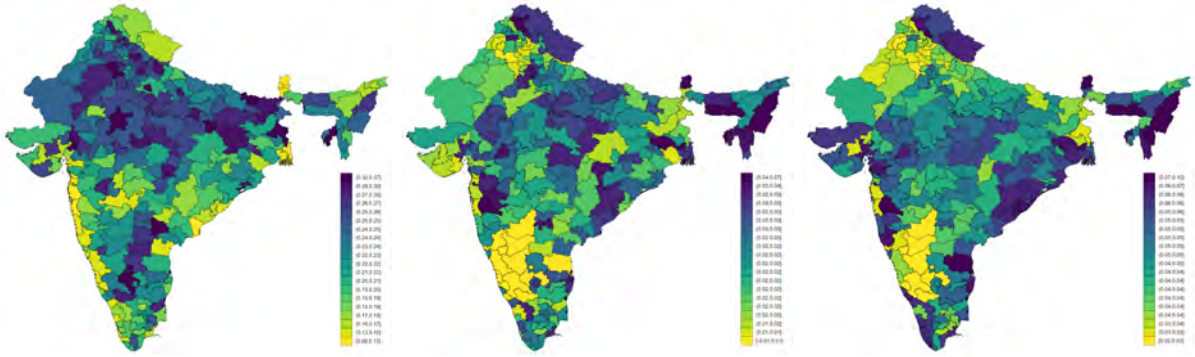

(a) Baseline (b) % Δ in Autarky (c) % Δ in Free Trade

Panel B: Variance of real wages

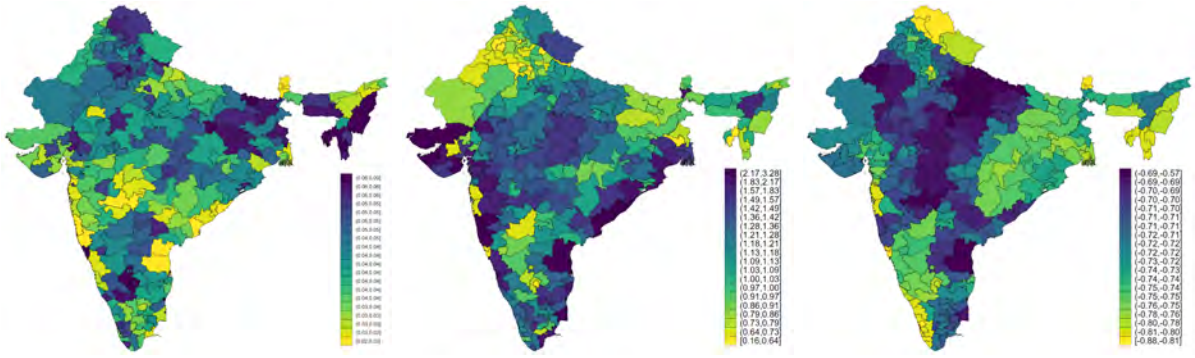

(d) Baseline (e) % Δ in Autarky (f) % Δ in Free Trade

Note. This figure shows expected real wages (Panel A) and their variance (Panel B). The left column shows expected real wages and their variance in the baseline calibrated model. In the middle and right columns, the figure shows the percentage changes in expected real wages under the autarky and the free trade counterfactuals relative to the baseline scenario. In the bottom panel, the middle and right figures show the percentage changes in the variance of real wages under the autarky and the free trade counterfactuals relative to the baseline scenario.

Figure A18: Counterfactuals: Climate Risk Increase – Projected Risk

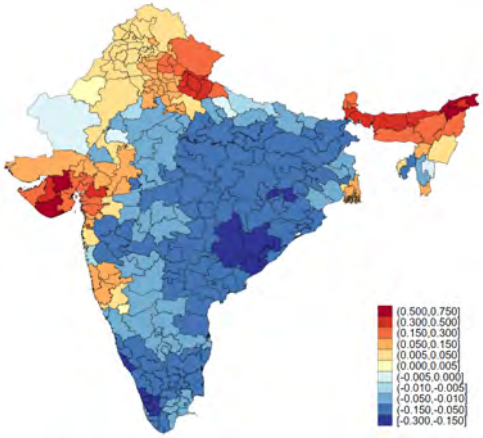

(a) A: Climate risk change

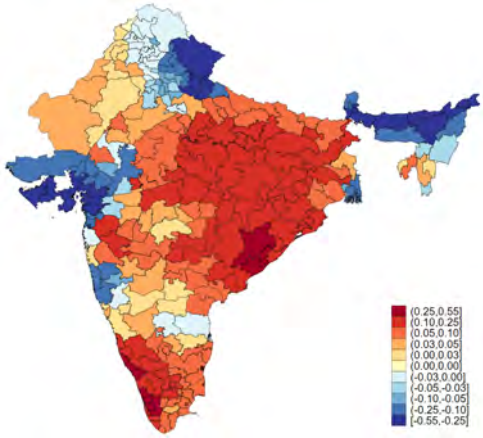

(b) B:% Δ input prices

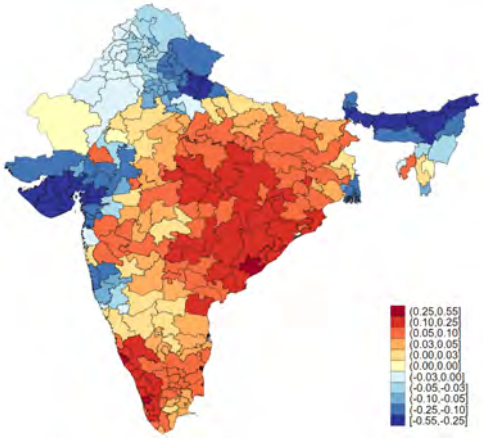

(c) C:% Δ Expected Real Wages

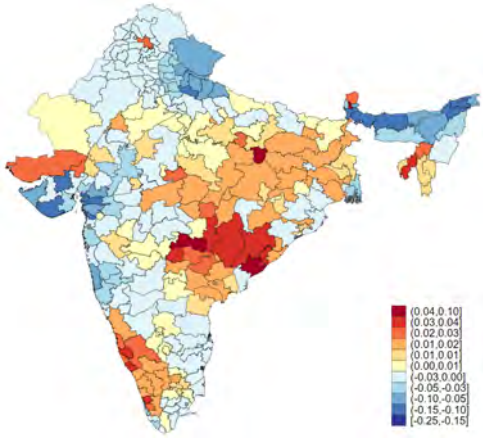

(d) D: % Δ Volatility

Note. In this figure, we plot the change in probabilities of climate risk (panel A), the change in district input prices (panel B) the change in expected real wages (panel C) and the change in the volatility of real wages (Panel D) as climate risk increases as described in Section 4.4.

F A Model with Finite Elasticity Across Inputs

In this Appendix, we develop a model in which we relax the assumption of perfect substitution of inputs across different regions by allowing for a finite elasticity of substitution, akin to an Armington model. In this model, firms will have two incentives to source input varieties from different regions. The first one is the diversification motive, which is the main focus of this paper. The second incentive corresponds to love for variety.

The only modification to the model in Section 3 is to allow for imperfect substitution in the aggregator of inputs in Equation 6. Thus, the expression becomes:

$$x_i(\omega) = \left(\sum_{j \in I} x_j^{\frac{\varepsilon-1}{\varepsilon}} \right)^{\frac{\varepsilon}{\varepsilon-1}}.$$

Since this assumption is just changing the way that the received input units are aggregated, the *ex-post* problem of the firm remains unchanged. Profits as a function of the total number of inputs the firm has are:

$$\pi_i(\boldsymbol{M_i}; \boldsymbol{\chi}) = \kappa w_i^{\frac{\beta(1-\sigma)}{\beta+\sigma(1-\beta)}} \left[\left[Y_i \mathbb{P}_i^{\sigma-1} \right] \phi_i^{\sigma-1} \left(\left(\sum_{j \in I} \left[\chi_j M_{ji} \right]^{\frac{\varepsilon-1}{\varepsilon}} \right)^{\frac{\varepsilon}{\varepsilon-1}} \right)^{(1-\beta)(\sigma-1)} \right]^{\frac{1}{\beta+\sigma(1-\beta)}},$$

where $\kappa = \left[\frac{\sigma(1-\beta)+\beta}{\beta(\sigma-1)} \right] \left[\frac{\beta(\sigma-1)}{\sigma} \right]^{\frac{\sigma}{\beta+\sigma(1-\beta)}}$. The sourcing problem of the firm is to choose M_{ij} to maximize expected profits minus order costs

$$\max_{M_{ij} \geq 0} \mathbb{E}_\chi \left(\kappa w_i^{\frac{\beta(1-\sigma)}{\beta+\sigma(1-\beta)}} \left[\left[Y_i \mathbb{P}_i^{\sigma-1} \right] \phi_i^{\sigma-1} \left(\left(\sum_{j \in I} \left[\chi_j M_{ji} \right]^{\frac{\varepsilon-1}{\varepsilon}} \right)^{\frac{\varepsilon}{\varepsilon-1}} \right)^{(1-\beta)(\sigma-1)} \right]^{\frac{1}{\beta+\sigma(1-\beta)}} \right) - \sum_{j \in I} p_j^I M_{ji}, \tag{32}$$

with first order condition,

$$\mathbb{E}_\chi \left(\chi_j \Theta_i \left[\sum_{j \in I} \left(\chi_j M_{ji} \right)^{\frac{\varepsilon-1}{\varepsilon}} \right]^{\frac{-\varepsilon+\beta+\sigma(1-\beta)}{\beta+\sigma(1-\beta)}} \left(\chi_j M_{ji} \right)^{-\frac{1}{\varepsilon}} \right) \leq p_j^I.$$

In this particular model due to an Inada condition, the solution will be interior, and is

implicitly given by:

$$M_{ji}^{-\frac{1}{\varepsilon}}\mathbb{E}_{\chi}\left(\chi_j^{\frac{\varepsilon-1}{\varepsilon}}\Theta_i\left[\sum_{j\in I}\left(\chi_j M_{ji}\right)^{\frac{\varepsilon-1}{\varepsilon}}\right]^{\frac{-\varepsilon+\beta+\sigma(1-\beta)}{(\varepsilon-1)(\beta+\sigma(1-\beta))}}\right)=p_j^I$$

$$M_{ji}=\frac{\left(p_j^I\right)^{-\varepsilon}}{\mathbb{E}_{\chi}\left(\chi_j^{\frac{\varepsilon-1}{\varepsilon}}\Theta_i\left[\sum_{j\in I}\left(\chi_j M_{ji}\right)^{\frac{\varepsilon-1}{\varepsilon}}\right]^{\frac{-\varepsilon+\beta+\sigma(1-\beta)}{(\varepsilon-1)(\beta+\sigma(1-\beta))}}\right)^{-\varepsilon}}$$

and can be simplied after plugging in the GE components to

$$M_{ji}=(1-\beta)^{\varepsilon}\left(w_i L_i\right)^{\varepsilon}\frac{\left(p_j^I\right)^{-\varepsilon}}{\mathbb{E}_{\chi}\left(\chi_j^{\frac{\varepsilon-1}{\varepsilon}}\left[\sum_{j\in I}\left(\chi_j M_{ji}\right)^{\frac{\varepsilon-1}{\varepsilon}}\right]^{-1}\right)^{-\varepsilon}}.$$

where

$$\Theta_i=(1-\beta)w_i L_i\left(\sum_{j\in I}\left[\chi_j M_{ji}\right]^{\frac{\varepsilon-1}{\varepsilon}}\right)^{-\frac{\varepsilon}{\varepsilon-1}\frac{(1-\beta)(\sigma-1)}{\beta+\sigma(1-\beta)}}$$

Notice that we cannot derive a closed-form solution for this expression, we can only define it implicitly, and solve for the demand of inputs numerically.

Proposition 3 *The ex-ante profit function described in Equation 32 is concave in orders of inputs M_{ji}.*

Proof. Since the cost of materials is linear in M_{ij} and the constraints are conventional (linear) non-negativity constraints, it suffices to show that the expected operating profits function $\mathbb{E}_{\chi}\left(\pi(\boldsymbol{M};\boldsymbol{\chi})\right)$ is concave in the vector $\boldsymbol{M}$. The expectation operator preserves the concavity of $\pi(\boldsymbol{M};\boldsymbol{\chi})$ which is the only thing required to prove. The concavity of the CES aggregator follows from the fact that it is a quasi-concave function that is homogeneous of degree 1. The concavity of ex-post profits, $\pi(\boldsymbol{M};\boldsymbol{\chi})$, follows from the parametric restriction, $\frac{(1-\beta)(\sigma-1)}{\beta+\sigma(1-\beta)}<1$, as the composition of concave functions is concave. ■